Distributed Resource Allocation Techniques in Interference-Limited Cellular Networks

Saad G. Kiani

THESE

présentée pour obtenir le grade de

Docteur de l'Ecole Nationale Supérieure des Télécommunications

Spécialité: Communication et Electronique

Saad Ghazanfar Kiani

Allocation Distribuée de Ressources dans les Réseaux Cellulaires Limités en Interférences

Thèse soutenue le 12 Fevrier 2008, devant le jury composé de :

Président	Prof. J.-C. Belfiore, ENST (Paris, France)
Rapporteurs	Dr. C. Antón-Haro, CTTC (Castelldefels, Spain)
	Prof. M. Zorzi, Universitá di Padova (Padova, Italy)
Examinateurs	Prof. R. Knopp, Institut Eurécom (Sophia Antipolis, France)
	Prof. G. Øien, NTNU (Trondheim, Norway)
Directeur de thèse	Prof. D. Gesbert, Institut Eurécom (Sophia Antipolis, France)

TELECOM PARIS
école nationale supérieure des télécommunications

EURECOM
Sophia Antipolis

THESIS

In Partial Fulfillment of the Requirements
for the Degree of Doctor of Philosophy
from Ecole Nationale Supérieure des Télécommunications

Specialization: Communication and Electronics

Saad Ghazanfar Kiani

Distributed Resource Allocation Techniques in Interference-Limited Cellular Networks

Defended on the 12th of February 2008 before a jury composed of:

President	Prof. J.-C. Belfiore, ENST (Paris, France)
Rapporteur	Dr. C. Antón-Haro, CTTC (Castelldefels, Spain)
	Prof. M. Zorzi, Universitá di Padova (Padova, Italy)
Examiners	Prof. R. Knopp, Institut Eurécom (Sophia Antipolis, France)
	Prof. G. Øien, NTNU (Trondheim, Norway)
Thesis supervisor	Prof. D. Gesbert, Institut Eurécom (Sophia Antipolis, France)

Abstract

In this dissertation, we study distributed resource allocation techniques in full reuse multicell networks. Throughout this work, we consider a system model in which simultaneous transmissions mutually interfere, and thus it is applicable to a number of wireless access schemes. On the basis of this model, we define the specific resource allocation problem addressed in this work: *joint power allocation and user scheduling* in view of maximizing network capacity, defined as the sum of individual link rates.

We initially investigate the behavior of interference in large random wireless networks, where analytical expressions are derived for the average interference as a function of distance between transmitter and receiver in cellular networks. Intuition from this study allows us to propose the interference-ideal network model, which enables us to approximate the instantaneous interference by its average value. This model is applied to the resource allocation problems considered later in the dissertation.

We then proceed to study the user scheduling sub-problem in the multicell context under a standard power allocation policy and a resource fairness constraint. We derive the network capacity optimal scheduling policy, based on which a distributed algorithm for the user scheduling problem is proposed.

Next, we investigate the optimal power allocation problem considering a weighted sum-rate objective function. Though this is a non-convex optimization problem, for two interfering links we are able to characterize the optimal power allocation solution. Interestingly, when the weights are equal, the optimal power allocation turns the links either on or off, and we term this binary power allocation.

Having looked at scheduling and power allocation individually, we proceed to propose algorithms for joint power allocation and scheduling to maximize the sum network capacity. In the first approach, we employ the interference-ideal network model and binary power allocation to derive a distributed iterative algorithm for power allocation and scheduling. The key idea in this approach is to switch off cells which do not contribute enough capacity to outweigh the interference caused to the network.

The previous approach relies on a large network assumption, and as such can not be employed for any number of cells. Thus, we propose a framework for distributed optimization of transmit powers based upon partitioning network parameters into local and non-local information. By assuming instantaneous knowledge of local, and statistical knowledge of non-local information, a distributed algorithm is derived which requires no information exchange between links. We also propose an algorithm which uses minimal information message passing (in this case one bit) to further improve the performance gain. User scheduling is shown to be easily incorporated into the power allocation algorithms.

In the end, we briefly touch upon an alternative approach called multicell access schemes, inspired by the classical multiple access problem in ad-hoc networks.

Contents

List of Figures

List of Tables

Acronyms

List of acronyms used in this document.

AWGN	Additive White Gaussian Noise
CDMA	Code Division Multiple Access
CSI	Channel State Information
CSIT	Channel State Information at Transmitter
FDMA	Frequency Division Mutiple Access
i.i.d.	independent and identically distributed
MAC	Mulitple Access Control
OFDMA	Orthogonal Frequency Division Mutiple Access
MIMO	Multiple-Input Multiple-Output
SDMA	Space Division Multiple Access
SINR	Signal-to-Interference-plus-Noise Ratio
SIR	Signal-to-Interference Ratio
SNR	Signal-to-Noise Ratio
TDMA	Time Division Multiple Access

Notations

List of the notations and symbols used in this document.

General Notations

$\mathbb{R}$	Set of real numbers
$\mathbb{E}$	Expectation operator
$\mathcal{CN}$	Complex Normal Distribution

Chapter 2 : System Model and Multicell Resource Allocation

N	Number of AP/cells/links
U_n	Number of users in cell n
u_n	A user in cell n
$G_{u_n,i}$	Channel gain from AP i to user u_n
η	Thermal noise
$\boldsymbol{U}$	Scheduling vector
Υ	Set of feasible scheduling vectors
P_{u_n}	Transmit power used for user u_n
$P_{\max}$	Maximum power constraint
$\boldsymbol{P}$	Transmit power vector
Ω	Feasible set of transmit power vectors
γ	Signal-to-interference-plus-noise ratio
$\mathcal{C}$	Sum network capacity

Chapter 3: Interference Modeling in Wireless Networks

R	Cell radius
D	Network radius
ϕ	Network density (number of AP per unit area)

K_{DL}	Number of interferers in the downlink
K_{UL}	Number of interferers in the uplink
$G_{\mathbf{r},i}$	Channel gain from interfering AP i to point $\mathbf{r}$
$d_{i,r}$	Distance between an interferer i and the receiver
ξ	Pathloss exponent
$h_{i,r}$	Fading at receiver from interferer i
σ^2	Lognormal shadowing variance

Chapter 4: Distributed Resource-Fair User Scheduling

K	Number of resource slots in a frame
ρ	Power control factor
$R_{u_n \leftarrow u_i}$	Received power at user u_n from AP of user u_i
φ	Scheduling policy
$\mathscr{I}^{(k)}$	Scheduling vector at slot k
$\mathbf{S}$	Scheduling matrix
$\mathbb{S}$	Set of all possible scheduling matrices
τ	Network capacity gain

Chapter 5: Weighted Sum-Rate Maximizing Power Allocation

$\mathcal{R}_n$	Rate of link n
w_n	Weight of link n
Ω^B	Binary feasible power allocation set

Chapter 7: Power Allocation Based on Statistical Knowledge

$\mathcal{G}$	Set of all network information
$\mathcal{G}_n^{\text{local}}$	Set of local information for link n
$\tilde{\mathcal{G}}_n$	Set of non-local information for link n
$\overline{\mathcal{C}}_n$	Expected network capacity at link n
$\overline{w}$	Average weight
$\overline{\mathcal{R}}$	Expected link capacity

Chapter 1

Introduction

1.1 Overview

Since the advent of cellular telephony in the late 80's, wireless communications has had a drastic impact on society and how we communicate. In the past, a fixed telephone number was attributed to a place, e.g. the home or office. With cellular communication, now we clearly think of a mobile phone number being associated with a person. It is thus not surprising that mobile connection market penetration in a number of countries has passed 100%; meaning there are more cell phones than people! The convenience of always being in touch has not only improved our productivity, but also opened up potential use of wireless communication for leisure and entertainment. Clearly, the myriad of consumer devices exploiting the wireless medium is testament to the role wireless technology plays, and will continue to play, in many aspects of our daily lives.

With the telecoms industry trying to fulfill the *anytime, anywhere* connectivity promise, wireless communication will take a lead role in achieving this goal. Though its early use was primarily for voice calls, users now want access to their work (email, documents, conferencing, etc.), as well as entertainment (streaming music, video-on-demand, networked gaming, etc.) no matter where they are. Data communication is thus being touted as the revenue generating service of the future, and wireless transmission is being seen as a viable and attractive medium for data communications. This is evidenced by the progression of standards from the few for early voice-centric networks e.g. AMPS, GSM, IS-95/CDMA to the numerous standards focusing on more recent data-rate intensive multimedia communications e.g. IEEE 802.11, 3GPP LTE, 3GPP2 UMB, IEEE 802.16 (WiMax) etc.

However, the announced convergence between mobile and data access internet-based services, initiated in systems such as WiMax [1] and 3GPP LTE [2], poses extraordinary challenges. For instance, in the downlink, LTE and WiMAX promise per-site data rates of 75Mbps and 100Mbps, requiring a spectral efficiency of 3.75 bits/sec/Hz and 5 bits/sec/Hz, respectively. The nature of data services (web-browsing, email, streaming video, etc) coupled with heavy user demand will place a significant load on the network in terms of data rate requirements. The designers of future generation wireless networks must come up with techniques to increase spectral efficiency (number of bits packed into unit spectrum) in order to cope with the scarcity of precious and expensive spectral resource. To this end, research has focused on innovative techniques to improve physical layer performance e.g. use of multiple antennas [3, 4, 5] and advanced error correction coding [6, 7]. Though these approaches offer gains in the point-to-point or point-to-multipoint scenarios, system-level performance is a different story. As one example, it has been shown that bringing co-channel interference into the picture significantly degrades performance of MIMO systems [8, 9]. Thus, it is of paramount importance to take a *system-level* view of the wireless network to not only exploit the system resources as efficiently as possible [10, 11], but also to increase the global performance. At the heart of this challenge lies the optimization of system resources across all dimensions allowed by the multiple access scheme (e.g. time, frequencies, codes, power, beams, etc.).

1.1.1 Traditional Resource Allocation Approach

Up till now, deploying a wireless network over a given geographical area has been done through a *divide and conquer* approach, as described in the following:

Divide: First, network frequency (or, more generally, resource) planning is used to fragment the network coverage area into smaller zones isolated from each other, from a radio point of view (Fig. 1.1) [12]. Within a cluster of neighboring cells, the spectral resource is not reused at all (such as e.g. in GSM), or reused only partially (e.g. CDMA networks, where each cell limits the number of assigned codes to a fraction of the theoretical limit defined by

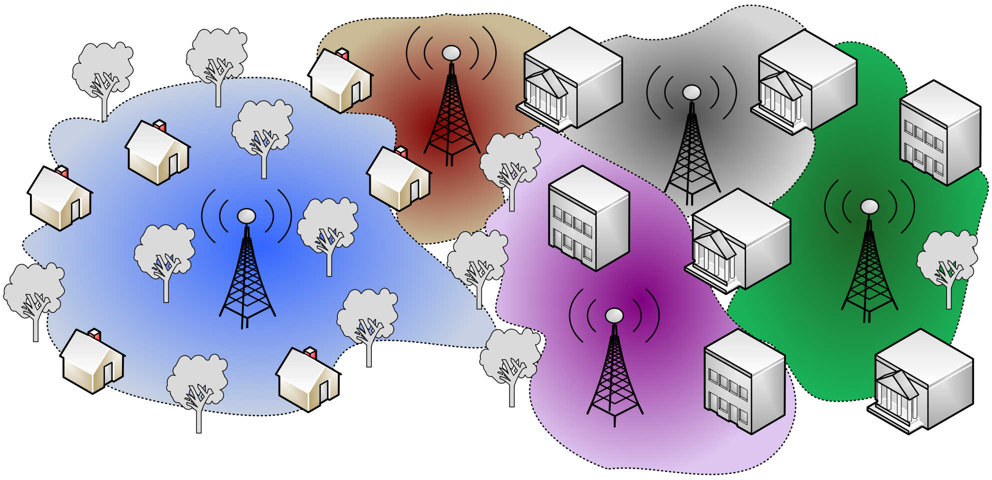

Figure 1.1: Traditional Cellular Network where coverage area is fragmented via orthogonal resource reuse to diminish the effect of interference.

the spreading factor). In ad-hoc networks, isolation of transmit-receive pairs from each other is also sought, via interference-avoidance multiple access control (MAC), typically by means of carrier sensing based protocols. The need for high efficiency figures however leads the system designer towards a planning featuring even more aggressive spectral reuse, for instance in the cellular case, from a cluster size of 5 to 7 in early GSM deployments, down to close to 1 in today's available networks such as WiMax. Power control techniques and per-cell dynamic resource allocation (e.g. frequency hopping) methods help alleviate the problem of out-of-cell interference, but in practice aggressive resource reuse will still inevitably lead to an increased level of interference in the network, which undermines the link-level performance.

Conquer: In turn, this loss of link efficiency (due to interference) for a given cell or local transmit-receive pair, may be compensated via a careful design of the radio air interface. The latter may exploit advanced processing such as efficient forward error correction (FEC) coding, fast link adaptation protocols, multiple-antenna transceivers [13], interference cancellation [14, 15] and more recently channel aware scheduling techniques [16]. In the *multiuser diversity* approach, the scheduling protocol is designed towards a better utilization of the spectrum inside each cell. This is done by encouraging at each scheduling instant, channel access for data-access users temporarily experiencing better propagation conditions (Fig. 1.2), giving

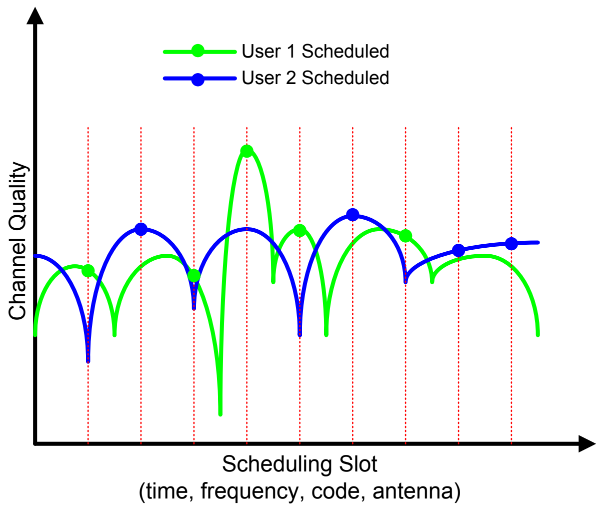

Figure 1.2: Multiuser diversity scheduling favors user with better channel conditions.

rise to the so-called multiuser diversity gain [17]. It is worth noting that this gain can be realized only if link adaptation techniques are available to take advantage of the improvement in channel conditions. Clearly multiuser diversity scheduling favors users which have on average better channel quality (e.g. those closer to the AP) and is gained at the expense of throughput fairness. This may be at least partially restored by modifying the scheduling criteria in one of several possible manners [18]. Interestingly, this idea of multiuser diversity, traditionally a single cell concept, is going to resurface later in a different form in the multicell context.

1.1.2 Voice-Centric vs. Data-Centric Networks

To a large extent the divide and conquer approach outlined above is initially motivated by voice-centric considerations. Traditionally, multicell resource planning and power control are aimed at allowing the network users to operate under a common minimum carrier-to-interference level (C/I), that is compatible with the receiver's sensitivity or operating point[1] at the access points and the user terminals. Consequently, most power control algorithms are designed to reach a signal-to-interference-plus-noise (SINR) target simultaneously for all interfering user terminals. This *SINR balancing* approach

[1]The operating point is the level of SINR needed to operate on the link, below which the call may be dropped.

ensures a worst-case outage probability necessary for connection oriented voice calls, as was done in famous contributions such as [19, 20, 21].

The concept of a modem's required SINR (operating point) is becoming less relevant in modern networks designed for data-dominated traffic, as these typically feature adaptive coding and modulation [22] protocols capable of adjusting the transmission rate to a wide range of channel conditions. Thus, the link utility is no longer a simple step function of the link SINR. Even if the number of coding rates remains limited in practice due to memory and complexity constraints, the strategy consisting of optimizing the spectral resource for a desired worst case interference level and then relying on advanced modem design alone for maximizing performance is losing some relevance. This in turn shows the limitation of the divide and conquer approach when it comes to network-wide optimization of performance. Moreover, the nature of data traffic is different from that of connection-oriented voice calls. The highly bursty nature of web and email traffic, coupled with the high data rate requirements of file downloading and peer-to-peer applications, necessitates the link rate to be able to adapt to highly variable network conditions. Getting as much data across to the end user is the need. Thus, for best-effort data access, the *sum network capacity*, defined as the sum of simultaneous transmit-receive link rates, appears as a more meaningful metric. However, additional constraints may be needed to include specific scenarios with QoS-driven traffic data (e.g. VoIP) into the resource optimization problem.

1.2 Coordinated Multicell Resource Allocation

The main thesis of our work is that significant performance gains can be realized by taking a holistic approach to network optimization. Taking an isolated view of each cell in the network is the not the best strategy. By per-cell allocation of system resources, not only does one not take advantage of the dynamics of the wireless medium, but also the enormous degrees of freedom available throughout the multicell network are not exploited.

1.2.1 Challenges

The strategy of increasing the re-use of the available resources throughout the network is blind to the detrimental effects of co-channel interference. Taking such an action alone will not prove beneficial for the system. Consequently, a *selfish* measure is not the answer to a *social* problem in which interference effects everybody. Interference management techniques will thus play a key role in future wireless networks, if we are to realize any benefit at the system level.

Moreover, the wireless channel is inherently a time-varying medium. This has significant impact on the data transfer rate which can be mathematically related to the channel state. The ability for a system to adapt to changing wireless conditions will obviously make the system robust. The more subtle and significant impact is a multiuser diversity gain through opportunistic communication by exploiting good channel conditions. With hard allocation of resources, the system cannot exploit the opportunities presented by nature. Adaptation is thus a highly desirable trait, which provides a two-fold benefit to the system.

One can naturally imagine that instead of decoupling cells and then performing single cell/link optimization, a joint optimization simultaneously across all links in the networks will yield better system performance. First of all, this will allow the network to allocate resources on the fly based on underlying channel conditions, thus extracting the maximum achievable gain. More importantly, all the optimization variables mentioned previously, e.g. code assignment, power control, multiple antenna beam design, time/frequency channel-aware scheduling, are now expanded to the take into account the dimensions offered by the multicell network (number of cells, number of users, number of possible scheduling slots, codes, power levels, etc.). The generalized concept that arises from the previous discussion is that of *coordination* or even cooperation in the wireless networks. The network has number of resources (power, bandwidth, users, cells, antennas, etc.) which can potentially offer substantial capacity gains. The actions of network nodes may be coordinated so that each one benefits, or some nodes may sacrifice for the good of the whole system. Simply put, coordination involves the entities in the network combining their efforts for the common benefit.

Global coordination across the whole networks however comes with several practical challenges. Slot-level synchronization for large network areas will be required to simultaneously allocate resources. This problem may in part be alleviated by clustering optimization over a subset of network cells. Another severe problem is the joint processing of network-wide traffic and channel quality parameters fed back to a network controller. This entails significant computation power and signaling overhead in order to realize the joint optimization of a given system objective. This is compounded in high mobility scenarios where the control unit and signaling will have to cope with fast-varying conditions.

Despite these important challenges, some recently published methods have hinted at how some of the gains offered by multicell coordination may be realized in practice and we review some of them here.

1.2.2 Existing Work on Multicell Resource Allocation

Following the recent literature, three leading and independent strategies may be identified in the effort toward making multicell coordination of resource more practical, though overall many interesting questions and challenges remain open. Some of these ideas are now briefly reviewed, while others are described in greater detail later in this dissertation.

Structuring

One of the major difficulties associated with interference avoidance in packet access communications is the lack of predictability of interference coming from other transmit-receive links due to burstiness of the traffic combined with the temporal channel variability. As an approach to counteract this effect, structure may be enforced on the resource planning grid to make interference more predictable. For instance, in the joint user scheduling and power allocation problem, a particular *power shaping* of the time frame can be exploited by allowing the access point (AP) to transmit with different powers in different portions of the frame, while users are allotted slots according to the amount of interference they can tolerate given their local channel conditions. This type of approach was pursued in e.g. [23, 24]. In an analogous strategy, power shaping over the cell sectors can be implemented by turning off sector beams according to a determined sequence, which permits users to measure the interference received and then tell their respective AP their preferred sub-frame for reception; this idea is referred to as *Time-Slot Reuse Partitioning* in [25]. In another approach, structure may be enforced by fixing the *order* in which time/frequency slots are being filled up with user packets. In the case of under-loaded systems, a predictable average portion of the slots remain unused (power-free) and the location of such slots on the multicell resource grid can be optimized to reduce interference for selected users [26]. The spatial position of users in the cell can also be used to coordinate inter-cell transmissions to avoid excessive interference [27]. Limited exchange of information between dominant interfering (neighboring) APs is yet another way of gaining knowledge about the worst-case interference, enabling the orthogonalization of these transmissions [28].

Such clever resource planning schemes are interesting as they offer additional flexibility in mitigating interference with very low complexity and little need for signaling. On the other hand, they are not fully exploiting the degrees of freedom provided by the joint multicell resource allocation problem, as the imposed structure tends to reduce the dimensions offered in the optimization.

Discretization

As certain quantities entering the resource allocation problem may be continuous, e.g. the transmit power levels, or the beamforming coefficients if multiple antennas are used, a potentially interesting tool in modifying the optimization problem consists of discretizing the optimization space. This would reduce the number of potential solutions to search over, and also reduce the feedback rate needed to communicate overhead data between network nodes. Discretization (via vector quantizing) of the optimal beamforming weights through the use of vector precoding has been proposed, but interestingly, mostly for the single cell scenario, and only for the purpose of feedback reduction (see e.g. [29]). In the case of beamforming weights, discretization can be applied posterior to beamforming weight computation. In the case of power control, discretization can be carried out prior to optimization, as a way to greatly simplify the power level search procedure. Remarkably, the discretization of power control, even to its extreme of binary on/off control, can be shown to yield quasi-optimal results in a number of cases [30], and as such constitutes a promising tool to making multicell coordination a reality. This is a central idea which is also developed in greater detail later in this dissertation.

Greedy and Iterative Optimization

Due to the non-convexity of many of the multicell resource optimization problems, finding globally optimal solutions from standard techniques proves difficult, and an analytical formulation of the solution is often out of reach. In this case, heuristic approaches based on alternating optimization or greedy search may provide a good performance/complexity compromise. While greedy search techniques have been popularized over the last few years in the area of resource allocation in multiuser spatial division multiple access [31] and OFDMA scheduling [32, 33], their application to multicell resource allocation seems to have drawn attention only recently. Greedy multicell optimization operates by optimizing on a cell by cell basis, sequentially, just as individual users are optimized sequentially in the single cell scenario. At each cell visited, the resource is optimized based on local channel conditions and newly updated interference conditions originating from the other cells [34, 35]. Such techniques may also be applied in an iterative manner by revisiting a sequence of cells several times until capacity convergence is reached.

1.2.3 Distributed versus Centralized Control

In most of the approaches above, the need exists for centralized knowledge of all channel and interference state conditions for all nodes in the network. In the case of the greedy approaches, the algorithm then only visits the cell *virtually*, and the actual computation takes place within the central control unit shown in Fig. 1.3(a). Centralized channel state information for a multiuser, multicell network involves immense signaling overhead and will not allow the extraction of diversity gains in fast-fading channel components. As first step to circumvent this problem, the design of so-called *distributed* resource allocation techniques is crucial. Distributed optimization refers to the ability for each cell to manage its local resources (say e.g. rate and power control, user scheduling) based only on locally observable channel conditions such as the channel gain between the access point and a chosen user, and possibly locally measured noise and interference Fig. 1.3(b).

At first sight, joint multicell resource allocation does not lend itself easily to distributed optimization because of the strong coupling between the locally allocated resources and the interference created elsewhere in the network. Hence the maximization of the cell capacities taken individually will not in general result in the best overall network capacity.

An interesting and recently explored path toward enforcing a distributed control of resource has been through the use of *game theoretic* concepts [36]. Game theory, in its non-cooperative setting, pitches individual players in a battle against each other, where each seeks to maximize a utility function by selecting one of several available strategic actions. In the resource allocation framework, players can be user terminals competing for access in a single cell, or interfering transmit-receive pairs of a multiple cell network or an ad-hoc network. The actions taken may be resource allocation strategies, and the utility may be capacity related. Non-cooperative game models allow transmit-receive pairs to maximize their capacity under reasonable guesses of what competing pairs might be doing [37]. In that respect, it naturally lends itself to distributed optimization. The game theoretic framework is very well suited to network scenarios where infrastructure is sparse or completely absent, as in peer-to-peer and ad-hoc networks. In infrastructure-based networks like cellular, broadband access and to some

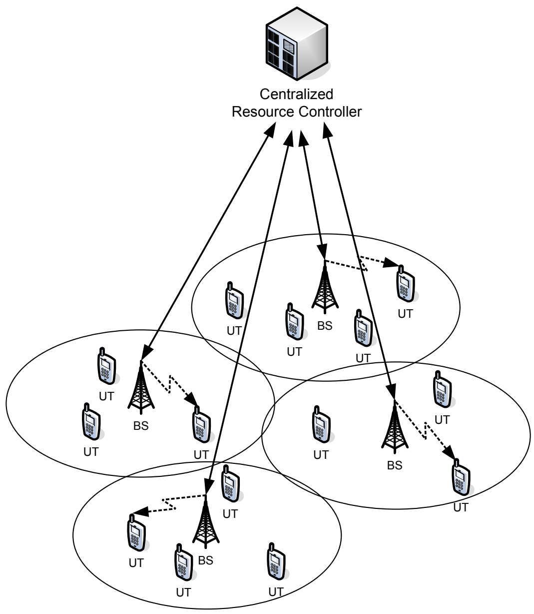

(a) A multicell system managed by centralized resource controller. This controller processes all network information jointly.

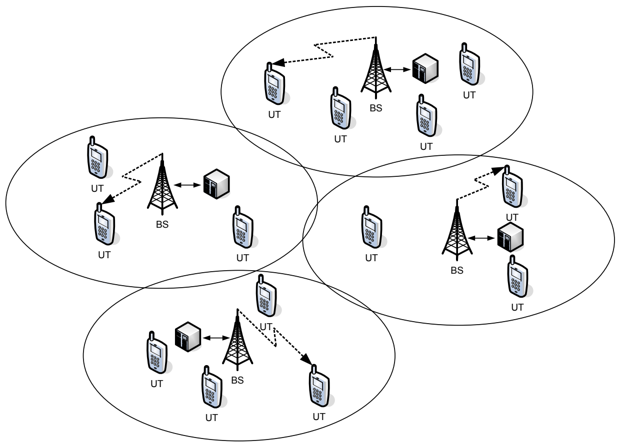

(b) A distributed multicell system requires no centralized control. Each cell performs resource allocation based on local channel knowledge (and possibly limited inter-cell information).

Figure 1.3: Centralized vs. Distributed Network Control.

extent WLAN networks, where a centralized operator retains control over the common resource, it remains to be seen if the purely non-cooperative model is overly pessimistic, as it may not be able to fully capture the gain that could be obtained from coordination. However, pricing-based game theoretic approaches have been proposed to alleviate this problem, by penalizing players with a cost for harming other players. There is a large body of literature considering various choices of utility and pricing mechanisms. In voice-oriented systems, utility can be a step function or sigmoid-like, geared toward trying to achieve a target SINR at each user as in [20]. In that case pricing may be used to stabilize power consumption when the SINR targets are close to the non-feasible region [38]. In data-oriented settings, the utility is usually a smoothly increasing function of the SINR. For instance the authors in [39, 40, 41] consider a function giving the amount of information successfully transferred per unit energy by each player, while the incurred cost is a linear function of the transmit power. An iterative algorithm is proposed which maximizes the net utility by updating individual transmit powers assuming other players' power vectors to be constant. The downlink of a two-cell CDMA data network is studied in [42], with the goal of finding the optimal transmit powers for utility and revenue maximization. The AP announces a price to the users, which then demand certain powers based on maximization of the net utility. Power control for transmit-receive pairs in an ad-hoc network is considered in [43]. Here, the cost is not a constant function, but is based on prices announced by the players to each other. Interestingly, the players charge each other for the interference created. The iterative algorithm updates the power and prices at every step, but this is not completely distributed as it requires channel gain information, as well as price updates, from all other users in the network. A truly distributed setting is obtained by making the pricing a simple linear function of the consumed power, as considered in some of the approaches discussed above. Clearly, an issue with pricing is that it should eventually be a function of the macroscopic parameters, like the number of cells, users, cell size etc. and itself needs to be optimized. Finally, it is worth noting that, although significant work on resource allocation using game theoretic frameworks can be found, it appears that the problem of user scheduling in cellular networks has been little or not addressed in this framework, a fact probably due to the historic ties between game theory approaches and adhoc networks. Though not distributed, recently cooperative game theory has been used to show the value of collaboration as opposed to competition [44].

1.3 Contributions

The end goal of this dissertation is to propose distributed schemes for multicell resource allocation with the view of improving the sum rate, which will thus be our main figure of merit. Specifically, we will consider the issues of multicell user scheduling and power allocation in a full reuse setting. Though the word multicell implies a cellular architecture, some of the results presented herein (particularly those related to power allocation) will carry to the ad-hoc network case as well.

We being in Chapter 2 by formally defining the basic system model and assumptions considered for most part of our work. We consider an interference prone system, in which a number of mutually interfering links are active. Practically, this can be the downlink of a synchronized, full reuse cellular network where the access point or base-station communicates with cell users. This can also represent communicating nodes of a wireless adhoc network. Moreover, this model is general enough for it to be applied to a number of access technologies (TDMA, O/FDMA, orthogonal CDMA within each cell). There is also no interference cancellation or joint decoding capability at the receivers. With help of the system model, we define the utility function to be optimized and consequently formulate the Multicell Resource Allocation problem in terms of power allocation and user scheduling. Utility optimal joint power allocation and user scheduling is the subject of the rest of the dissertation.

As interference plays a key role in the system model we consider, in Chapter 3 we investigate the behavior of interference in large wireless networks. We present a simple geometric network model for a large random wireless network which applies to cellular, as well as certain classes of ad-hoc networks. With the help of this model we are able to derive upper and lower bounds on the interference experienced in the network and also analyze the behavior of cellular network capacity with different network parameters. As the instantaneous interference experienced by any node in the network is difficult, if not impossible to predict, the goal is to characterize the behavior of interference in large wireless networks. The end result is a simple method to model interference in wireless networks, which is later used to derive distributed algorithms for multicell user scheduling and power allocation.
The work in this chapter has been submitted for publication in:

S. G. Kiani, D. Gesbert, "**Interference Modeling in Full Reuse Wireless Network**", *IEEE Transactions on Wireless Communications*, submitted April 2007.

In Chapter 4, we initially focus on the user scheduling sub-problem in a cellular environment considering a standard inverse power control policy. We also impose a resource-fairness constraint on the network, guaranteeing each user in the network a scheduling slot. Under this setting, with the help of the interference model derived in Chapter 3, we are able to find the network capacity-optimal scheduling policy. Based on this policy, we propose a completely distributed user scheduling algorithm which requires only knowledge of local channel gains.
The work in this chapter has been published in:

S. G. Kiani, D. Gesbert, "**Maximizing the Capacity of Large Wireless Networks: Optimal and Distributed Solutions**", in Proceedings of the *IEEE International Symposium on Information Theory* (ISIT), July 9-14, 2006, Seattle, USA.

S. G. Kiani, D. Gesbert, "**Optimal and Distributed Scheduling for Multicell Capacity Maximization**", *IEEE Transactions on Wireless Communications*, vol. 7, no. 1, January 2008.

In Chapter 5, we tackle the optimal power allocation problem for multiple interfering links, considering a weighted sum-rate utility function. Though the solution to this problem for many links is difficult to obtain, we are able to characterize the optimal power allocation for two interfering links. The motivation for considering weighted sum-rate is that it allows adaptive allocation of resources by adjusting the link weights and thus enables incorporation of QoS in the network. Moreover, it is a generalization of the equal weighted sum-rate, which itself has a remarkably simple solution.
The work in this chapter has been published in:

A. Gjendemsjø, D. Gesbert, G. Øien, S. G. Kiani, "**Optimal Power Allocation and Scheduling for Two-Cell Capacity Maximization**", in Proceedings of the *Workshop on Resource Allocation in Wireless Networks* (WiOpt), April 3-7, 2006, Boston, USA 2006.

A. Gjendemsjø, D. Gesbert, G. Øien, S. G. Kiani, "**Binary Power Control for Multicell Capacity Maximization**", *IEEE Transactions on Wireless Communications*, accepted August 2007.

S. G. Kiani, D. Gesbert, G. Øien, A. Gjendemsjø, "**Sum-Rate Maxi-**

mizing Power Allocation for Mutually Interfering Links: A Distributed Approach", *IEEE Transactions on Wireless Communications*, submitted January 2008.

where the first two papers recently appeared in the PhD dissertation of our collaborator Anders Gjendemsjø.

In Chapter 6, we go on to consider the problem of joint power allocation and user scheduling with the goal of maximizing the sum rate with out explicit fairness constraints. Using the optimal power characterization and the interference model derived in previous chapters, we propose fully distributed iterative algorithms to solve this problem for interference-limited networks with many cells. The key idea in this approach to compare the benefit a cell gives to the network in terms of capacity to the harm it causes in terms of interference.
The work in this chapter has been published in:

S. G. Kiani, G. Øien, D. Gesbert, "**Maximizing Multicell Capacity Using Distributed Power Allocation and Scheduling**", in the Proceedings of the *IEEE Wireless Communications and Networking Conference* (WCNC), March 11-15, 2007, Hong Kong.

D. Gesbert, S. G. Kiani, A. Gjendemsjø, G. E. Øien, "**Adaptation, Coordination and Distributed Resource Allocation in Interference-Limited Wireless Networks**", *Proceeding of the IEEE*, vol. 95, no. 12, December 2007.

where the second publication appeared as a tutorial paper.

In Chapter 7, we propose an alternate framework for the distributed power allocation problem which does not rely on a large network size. In this approach, we assume statistical knowledge of unknown non-local information and based on the developed framework, obtain a distributed algorithm for power allocation. By allowing a minimum exchange of information between links, substantial improvement in performance of the distributed algorithm is observed. We also demonstrate how user scheduling can be easily incorporated into the power allocation algorithm.
The work in this chapter has been published in:

S. G. Kiani. D. Gesbert, "**Capacity Maximizing Power Allocation for Interfering Wireless Links: A Distributed Approach**", in the Proceedings of *IEEE Global Communications Conference* (GLOBECOM), November 26-30, 2007, Washington D.C., USA.

S. G. Kiani, D. Gesbert, G. Øien, A. Gjendemsjø, "**Sum-Rate Maximizing Power Allocation for Mutually Interfering Links: A Distributed Approach**", *IEEE Transactions on Wireless Communications*, submitted January 2008.

In Chapter 8, we give a brief overview of an alternate approach to solving the joint power allocation and scheduling problem based on so called *multi-cell access schemes* (MCA). The approach is reminiscent of random access protocols in ad-hoc networks, however in MCA, cells rather than users compete for a chance to transmit. The notion of credit is used to allow cells to probabilistically transmit, where the credit is dependent on channel gain. Initially a simple function is used to map the credit onto the probability of access and then subsequently, the access function is optimized to maximize the sum network capacity.
The work in this chapter has been done in collaboration with fellow PhD student, Jan-Egil Kirkebø and been published in:

J. -E. Kirkebø, D. Gesbert, S. G. Kiani, "**Maximizing the Capacity of Wireless Networks Using Multi-Cell Access Schemes**", in Proceedings of the *IEEE International Workshop on Signal Processing Advances for Wireless Communications* (SPAWC), July 2-5, 2006, Cannes, France.

J. -E. Kirkebø, D. Gesbert, S. G. Kiani, "**Probabilistic Access Functions for Multicell Wireless Schemes**", in Proceedings of the *IEEE International Telecommunication Symposium* (ITS), September 3-6, 2006, Fortaleza, Brazil.

Chapter 2

System Model and Multicell Resource Allocation

In this chapter, we begin by presenting the system model and assumptions used throughout most of this dissertation. We consider a cellular network architecture in which users are spread randomly over each cell, however, some of the results presented in later chapters also carry forward to the ad-hoc case. Due to users fully sharing the same spectral resource, co-channel interference is experienced from concurrent transmissions. The advantage of such a model is that it is independent of the underlying radio interface and can be used to evaluate the system performance for a number of radio access mechanisms, e.g. TDMA,O/FDMA, orthogonal-CDMA, etc.

We then introduce the scope of Multicell Resource Allocation, focusing on power allocation and user scheduling. We define the figure of merit used throughout this work as the sum of individual link rates. We then formulate the joint power allocation and scheduling problem for sum-rate maximization, for which we will investigate solutions and algorithms in later chapters.

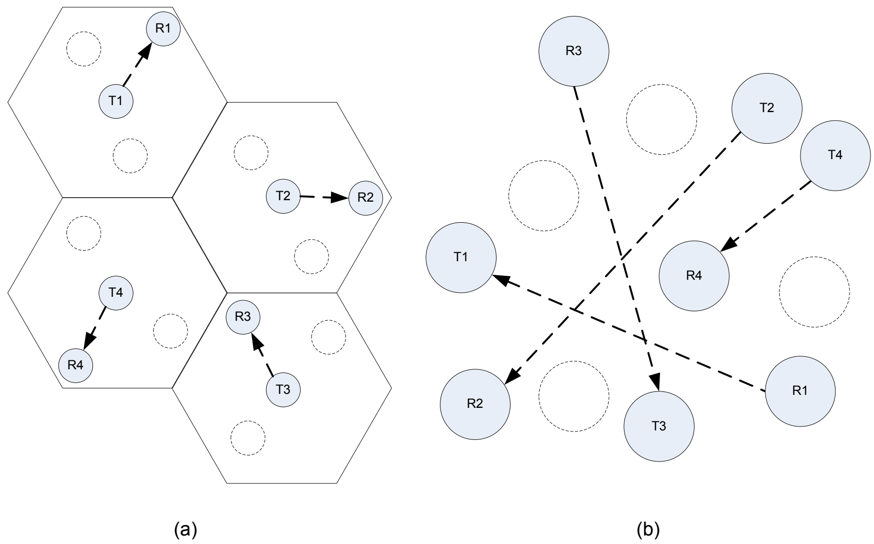

Figure 2.1: Snapshot of network model, with $N = 4$ interfering pairs of transmitters and receivers. The cellular model (a) and the single-hop peer-to-peer or ad-hoc model (b).

2.1 System Model

We consider a wireless network with a collection of nodes, which can be both transmitters and receivers. By virtue of a scheduling protocol, N transmit-receive active pairs are simultaneously selected from these nodes to communicate at a given time instant, while others remain silent. In this network, each transmitter sends a message which is intended for its receiver only. Due to full reuse of spectral resource, a receiver hears the signals from all transmitters. We assume that there is no interference cancellation capability at the receivers, nor can they jointly decode signals. In such circumstances, the receiver is interfered by all other active links and this interference contributes as noise in the intended signal. Such a setup can be seen as an instance of the interference channel, the analysis of which is a famously difficult problem in information theory [45].

The architecture resulting from the situation depicted above can be that of a cellular network with reuse factor one i.e. all the spectral resource is reused in all cells. For example, the downlink in which access points (AP) or base stations send data to the users results in parallel interfering links (Fig. 2.1(a)). In this case, the AP buffers users' data and then serves individual users within its coverage area, on a given resource slot. However, one added aspect in cellular networks is the user population which enables the selection of the user to be served at any given instant. This is called user scheduling and will be discussed further, later in the chapter.

Another architecture that also corresponds to the aforementioned model is a snapshot of nodes in an ad-hoc network (Fig. 2.1(b)). In this case source-destination pairs are setup randomly and the concept of user scheduling does not really exist. The shared channel is secured for transmission through a medium access control (MAC) protocol, which aims at providing spatial separation of simultaneously transmitting links. None the less, due to concurrent transmission the links cause interference to each other.

2.1.1 Signal Model

Mathematically, the ad-hoc and cellular scenario give the same model and as the cellular system allows us to perform user scheduling, we shall adopt a cellular terminology from here on. We thus consider N time-synchronized cells[1] with U_n users randomly distributed over each cell $n \in [1, \ldots, N]$ and infinite backlog of traffic so that there is always data to send to a user. Within each cell, we consider an orthogonal multiple access scheme so that on any given *spectral resource slot* (where resource slots can be time or frequency slots in TDMA/FDMA/OFDMA, or code in orthogonal-CDMA) a single user is supported. Therefore, focus is on inter-cell interference rather than on intra-cell interference and the latter would come as a further extension of the work presented herein. On any given spectral resource slot, shared by all cells, let $u_n \in [1, \ldots, U_n]$ be the index of the user that is granted access to the channel in cell n.

We denote the downlink channel from AP i to user u_n in cell n by $G_{u_n,i}$ which models the attenuation effects of the channel possibly including distance based pathloss, log-normal shadowing and random complex fading. We hereby focus on the downlink, but some of the ideas presented in this dissertation carry over to the uplink as well. We shall assume that the coherence time of the channel is long enough so that the receiver can estimate the gain (in each resource slot) and send this information to a local or global resource allocation unit via a feedback channel if necessary. The received

[1]In this dissertation, we will use the words cell and link to signify a transmit-receive pair.

signal Y_{u_n} at the user in a given resource slot is then given by

$$Y_{u_n} = \sqrt{G_{u_n,n}} X_{u_n} + \sum_{i \neq n}^{N} \sqrt{G_{u_n,i}} X_{u_i} + Z_{u_n}, \tag{2.1}$$

where X_{u_n} is the intended signal from the serving AP, $\sum_{i \neq n}^{N} \sqrt{G_{u_n,i}} X_{u_i}$ is the sum of interfering signals from all other cells, and Z_{u_n} is additive noise or additional interference. Z_{u_n} is modeled for convenience as complex AWGN, with power $\mathbb{E}|Z_{u_n}|^2 = \eta$.

2.1.2 Resource Fair vs. Throughput Fair vs. Max Sum-Rate Resource Allocation

An issue that arises when performing resource allocation is that of fairness. The notion of fairness can have a number of meanings depending on the underlying objectives. Thus we define here the following resource allocation policies which will be encountered in the dissertation.

Resource fairness is when each user in the network is guaranteed access to resource slot over a given time frame. For example, in a time-slotted frame with K slots, a maximum of K users are guaranteed access in a frame. Similarly, an OFDMA system with K sub-carriers guarantees access to a maximum of K users at a time. We will enforce this kind of fairness constraint when we consider the multicell scheduling problem in Chapter 4.

Rate fair policies are those that try to equalize the throughput achieved by all the users in the network over a given time frame. Proportional Fair Scheduling [46, 47] is one such policy which schedules the user with the maximum instantaneous rate normalized by the user throughput already enjoyed over a given time horizon.

In *Max Sum-Rate* resource allocation there is no fairness guarantee and at each scheduling instant, resources are allocated such that the sum of instantaneous user rates is maximized.

With the exception of Chapter 4, where resource fairness is enforced, we will consider a max sum-rate policy for the resource allocation algorithms proposed in this dissertation.

2.2 The Multicell Resource Allocation Problem

In this section, we define the core problem of resource allocation in the multicell context. Given the system model described previously, we will focus on two aspects of the resource allocation problem: *power allocation* and *user scheduling*. Power allocation is the adjustment of the transmitter power to take into account both the rate enjoyed by the link, as well as the interference caused to other active links. User scheduling is the attribution of a given resource slot to a user based upon underlying channel conditions. Specifically, we consider resource allocation policies based on *sum-rate maximization*, rather than *fairness-oriented* ones. In this setting, the optimization of resources in the various resource slots decouples, and we may consider the power allocation and user scheduling which maximize capacity in a particular slot, independently of others. However, we will touch upon fairness isses in the Chapter 4, where a resource fairness constraint is enforced.

A peak transmit power constraint $P_{\max}$ is imposed at each AP and to simplify exposition, we shall assume that it is identical for all transmitters. In order to facilitate the problem formulation of the joint power allocation and scheduling problem, we state the following definitions:

Definition 2.1 *A* **scheduling vector** $\boldsymbol{U}$ *for a given resource slot contains the set of users simultaneously scheduled across all cells:*

$$\boldsymbol{U} = [u_1\, u_2\, \cdots\, u_n\, \cdots\, u_N]$$

where $[\boldsymbol{U}]_n = u_n$*. Noting that* $1 \leq u_n \leq U_n$*, the feasible set of scheduling vectors is given by* $\Upsilon = \{\boldsymbol{U} \mid 1 \leq u_n \leq U_n\ \forall\ n = 1, \ldots, N\}$.

Definition 2.2 *A* **transmit power vector** $\boldsymbol{P}$ *for a given resource slot contains the transmit power values used by each AP to communicate with its respective user:*

$$\boldsymbol{P} = [P_{u_1}\, P_{u_2}\, \cdots\, P_{u_n}\, \cdots\, P_{u_N}]$$

where $[\boldsymbol{P}]_n = P_{u_n} = \mathbb{E}|X_{u_n}|^2$*. Due to the peak power constraint* $0 \leq P_{u_n} \leq P_{\max}$*, the feasible set of transmit power vectors is given by* $\Omega = \{\boldsymbol{P} \mid 0 \leq P_{u_n} \leq P_{\max}\ \forall\ n = 1, \ldots, N\}$.

2.2.1 Utility-Optimal Resource Allocation

The merit associated with a particular choice of resource allocation strategy can be measured via the help of a *utility function* which, in our case is denoted by $F(\boldsymbol{U}, \boldsymbol{P}) : \Upsilon \times \Omega \longrightarrow \mathbb{R}_+$. Because N pairs are served in parallel, the total utility is typically represented by the sum $F(\boldsymbol{U}, \boldsymbol{P}) =$

$\sum_n f_n(\boldsymbol{U}, \boldsymbol{P})$, where $f_n(\cdot)$ is the individual utility enjoyed by cell n. A logical choice for the utility in the above interference limited system is to pick a function of the signal-to-interference-plus-noise ratio (SINR), $f_n(\boldsymbol{U}, \boldsymbol{P}) = f(\gamma([\boldsymbol{U}]_n, \boldsymbol{P}))$, where $\gamma([\boldsymbol{U}]_n, \boldsymbol{P})$ refers to the SINR experienced by the user u_n scheduled in cell n as a result of power allocation in all cells. This SINR is given by

$$\gamma([\boldsymbol{U}]_n, \boldsymbol{P}) = \frac{G_{u_n,n} P_{u_n}}{\eta + \sum_{i \neq n}^{N} G_{u_n,i} P_{u_i}}. \tag{2.2}$$

Sum-Rate Optimal Resource Allocation

In connection-oriented communication, utility is typically a step function of the SINR, where the SINR threshold is dictated by the receiver's sensitivity. In data-centric applications however, where rate adaptation is implemented, a more reasonable choice of utility is a monotonically piece-wise increasing function of the SINR, reflecting the various coding rates implemented in the system. Assuming an idealized link adaptation protocol, i.e assuming Shannon capacity can be achieved at any SINR in any resource slot, the utility eventually converges to a smooth function reflecting the user's instantaneous rate in bits/sec/Hz. For the overall network utility we thus define the *sum network capacity*[2] [45] as

$$\mathcal{C}(\boldsymbol{U}, \boldsymbol{P}) \triangleq \frac{1}{N} \sum_{n=1}^{N} \log\Big(1 + \gamma([\boldsymbol{U}]_n, \boldsymbol{P})\Big). \tag{2.3}$$

The sum network capacity and variations based on it, will be the utility functions used throughout this dissertation. The capacity optimal resource allocation problem can now be formalized simply as:

$$(\boldsymbol{U}^*, \boldsymbol{P}^*) = \arg \max_{\substack{\boldsymbol{U} \in \Upsilon \\ \boldsymbol{P} \in \Omega}} \mathcal{C}(\boldsymbol{U}, \boldsymbol{P}), \tag{2.4}$$

The optimization problem above can be seen as generalizing known approaches in two ways: First, the capacity-maximizing scheduling problem is well studied for a single cell scenario, but traditionally not jointly over multiple cells. Second, the problem above extends the classical multicell power control problem (which usually aims at achieving SINR balancing) to

[2] We use the word capacity to refer to the sum of single user rates rather than capacity in the information-theoretic sense

include joint optimization with the scheduler. Despite its promise, solving (2.4) presents the system designer with several serious challenges.

To begin with, the problem above is known to be non-convex [48], and standard optimization techniques do not apply directly [3]. On the other hand, an exhaustive search for the $(\boldsymbol{U}^*, \boldsymbol{P}^*)$ pair over the feasible set is prohibitive. Finally, even if computational issues were to be resolved, the optimal solution still requires a centralized controller updated with instantaneous inter-cell channel gains which would create acute signaling overhead issues in practice.

The central theme of this dissertation thus arises: How do we extract all or some of the gain related to multicell resource allocation using the solution of (2.4), within reasonable complexity and signaling constraints? During the course of this thesis, we will present constructive results which demonstrate the value of multicell resource allocation and provide insight into solving this problem. Moreover, we will also focus on *distributed* algorithms requiring only local information, which would be the first step to making some of these gains realizable in practice.

In the first instance, we try to gain an insight into the behavior of expected interference in large wireless networks. As knowledge of instantaneous interference is difficult to obtain on the fly, the motivation behind such a study is that a simple model can be derived to predict interference in the large number of nodes case. This can then be applied to the problem of multicell resource allocation allowing us to achieve computationally simple and distributed algorithms.

[3] Note that by considering the high or low SIR regime, geometric programming techniques have been applied to non-convex power control problems [49]

Chapter 3

Interference Modeling in Wireless Networks

In this chapter, we study interference in a dense wireless network with frequency reuse one. In the presence of a large number of interferers, the instantaneous interference is approximated by its expectation with reasonable modeling loss. We first propose a geometric network model for a random cellular wireless system, which can also be easily extended to the case of single-hop ad-hoc networks for certain classes of MAC protocols. Based on this model, analytical expressions for the expected interference as a function of different system parameters are derived. These allow us to characterize the interference power as a function of the distance between the transmitter and the receiver of interest. Bounds on the signal-to-interference ratio are then derived which can be used to investigate network capacity behavior with network density. Interestingly, we show that the per-cell capacity is independent of network density and thus the sum network capacity scales linearly with the network size. This simple model finds several useful applications one of which is its application for distributed multicell power allocation and user scheduling discussed in later chapters.

3.1 Introduction

Interference in wireless networks is known to hinder reliable communication and ultimately limit the achievable network capacity. This effect is even more severe in forthcoming wireless data networks (e.g. WiFi, WiMAX), where the limited spectral resource is aggressively reused and networks grow denser due to the use of micro and pico-cells. In such interference-limited environments, the capacity is a direct function of the total interference level seen at any receiver. Modeling interference for such specific scenarios has thus become a critical task and is receiving increasing attention in the literature.

In previous work, the primary focus for interference models has been on CDMA (hexagonal-cell) networks for which analytical interference expressions are obtained to evaluate performance measures like packet error probability [50], system capacity [51] and outage probability [52]. Interference modeling also serves to address system design issues such as access point density optimization and placement [53, 54]. In these studies, the network is considered to be regular in geometry and thus, the base stations or access points (AP) are considered to lie at deterministic positions. This simplifies analysis of the distance-dependent pathloss by permitting the use of the "*at most n-tier*" interference approximation. This approach assumes the closet n-tiers of cells (neighbors) cause the most interference while neglecting the other cells in the network. Interference also plays a major role in determining the performance of ad-hoc networks. However, due to the random spatial position of nodes and random nature of communication link buildup and ultimate breakdown, studying interference in ad-hoc networks is a more challenging task[1]. However, the utility of a random network model is found for ad-hoc networks as well, where analysis of interference power is also attracting attention [55, 56, 57] and is instrumental in predicting the capacity. As modern networks grow denser and placement of access points (AP) mostly fail to follow a regular pattern due to zoning restriction, the need for interference analysis tools which are suited to dense random networks appears clearly.

In light of the arguments presented above, here we study interference in dense random wireless networks. The contributions presented in this chapter are as follows:

- We first present a simple geometric model for a large (many transmit-

[1] This is compounded by the interaction/impact of the resource allocation and routing protocols.

ters) *random* wireless network, where all receivers are assumed to communicate with their *neighboring* AP. This setup is relevant to practical scenarios such as WiFi, WiMAX, 3G/4G etc. In contrast with previous work, we consider the interferers to lie at discrete random points instead of following a fixed topology [53, 55, 56] or being a "uniform continuum" over the network area [51, 54]. Moreover, we take into consideration interference from *all nodes* present in the network and not just closest interferers. In our network model, the topology is governed by a key parameter which is the network density (number of AP per unit area).

- Using this model, for a cellular network we obtain analytical expressions for the downlink and uplink average interference power as a function of the distance to the intended receiver and network density, among other parameters. We show that the expected interference power is a *slowly* increasing function of the distance between the transmitter and the intended receiver.

- Using these expressions, we are able to obtain lower bounds on the signal-to-interference ratio (SIR), which can be used to investigate the behavior of the system capacity with respect to different parameters.

- Furthermore, the presented model can be extended to single-hop ad-hoc networks under certain classes of MAC protocols. This work differs from previous studies on interference in ad-hoc settings [56] in that we do not impose a spatial structure on the ad-hoc network, but consider the random positions and consequentially the random distance based pathloss from different nodes. Nor do we consider the interference as just a sum of log-normal random variables [57], but rather each interference term to be a product of fading (which may include log-normal shadowing) as well as distance based pathloss. As a result, these expressions allow us to analytically predict the best case and worst case interference in a truly ad-hoc network setting.

- Finally, modeling insights gained from this study find practical application e.g. when deriving distributed algorithms for scheduling and power control in multicell networks with aggressive reuse.

In Section 3.2 we describe in detail the proposed random network model as well as parameters governing this model. Based on this model, analytical expressions for interference are derived in Section 3.3. Section 3.4 exploits these expressions to analyze SIR and its implications on system capacity and design. The model is extended to ad-hoc networks in Section 3.5. In Section 3.6, we discuss how the average interference may be used for distributed resource allocation where as in Section 3.7 we consider the validity of the asymptotic network interference for a finite network area.

3.2 A Model for Large Random Networks

Cellular networks are traditionally modeled by a number of hexagonal cells spread over the coverage area with an AP present at the center of each cell. Although not realistic, a hexagonal cell representation allows coverage without overlap of cells or holes in the service area and serves as a mathematically tractable geometric model. However, due to the random propagation environment, the actual cell shape is neither hexagonal nor circular. Moreover, due to practical site selection constraints, AP are seldom equidistant from each other and inter-AP distance can be considered random. However, it is clearly unlikely that two AP sites will be chosen very close to each other thanks to human intervention in the site selection. The characteristics of a good network model for cellular networks must therefore reflect two effects; which make interference modeling a challenging task. First of all, APs are essentially located randomly. However, the distance between a target AP and any interfering AP can be lower bounded by a constant. As will be explained later in the section, this constant will be denoted $2R$ where R can be interpreted as the cell radius. We propose such a model in Sections 3.2.1 & 3.2.2.

Ad-hoc networks on the other hand are infrastructureless and communication links are created by virtue of a medium access control (MAC) protocol. By employing a handshaking procedure, the MAC protocol, ensures reliable communication through sufficient spatial separation of the concurrent transmit-receive links. Numerous MAC protocols have been proposed in the networking research literature for equally numerous objectives. As nodes in an ad-hoc network take on random locations, the creation of communication links are also random over a given area. However, they share a common point with cellular networks in the sense that an an exclusion area is set up around a transmit-receive pair, where no other transmission takes place to avoid collisions. We thus seek a network model which can capture the random spatial characteristics of an ad-hoc network, while still being mathematically tractable. We will see in Section 3.5 how the network model presented here can be extended to ad-hoc networks under certain classes of MAC protocols.

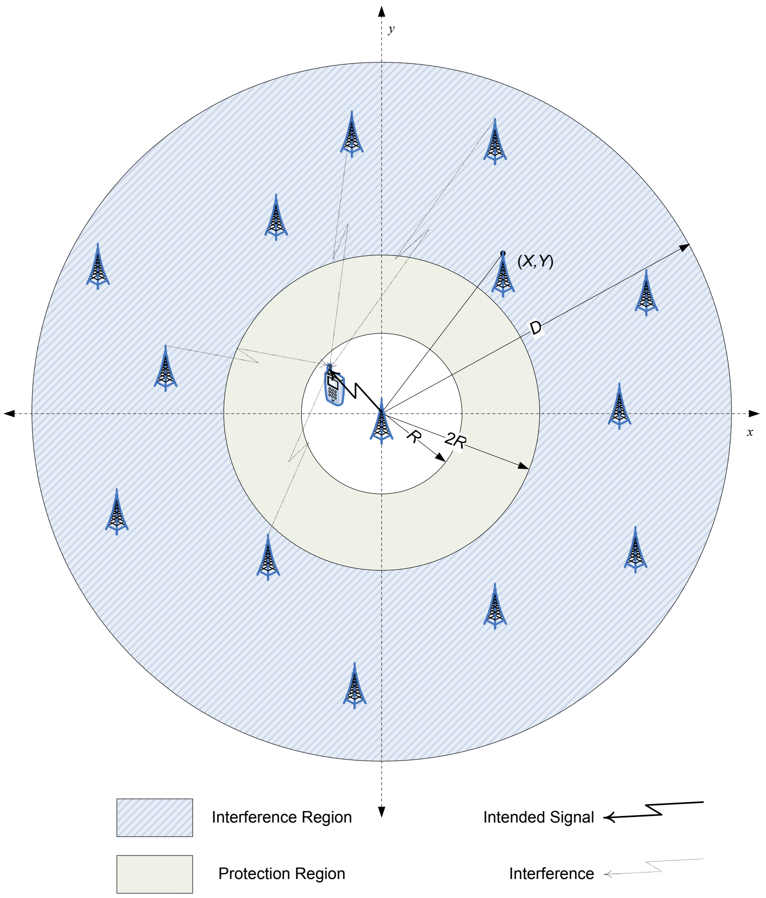

Figure 3.1: Random network model in the downlink. Closest interferer (AP) is at a distance at least $2R$ from target AP.

3.2.1 Downlink Network Model

We propose a random network model with full reuse, in which APs are located randomly according to a two-dimensional uniform distribution over a plane. Without loss of generality, a reference AP is chosen, located at the origin and all other APs (assumed then to be the sources of interference) are distributed on a ring centered at the origin with inner radius $2R$ (Fig. 3.1). The outer radius of the ring is denoted D and governs the total network area. To avoid edge effects, D will be assumed large in the rest of the paper, i.e. $D >> R$.

In this paper, we study the interference power (sum of powers received from all interference sources) at a user located within a target region, which for simplicity is represented by a disc centered at the origin (the white inner disc in Fig. 3.1). The inner disc has radius R (thus half of the interference-free disc's radius). The target region can be roughly interpreted as the service area for the reference AP, i.e. the region containing the users which communicate with the reference AP rather than with any other AP. In practical networks, users will preferably connect to a AP that yields the minimum signal propagation loss[2]. On average (i.e. when averaging over local fading and shadowing effects), a user will connect to the reference AP when it is located less than R meters away from it, as the user will then be at a greater distance from any other AP.

The network density ϕ (average number of AP per m^2) is a key parameter in this study as it will allow us to investigate how interference scales with network size. For cellular networks, it can be related to R by setting the expected number of AP in the cell area (πR^2) to be one. We thus obtain:

$$R = \sqrt{\frac{1}{\pi\phi}}. \tag{3.1}$$

Note that the density can be adjusted to take into account different cell size. Additionally, the equation above corresponds to a reuse one setting, but could be generalized without difficulty to reflect different reuse factors. Using the network density, the total expected number of *interfering* AP in the downlink is given by $K_{DL} = \phi(\pi D^2 - \pi R^2)$.

3.2.2 Uplink Network Model

In the uplink, the out-of-cell co-channel users cause interference to the target AP located at the origin (Fig. 3.2). The co-channel users are assumed to be randomly located over a ring of outer radius D with a uniform distribution consistent with the downlink model. The closest interfering users lie in the neighboring cells and thus can arise on the reference AP's cell boundary. So the inner radius for the interference ring is R. As we assume single-user communication in both the downlink and uplink, the densities of transmitters in the uplink and in the downlink naturally coincide for a given network. The total number of interfering users in the uplink is thus given by $K_{UL} = \phi(\pi D^2 - \pi R^2)$.

[2]Ignoring other factors in cell selection, such as the use of traffic-driven cell loading/balancing algorithms

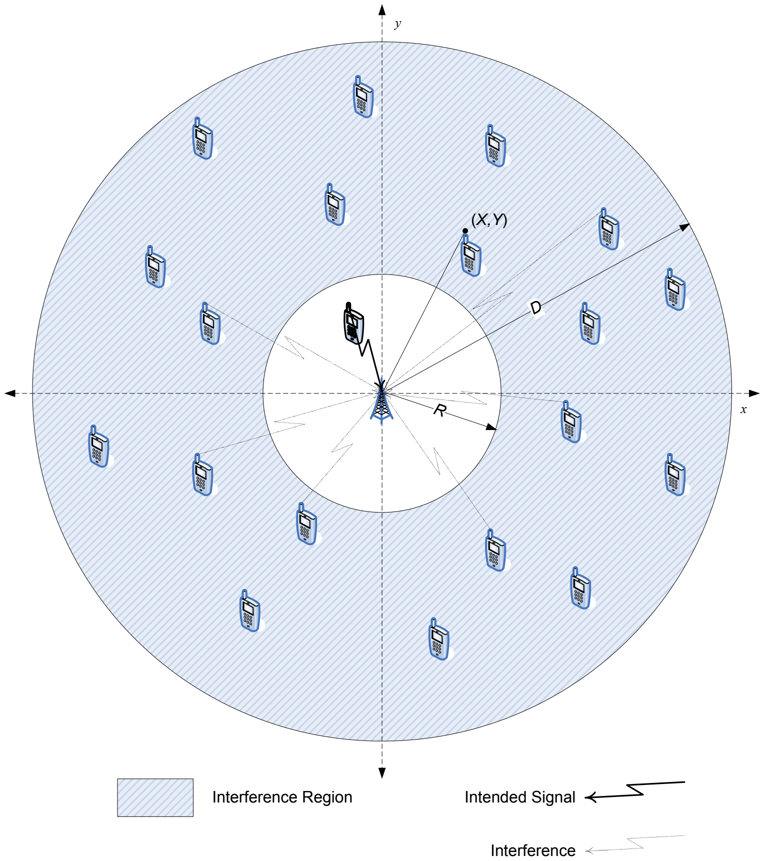

Figure 3.2: Random network model in the uplink. Closest interferer (user) is at a distance at least R from target AP.

3.3 Modeling Interference Power

Using the random network model presented, we now derive analytical expressions for the total interference power. Since the interference power is a random variable, with randomness arising from the random AP (downlink) or user (uplink) locations as well as fading, we choose to focus on the *average interference power*.

3.3.1 Downlink Interference

The interference received at a point inside the cell is the sum of powers from all APs in the interference region. Thus, the total interference received from the K_{DL} interferers at a point $\mathbf{r}$ in the 2-D plane can be expressed as,

$$I_{DL}(\mathbf{r}) = \sum_{i=1}^{K_{DL}} G_{\mathbf{r},i} P_i, \tag{3.2}$$

where $G_{\mathbf{r},i}$ is a random variable representing channel gain between the point $\mathbf{r}$ and an arbitrary interfering AP i in the interfering region, and P_i is the transmit power of AP i. If power control is employed in the network, then we can consider P_i also to be a random variable independent of $G_{r,i}$. This might be the case if e.g. a standard received-signal level power control policy is adopted where the transmit power is adjusted based on intra-cell channel gain [58]. For other power control policies, an approximate independence only may be obtained.

Average Downlink Interference

We are interested in modeling the average interference power defined by:

$$\mathbb{E}\left\{I_{DL}(\mathbf{r})\right\} = K_{DL}\mathbb{E}\left\{G_{\mathbf{r},i}\right\}\mathbb{E}\left\{P_i\right\} \tag{3.3}$$

where expectation is carried out over the random channel gain and random power levels. Moreover, due to rotational symmetry of the network model, all points on the circle of radius $0 \leq r \leq R$ will experience the same average interference. Thus, from now on we assume the receiver to lie on the y-axis (Fig. 3.3) and we have

$$\mathbb{E}\left\{I_{DL}(\mathbf{r})\right\} = \mathbb{E}\left\{I_{DL}(r)\right\}.$$

We consider the link gains to be based on an exponential distance-based pathloss model plus fading. Thus

$$G_{r,i} = h_{r,i} d_{r,i}^{-\xi}, \tag{3.4}$$

where $d_{r,i}$ is a random variable representing the distance between an interferer i and the receiver. ξ is the pathloss exponent, the value of which is greater than 2 (free-space propagation) and often close to 4 (urban environment) [59]. $h_{r,i}$ is a random variable representing fading experienced from the interferer i at the receiver and is independent of the distance-based pathloss.

Remark: Strictly speaking, the pathloss model is relevant for the far-field region. Clearly $d_{r,i}^{-\xi}$ explodes as $d_{r,i} \to 0$. We thus assume that, where applicable, the results in this work are valid for the far-field region (typically

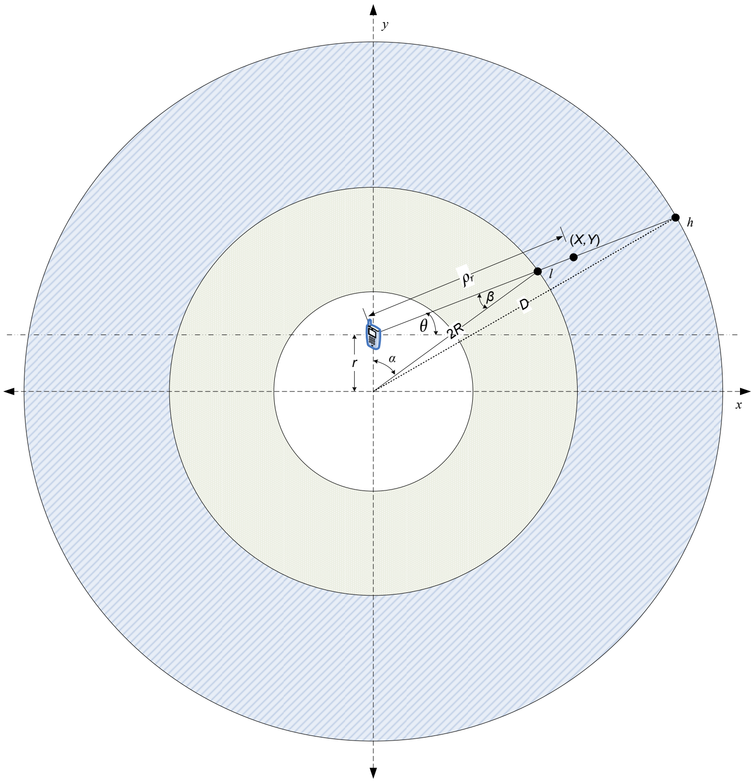

Figure 3.3: User at a distance of r from cell center. Limits of ρ_r are a function of θ, the angle with the horizontal

when $d_{r,i}$ is not in the order of the carrier wavelength). Moreover, for the analysis that follows, we also assume the pathloss exponent to be strictly greater than 2, i.e. $\xi > 2$.

Based on the above channel model we first derive the expectation of the channel gain and then use this to obtain the expected interference at any point inside the cell.

Lemma 3.1 *The* ***expected intercell channel gain*** *for the downlink of the random network model can be expressed as*

$$\mathbb{E}\left\{G_{r,i}\right\} = \frac{e^{\left(\frac{\sigma \ln 10}{10}\right)^2/2}}{(\pi D^2 - 4\pi R^2)(-\xi+2)} \int_0^{2\pi} \left(D\left(1 - \frac{r^2}{D^2}\cos^2\theta\right)^{\frac{1}{2}} - r\sin\theta\right)^{-\xi+2} - \left(2R\left(1 - \frac{r^2}{4R^2}\cos^2\theta\right)^{\frac{1}{2}} - r\sin\theta\right)^{-\xi+2} d\theta \tag{3.5}$$

Proof: The distance pathloss and fading being independent, the expectation of intercell channel gain is given by

$$\mathbb{E}\left\{G_{r,i}\right\} = \mathbb{E}\left\{h_{r,i}\right\} \mathbb{E}\left\{d_{r,i}^{-\xi}\right\}. \tag{3.6}$$

We will first determine $\mathbb{E}\left\{d_{r,i}^{-\xi}\right\}$. Imagine the disc to be centered at the origin of a cartesian plane (Fig. 3.3). Consider a random point (X, Y) for which the x and y cartesian coordinates are i.i.d. according to a uniform distribution inside the interference region. The joint density function of the random variables X and Y is given by

$$f(x, y) = \begin{cases} c & \text{if } (2R)^2 \leq x^2 + y^2 \leq D^2 \\ 0 & \text{otherwise} \end{cases}$$

We have

$$\begin{aligned} \iint_{-\infty}^{\infty} f(x, y) \mathrm{d}x \mathrm{d}y &= 1 \\ c \iint_{(2R)^2 \leq x^2 + y^2 \leq D^2} \mathrm{d}x \mathrm{d}y &= 1 \end{aligned}$$

and evaluating the integral actually gives us the area of the interference region and therefore,

$$c = \frac{1}{\pi D^2 - 4\pi R^2}$$

The joint density function is thus,

$$f(x, y) = \begin{cases} \frac{1}{\pi D^2 - 4\pi R^2} & \text{if } (2R)^2 \leq x^2 + y^2 \leq D^2 \\ 0 & \text{otherwise} \end{cases} \tag{3.7}$$

We can then derive the joint density function of the random variables ρ_r and θ (Fig. 3.3), the polar coordinates transformation of the point (X, Y) with r as origin (see Appendix 3.A),

$$f\left(\rho_r, \theta\right) = \frac{\rho_r}{\pi D^2 - 4\pi R^2} \quad \text{for} \quad \begin{array}{c} l \leq \rho_r \leq h \\ 0 \leq \theta \leq 2\pi \end{array} \tag{3.8}$$

We point out here that the limits l and h for ρ_r will be a function of θ (Fig. 3.3). As $\mathbb{E}\left\{d_{r,i}^{-\xi}\right\} = \mathbb{E}\left\{\rho_r^{-\xi}\right\}$, we can use the joint density of ρ_r and θ to find

$\mathbb{E}\left\{d_{r,i}^{-\xi}\right\}$. Using the marginal density of ρ_r, we can express the expectation as follows

$$\begin{aligned}
\mathbb{E}\left\{\rho_r^{-\xi}\right\} &= \iint_{-\infty}^{\infty} \rho_r^{-\xi} f\left(\rho_r, \theta\right) \mathrm{d}\rho_r \mathrm{d}\theta \\
&= \int_0^{2\pi} \int_l^h \frac{\rho_r^{-\xi+1}}{\pi D^2 - 4\pi R^2} \mathrm{d}\rho_r \mathrm{d}\theta \\
&= \frac{1}{(\pi D^2 - 4\pi R^2)(-\xi+2)} \int_0^{2\pi} h^{-\xi+2} - l^{-\xi+2} \mathrm{d}\theta. \qquad (3.9)
\end{aligned}$$

The limits can be easily derived (see Appendix 3.B) to give

$$\begin{aligned}
l &= 2R\left(1 - \frac{r^2}{4R^2}\cos^2\theta\right)^{\frac{1}{2}} - r\sin\theta, \\
h &= D\left(1 - \frac{r^2}{D^2}\cos^2\theta\right)^{\frac{1}{2}} - r\sin\theta. \qquad (3.10)
\end{aligned}$$

The expectation of the fading term can be obtained based on the environment considered. If we consider independent zero mean lognormal shadowing with σ^2 variance in dB and fast fading $\sim \mathcal{CN}(0,1)$ then

$$\mathbb{E}\left\{h_i\right\} = e^{\left(\frac{\sigma \ln 10}{10}\right)^2/2} \times 1$$

Thus, the expected downlink intercell channel gain at a distance r from the cell center can be expressed as

$$\mathbb{E}\left\{G_{r,i}\right\} = \frac{e^{\left(\frac{\sigma \ln 10}{10}\right)^2/2}}{(\pi D^2 - 4\pi R^2)(-\xi+2)} \int_0^{2\pi} h^{-\xi+2} - l^{-\xi+2} \mathrm{d}\theta, \qquad (3.11)$$

which, together with (3.10), gives (3.5). ■

Assuming all nodes to transmit at constant power, the average transmit power of each node is set equal to 1. We now present the following theorem:

Theorem 3.1 *The* ***expected downlink interference*** *at point r, for an asymptotically large network area (with fixed density) can be expressed as,*

$$\mathbb{E}\left\{I_{DL}(r)\right\} = \phi \frac{e^{\left(\frac{\sigma \ln 10}{10}\right)^2/2}}{(\xi-2)} \int_0^{2\pi} \left(2R\left(1 - \frac{r^2}{4R^2}\cos^2\theta\right)^{\frac{1}{2}} - r\sin\theta\right)^{-\xi+2} d\theta \qquad (3.12)$$

Proof: This is straightforward from (3.3) by substituting the value of K_{DL},

$$
\begin{aligned}
\mathbb{E}\left\{I_{DL}(r)\right\} &= K_{DL}\mathbb{E}\left\{G_{r,i}\right\} \\
&= \phi\frac{(\pi D^2-\pi R^2)}{(\pi D^2-4\pi R^2)}\frac{e^{(\frac{\sigma\ln 10}{10})^2/2}}{(-\xi+2)}\int_0^{2\pi}\left(D\left(1-\frac{r^2}{D^2}\cos^2\theta\right)^{\frac{1}{2}}-r\sin\theta\right)^{-\xi+2} \\
&\quad -\left(2R\left(1-\frac{r^2}{4R^2}\cos^2\theta\right)^{\frac{1}{2}}-r\sin\theta\right)^{-\xi+2}\mathrm{d}\theta
\end{aligned}
\tag{3.13}
$$

and then taking $\lim_{D\to\infty}\mathbb{E}\left\{I_{DL}(r)\right\}$ gives (3.12). ■

Unfortunately, further simplification of this expression seems difficult to obtain. Nevertheless it is easy to evaluate numerically and interesting insights can be gained from it, as discussed below.

Variation of downlink interference with network density

By normalizing r with respect to the cell radius, $\{\overline{r}=\frac{r}{R}:0\leq\overline{r}\leq 1\}$, we can express the downlink interference in terms of the network density as

$$\mathbb{E}\left\{I_{DL}(\overline{r})\right\}=\phi^{\frac{\xi}{2}}\Upsilon(\overline{r}), \tag{3.14}$$

where

$$\Upsilon(\overline{r})=\frac{(\pi)^{\frac{\xi}{2}-1}e^{(\frac{\sigma\ln 10}{10})^2/2}}{(\xi-2)}\int_0^{2\pi}\left(\left(4-\overline{r}^2\cos^2\theta\right)^{\frac{1}{2}}-\overline{r}\sin\theta\right)^{-\xi+2}\mathrm{d}\theta.$$

From (3.14), we easily see that interference increases with increasing density as expected. What is less obvious is whether the increase of interference will be compensated by the gain in desired signal power. This point is important in view of the network capacity calculation for very dense networks, and will be addressed in a later section.

Variation of downlink interference with distance from the target AP

In Fig. 3.4, we plot (3.14) which shows that interference increases monotonically, although only slightly, from the cell center up to cell edge. In fact, this behavior is valid for a range of practical values for the pathloss exponent in realistic propagation environments. Moreover, the interference decreases with increasing pathloss exponent due to increased signal attenuation (Fig. 3.4). This monotonic behavior of the interference power as function of the user location has some useful implications in terms of deriving best-case and worst-case behavior of the average interference and thus capacity.

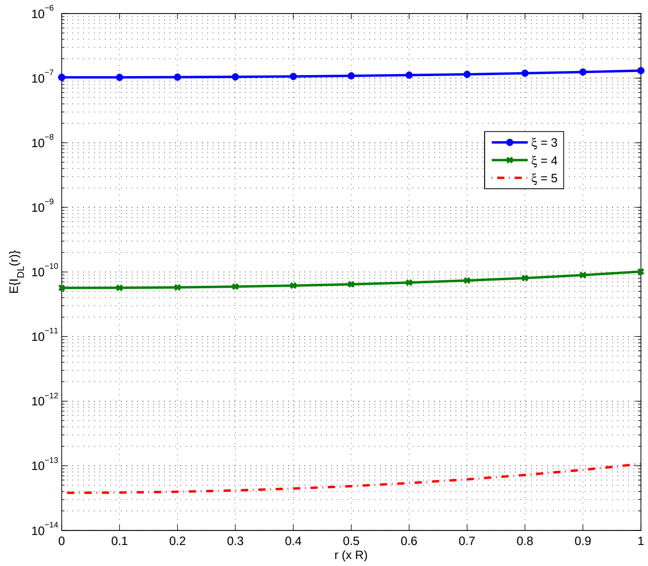

Figure 3.4: Variation of expected downlink interference with distance r from cell center for different pathloss exponents. For practical values of ξ, average interference increases slowly from cell center to cell edge.

3.3.2 Uplink Interference

In the uplink, the scheduled user in each cell communicates with its respective AP and causes interference to other AP in the network (Fig. 3.2). The average interference in the uplink can be treated in a similar way as the downlink, i.e.

$$\mathbb{E}\left\{I_{UL}\right\} = K_{UL}\mathbb{E}\left\{G_i\right\}, \tag{3.15}$$

where G_i is a random variable representing channel gain between the AP under consideration and a random user i.

Lemma 3.2 *The* ***expected intercell channel gain*** *for the uplink of the random network model is given by*

$$\mathbb{E}\left\{G_i\right\} = e^{\left(\frac{\sigma \ln 10}{10}\right)^2/2} \frac{2(D^{-\xi+2} - R^{-\xi+2})}{(-\xi+2)(D^2 - R^2)}. \tag{3.16}$$

Proof: In the uplink the position of the AP remains fixed and only the interferer position varies. We denote the distance pathloss by $d_i^{-\xi}$ and assume that fading distribution remains the same as the downlink. The joint density function of a random point (X, Y) in the interference region uniformly distributed in x and y coordinates is given by

$$f(x,y) = \frac{1}{\pi D^2 - \pi R^2} \text{ for } R^2 \leq x^2 + y^2 \leq D^2.$$

The cumulative distribution function of $d_i = \sqrt{X^2 + Y^2}$ is given by (Appendix 3.C)

$$F_{d_i}(a) = \frac{a^2 - R^2}{D^2 - R^2} \text{ for } R \leq a \leq D. \tag{3.17}$$

We can thus obtain the density function as

$$f_{d_i}(a) = \frac{\partial F_{d_i}(a)}{\partial a} = \frac{2a}{D^2 - R^2} \text{ for } R \leq a \leq D$$

Finally, we have

$$\begin{aligned} \mathbb{E}\left\{d_i^{-\xi}\right\} &= \int_R^D a^{-\xi} f_{d_i}(a)\mathrm{d}a \\ &= \frac{2}{D^2 - R^2} \int_R^D a^{-\xi+1}\mathrm{d}a \\ &= \frac{2(D^{-\xi+2} - R^{-\xi+2})}{(-\xi+2)(D^2 - R^2)}. \end{aligned}$$

The expected intercell channel gain is given by,

$$\mathbb{E}\{G_i\} = \mathbb{E}\{h_i\}\,\mathbb{E}\left\{d_i^{-\xi}\right\} \tag{3.18}$$

which gives (3.16). ■

This leads us to the following theorem for the uplink interference:

Theorem 3.2 *The* ***expected uplink interference*** *for an asymptotically large network area (with fixed density) can be expressed as*

$$\mathbb{E}\{I_{UL}\} = 2\pi\phi e^{(\frac{\sigma \ln 10}{10})^2/2} \frac{R^{-\xi+2}}{(\xi-2)} \tag{3.19}$$

Proof: This is straightforward by substituting respective values in (3.15) to obtain,

$$\begin{aligned}\mathbb{E}\{I_{UL}\} &= K_{UL}\mathbb{E}\{G_i\} \\ &= 2\pi\phi e^{(\frac{\sigma \ln 10}{10})^2/2}\frac{(D^{-\xi+2} - R^{-\xi+2})}{(-\xi+2)},\end{aligned} \tag{3.20}$$

and then taking $\lim\limits_{D\to\infty} \mathbb{E}\{I_{UL}\}$ gives (3.19). ■

Variation of uplink interference with network density

We can express the uplink interference in terms of the network density as follows

$$\mathbb{E}\{I_{UL}\} = \phi^{\frac{\xi}{2}}\Psi \tag{3.21}$$

where the constant Ψ is given by,

$$\Psi = \frac{2\pi^{\frac{\xi}{2}} e^{(\frac{\sigma \ln 10}{10})^2/2}}{(\xi-2)}.$$

Clearly, the uplink average interference also increases with network density, as intuitively expected. We also see that interference increases with decreasing ξ (Fig. 3.5) and will become unbounded as $\xi \to 2$. This again demonstrates the desirable effect of having a pathloss exponent greater than 2 in practice, as it offers protection from strong interference.

3.4 SIR & Capacity Analysis

The expected interference expressions obtained in the previous section are not only useful for predicting interference in the network, but they can also be used to study the network capacity scaling with the density in the interference-limited regime. Link capacity can be expressed as $f(\text{SIR})$ where $f(\cdot)$ is a monotonically increasing function of the SIR. We thus turn our attention to the effect of network density on the expected SIR which, in turn reflects the effect on the network capacity. We first express the SIR as a function of the distance from the reference AP. Then, we turn our attention to the worst case scenarios for both the downlink and uplink, which by our previous results are when the user is at the cell edge.

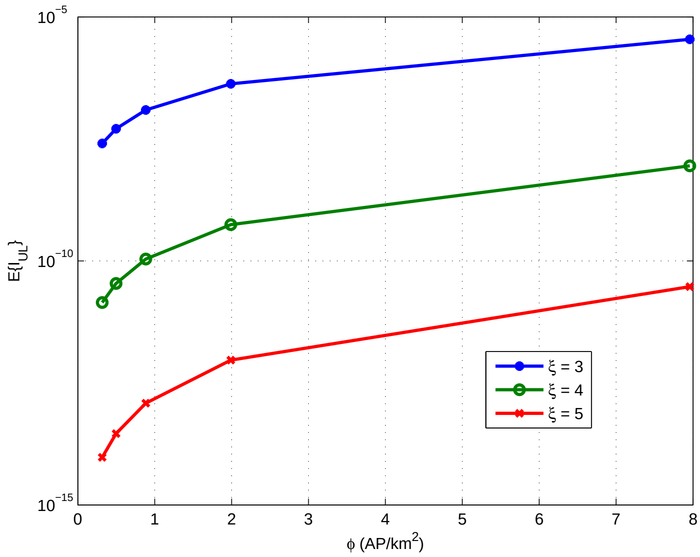

Figure 3.5: Variation of expected uplink interference with network density for different pathloss exponents. For practical values of ξ, average interference increases with increasing network density.

3.4.1 Lower Bound on Downlink SIR

The expectation of the downlink SIR is given by:

$$\mathbb{E}\{\mathrm{SIR}_{DL}(r)\} = \mathbb{E}\left\{\frac{G_{r,0}}{I_{DL}(r)}\right\}, \tag{3.22}$$

where the AP under consideration is indexed 0. Through Jensen's inequality [45] we can lower bound the expected SIR as,

$$\mathbb{E}\{\mathrm{SIR}_{DL}(r)\} \geq \frac{\mathbb{E}\{G_{r,0}\}}{\mathbb{E}\{I_{DL}(r)\}} = \overline{\mathrm{SIR}}^{LB}_{DL}(r) \tag{3.23}$$

Assuming identical fading distribution for all links, we obtain

$$\overline{\mathrm{SIR}}^{LB}_{DL}(r) = \frac{r^{-\xi}}{\frac{\phi}{(-\xi+2)}\int_0^{2\pi} -\left(2R\left(1-\frac{r^2}{4R^2}\cos^2\theta\right)^{\frac{1}{2}} - r\sin\theta\right)^{-\xi+2} \mathrm{d}\theta}. \tag{3.24}$$

Using $\phi = \frac{1}{\pi R^2}$ and the normalized distance $\overline{r}$ we obtain

$$\overline{\text{SIR}}^{LB}_{DL}(\overline{r}) = (\overline{r})^{-\xi} \frac{\pi(\xi - 2)}{\displaystyle\int_0^{2\pi} \left(\left(4 - \overline{r}^2 \cos^2\theta\right)^{\frac{1}{2}} - \overline{r}\sin\theta\right)^{-\xi+2} \mathrm{d}\theta}. \tag{3.25}$$

Clearly, the downlink SIR will decrease with $\overline{r}$, as the signal power (numerator) decreases and interference (denominator) increases from cell center to cell edge. More importantly, we note that the SIR is independent of the network density. It depends only on the position of the user in the cell and on the pathloss exponent.

3.4.2 Downlink Cell Capacity

Using the lower bound obtained in the previous section we can calculate the lower bound on the downlink cell capacity as follows:

$$\overline{C}_{DL} = \frac{1}{R^2} \int_0^R \log_2\left(1 + \overline{\text{SIR}}^{LB}_{DL}(r)\right) 2r\mathrm{d}r. \tag{3.26}$$

By using the normalized distance $\overline{r} = \frac{r}{R}$ we can rewrite the above expression as

$$\overline{C}_{DL} = 2\int_0^1 \log_2\left(1 + \overline{\text{SIR}}^{LB}_{DL}(\overline{r})\right) \overline{r}\mathrm{d}\overline{r}. \tag{3.27}$$

which we see is independent of the cell size. This expression however is difficult to simplify analytically. None the less, it can be solved numerically for a given pathloss exponent to obtain the lower bound on the downlink cell capacity.

3.4.3 Lower Bound on Uplink SIR

Proceeding along the same lines as the downlink, the expected uplink SIR is lower bounded by

$$\mathbb{E}\{\text{SIR}_{UL}\}(r) \geq \frac{\mathbb{E}\{G_r\}}{\mathbb{E}\left\{I_{UL}\right\}} = \overline{\text{SIR}}^{LB}_{UL}(r)$$

where G_r is the power received at the AP under consideration from a user situated at a distance r from the cell center. The lower bound on the uplink SIR is given by

$$\overline{\text{SIR}}^{LB}_{UL}(r) = \frac{r^{-\xi}}{2\pi\phi \dfrac{-R^{-\xi+2}}{(-\xi+2)}} \tag{3.28}$$

Substituting $\phi = \frac{1}{\pi R^2}$ and using the normalized distance $\overline{r}$, we have

$$\overline{\mathrm{SIR}}_{UL}^{LB}(\overline{r}) = (\overline{r})^{-\xi}\left(\frac{\xi}{2} - 1\right) \tag{3.29}$$

Again, we see that the uplink SIR decreases from cell center to cell edge and is independent of network density. It is only a function of the position of the user and the pathloss exponent.

3.4.4 Uplink Cell Capacity

Again using the lower bound on the uplink SIR, we can calculate the uplink cell capacity as

$$\overline{C}_{UL} = \frac{1}{R^2}\int_0^R \log_2\left(1 + \overline{\mathrm{SIR}}_{UL}^{LB}(r)\right) 2r\mathrm{d}r. \tag{3.30}$$

Using the normalized distance $\overline{r}$ we obtain

$$\overline{C}_{UL} = 2\int_0^1 \log_2\left(1 + (\overline{r})^{-\xi}\left(\frac{\xi}{2} - 1\right)\right)\overline{r}\mathrm{d}\overline{r}. \tag{3.31}$$

We see that the uplink capacity is also independent upon the cell size. Thus, we see that increasing the network density (keeping network area constant) will not effect the uplink cell capacity.

3.4.5 Network Design Implications

First of all, we note the effect of the pathloss exponent ξ on cell capacity. It is straightforward from eqs. (3.25) & (3.29) that when $\xi \to 2$, both uplink and downlink SIR tends to zero. This goes to demonstrate that even though a large pathloss exponent causes greater signal attenuation, it actually facilitates communication over the wireless medium by causing degradation to interfering signals as well. It turns out that as ξ increases, the ratio of the desired signal to interference i.e. SIR increases. As capacity at a given position $\overline{r}$ is a monotonically increasing function of SIR, *we can thus conclude that cell capacity will increase with a greater pathloss exponent.* This is an analytical explanation of what has been observed through simulations in previous studies [60].

Secondly, we see that for an asymptotically large network (number of transmit-receive pairs) the lower bounds on the uplink and downlink cell capacities are independent of the network density. Thus, increasing the AP density will not degrade the per cell capacity. This follows intuitively from that fact that although interference increases as network density increases, the distance between transmit-receive pairs (cell radius) decreases. Thus, increased interference is exactly compensated by the fact that the receiver becomes closer and closer to its serving AP as density increases. Note also that as we increase the network density, the number of cells over a given area naturally increases and thus *the total capacity of the fixed-area network will increase with the network density*.

From a network design point of view, as the SIR (and thus capacity) is not effected by the transmit power, smaller cells can be accommodated by reducing power. However, the power cannot be made arbitrarily small due to the fact that a) the underlying propagation model is valid only for the far field region, and b) the signal power should not fall below the noise floor. As has been seen from practical deployment experience, these arguments further motivate employing pico-cells with full-reuse as a means of providing capacity enhancement in harsh propagation environments.

3.5 Interference in Ad-hoc Networks

In ad-hoc networks, any node can communicate with any other node within its transmission/listening range. There is no imposed structure which restricts the source-destination pairs to lie within a given area (e.g. cells). So the source and destination lie at completely random locations in the network. This presents a significant challenge in terms of network modeling due to the random nature of link creation. However, completely random communication is not feasible as there would be too much interference to allow any of the links to communicate. That is why links are autonomously created according to the multiple access control (MAC) protocol, which reserves the shared medium over a given spatial region so that two nodes may communicate without any other node interfering.

MAC protocols for ad-hoc networks have been extensively studied in the networking community. It is out of the scope of the paper to detail all of these here. These have, however, been categorized into three different classes in [57]. Keeping with the classification introduced therein, in what follows, we discuss how the proposed random network model can also serve to model a single-hop ad-hoc network using Class 1 and Class 3 MAC protocols.

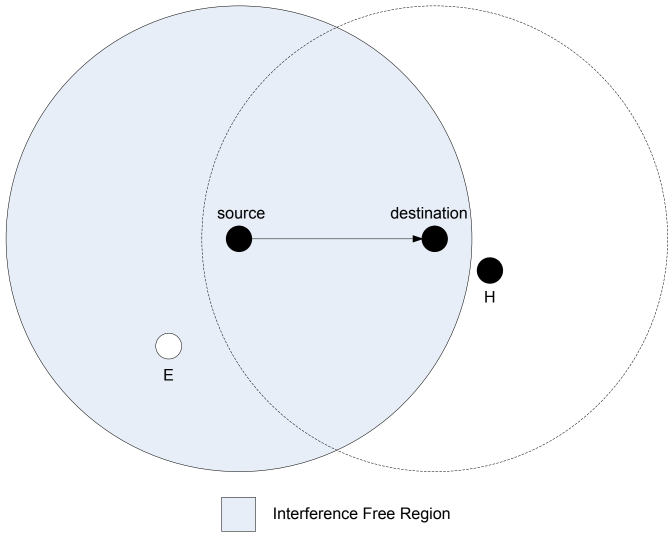

Figure 3.6: Class 1 MAC protocol leaves hidden and exposed node problem unsolved. Node H can severely interfere with the destination while node E is not allowed to transmit although it would not cause major interference to the destination.

3.5.1 Expected Interference for Class 1 MAC Protocols

In Class 1 MAC protocols, only nodes inside the transmission range of the source are prohibited from transmitting. This leaves both the hidden and exposed node problems unsolved as demonstrated in Fig. 3.6. The source reserves the medium in its radius of coverage[3] preventing other nodes from simultaneously transmitting. However, node H can transmit and cause severe interference to the destination. Node E on the other hand, though not causing that much interference to the destination cannot transmit. The widely adopted CSMA/CA protocol [61] without reservation is an example of this class.

It is easy to see that as a result of a Class 1 MAC protocol, all interfering nodes will lie outside the transmission range of the source. This will result in a similar network model as the downlink discussed previously, but there is no protection region (Fig. 3.7). The expected interference will be a function of the distance between source and destination. Using the same approach

[3]We assume that the distance beyond which the signal power falls below a certain threshold is the coverage radius. Beyond this distance, the signal is not perceived as interference by other nodes, which can thus create links without regard to this signal.

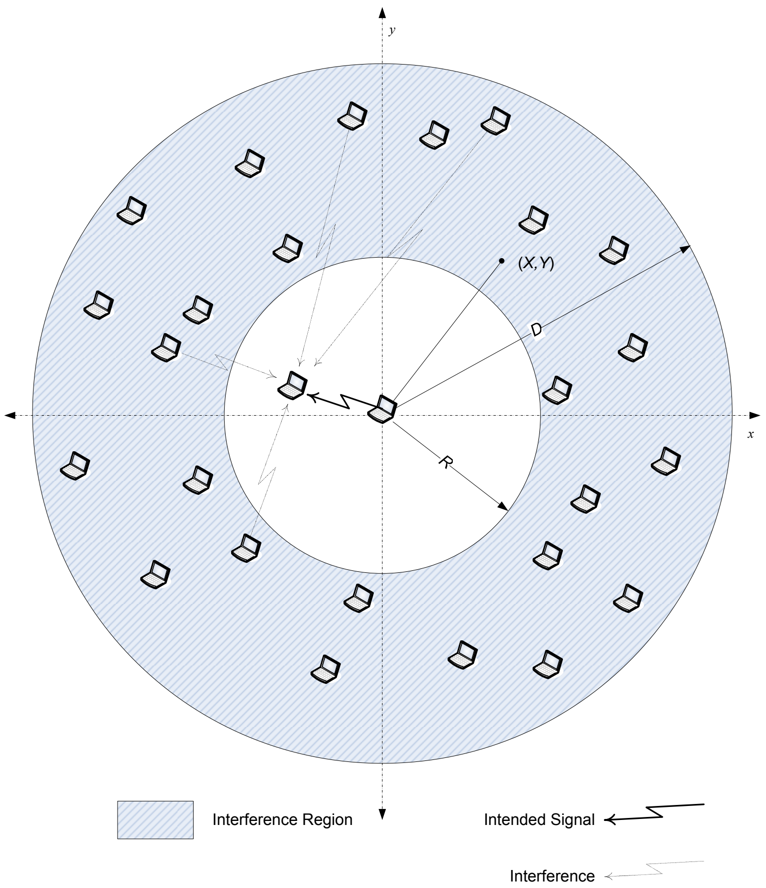

Figure 3.7: Random adhoc network model in Class 1 MAC protocol. Closest interfering node can lie at a distance of at least R from source.

as before, the expected interference can be calculated in the same way as the downlink scenario, however, the lower limit will change. Consider an asymptotically large network area ($D \to \infty$) with nodes located randomly according to a uniform distribution. Letting R represent the transmission range of the source node, the expected interference experienced by a destination at a distance r from the source can be written as

$$\mathbb{E}\left\{I_{\text{Class 1}}(r)\right\} = \phi_{\text{Class 1}} \frac{e^{\left(\frac{\sigma \ln 10}{10}\right)^2/2}}{(\xi-2)} \int_0^{2\pi} \left(R\left(1-\frac{r^2}{R^2}\cos^2\theta\right)^{\frac{1}{2}} - r\sin\theta\right)^{-\xi+2} \mathrm{d}\theta. \tag{3.32}$$

In contrast to the cellular network model considered above, due to the

MAC protocol, not all nodes in an ad-hoc network can be active simultaneously. However, the density of active (interfering) nodes under a Class 1 MAC protocol $\phi_{\text{Class 1}}$, has been studied in [57], where a simple mathematical expression relates it to the pathloss exponent and the total node density. Thus, ϕ_{Class1} can be easily calculated and plugged into eq. (3.32) to find the expected interference at a destination at any point inside the transmission range of the source.

Notice that when the destination lies on the border of the coverage area, i.e. $r = R$ in (3.32), the expected interference is infinite. This is due to a modeling irregularity when calculating the limits of integration for the interference region. The lower limit of the interference region should start at a distance $R + \epsilon$ for very small ϵ, thus avoiding this infinite interference observation. Alternatively, we can consider that $1 \leq r < R$. However, this analytically demonstrates the severity of the hidden node problem in Class 1 MAC protocols for dense ad-hoc networks. Intuitively, as the density of the network grows, it is more and more probable that an interfering node will lie closer and closer to the node on the coverage border of the source, thus causing severe interference to the destination.

3.5.2 Expected Interference for Class 3 MAC Protocols

This class of MAC protocols solves the hidden and exposed node problems. As demonstrated in Fig. 3.8, node H is not allowed to transmit, preventing excess interference to the destination, while node E is allowed to transmit as it will not cause severe interference. Examples of Class 3 MAC protocols are RBCS [62] and DBTMA [63]. Due to space limitations, we do not detail the exact workings of these protocols.

It is straightforward to see that under a Class 3 MAC protocol, the network model that arises is the same as the uplink of the cellular network studied previously (Fig. 3.2). Under previous assumptions of random node location and infinite network area, we can rewrite the expected interference in this case as,

$$\mathbb{E}\left\{I_{\text{Class 3}}\right\} = 2\pi\phi_{\text{Class 3}} e^{\left(\frac{\sigma \ln 10}{10}\right)^2/2} \frac{R^{-\xi+2}}{(\xi - 2)} \tag{3.33}$$

Again, an expression for the density of interfering nodes under a Class 3 MAC protocol ϕ_{Class3}, has been obtained in [57], thus allowing us to easily calculate the interference at the destination. Notice that the interference under a Class 3 MAC protocol is not a function of the distance between source and destination.

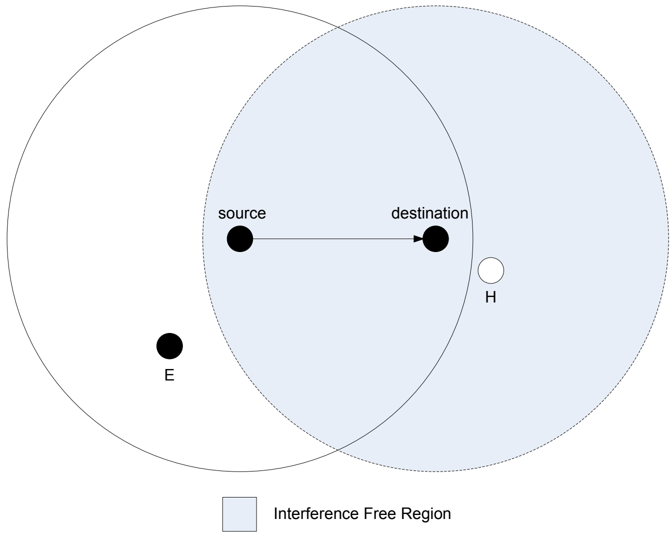

Figure 3.8: Class 3 MAC protocol solves hidden and exposed node problem. Node H cannot transmit, whereas node E is allowed to transmit.

3.6 Average vs. Instantaneous Interference

We see that through knowledge of the propagation environment, we are able to predict the average interference seen in dense multicell networks. Although some information is lost by restricting to the first order moment, we point out that this loss is acceptable from a system analysis point of view in regard of the following argument: For a large number of interferers, we have

$$\begin{aligned} I_{DL}(\mathbf{r}) &= K_{DL}\frac{1}{K_{DL}}\sum_{i=1}^{K_{DL}} G_{\mathbf{r},i}P_i \\ &\approx K_{DL}\mathbb{E}\{G_{\mathbf{r},i}P_i\} \quad \text{as } (K_{DL}\to\infty) \\ &\approx K_{DL}\mathbb{E}\{G_{\mathbf{r},i}\}\,\mathbb{E}\{P_i\} = \mathbb{E}\{I_{DL}(\mathbf{r})\} \end{aligned} \tag{3.34}$$

Rigorously speaking, the variance of I_{DL} does not decay with K_{DL}. Numerical evaluation of downlink interference however, shows the variation from cell center to cell boundary to be quite small and for the uplink, it is a constant. Based on this observation we define the concept of an *interference-ideal network* as one in which, *the total interference received at any point in the cell is independent of its location in the cell.* Though not rigorously true in practice, this model proves remarkably useful for approximating interference in large cellular networks.

Definition: A network is interference-ideal if, for any point r in the cell:

$$\sum_{i=1}^{K_{DL}} G_{r,i} P_i \approx G \sum_{i=1}^{K_{DL}} P_i.$$

The value of G can be selected as either the intercell channel gain at the cell center, $\mathbb{E}\{G_{0,i}\}$ or cell boundary, $\mathbb{E}\{G_{R,i}\}$, thus modeling best-case or worst-case performance. This model basically allows us to approximate intercell channel gain as a constant. This simple approximation can be used for multicell capacity analysis and in order to obtain distributed solutions for joint user scheduling and power allocation [64, 65, 66] as we will see in later chapters.

3.7 Asymptotic vs. Finite Network Area

In this section, we investigate for what network area the expected interference approaches that of an infinite network. We consider a cell radius $R = 200$ m. and a realistic pathloss exponent $\xi = 4$, as well as log-normal shadowing standard deviation $\sigma = 10$ dB. By varying the network radius D we plot the expected downlink interference obtained by (3.13) and compare it with that of an infinite network given by (3.12). Fig. 3.9 shows that for a network radius in the order of 10-20 times the cell radius, the asymptotic expression models well the interference in a finite network. For the uplink, a finite network radius which is more than 10 times the cell radius (Fig. 3.10) approaches the asymptotic interference given by (3.19). In practical wireless system deployments, the network to cell radius ratio is usually of a much higher order than those considered above, thus allowing us to easily employ the asymptotic expected interference expressions.

3.8 Conclusion

In this chapter, we proposed a geometric network model to study random wireless networks. We derived analytical expressions for the expected interference as a function of different network parameters and characterized its behavior as a function of the distance between transmitter and receiver. We then obtained lower bounds on the SIR, which can be used to evaluate cell capacity. We showed cell capacity to be independent of network density and to increase with the pathloss exponent. As a result we conclude that the

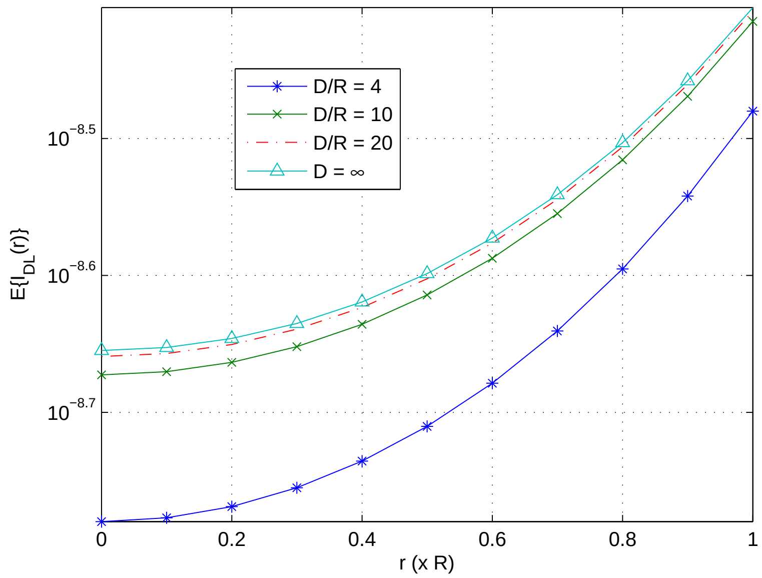

Figure 3.9: Comparison of expected downlink interference of finite network radius to an asymptotic network size. With D/R of the order 10-20, the expected downlink interference approaches the asymptotic interference.

system capacity increases with network density and pathloss exponent. The proposed model was also shown to be easily extendable to ad-hoc networks for certain classes of MAC protocols where this proves valuable in predicting expected interference. Intuition from this model allowed us to propose the interference-ideal model which proves useful for obtaining distributed solutions for multicell resource allocation problems, as we will see in the following chapters.

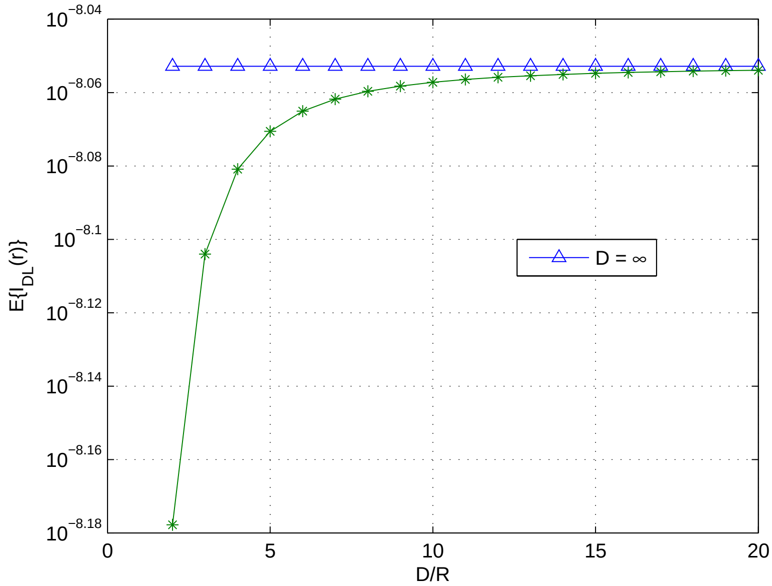

Figure 3.10: Comparison of expected uplink interference of finite network radius to an asymptotic network size. With D/R of the order 10-20, the expected downlink interference approaches the asymptotic interference.

APPENDIX

3.A Joint P.D.F of the Random Variables ρ_r and θ

We have

$$\begin{array}{rcccl} \rho_r & = & g_1(x,y) & = & \sqrt{x^2+(y-r)^2}, \\ \theta & = & g_2(x,y) & = & \tan^{-1}(\frac{y-r}{x}), \end{array}$$

where $g_1(x,y)$ and $g_2(x,y)$ are continuous and differentiable functions. The Jacobian of this transformation is given by

$$J(x,y) = \begin{vmatrix} \frac{\delta g_1}{\delta x} & \frac{\delta g_1}{\delta y} \\ \frac{\delta g_2}{\delta x} & \frac{\delta g_2}{\delta y} \end{vmatrix}$$

where

$$\begin{array}{rclrcl} \frac{\delta g_1}{\delta x} & = & \frac{x}{\sqrt{x^2+(y-r)^2}} & \frac{\delta g_1}{\delta y} & = & \frac{y-r}{\sqrt{x^2+(y-r)^2}} \\ \frac{\delta g_2}{\delta x} & = & -\frac{y-r}{x^2+(y-r)^2} & \frac{\delta g_2}{\delta y} & = & \frac{x}{x^2+(y-r)^2} \end{array}$$

We have

$$\begin{aligned} J(x,y) &= \left(\frac{x}{\sqrt{x^2+(y-r)^2}}\right)\left(\frac{x}{x^2+(y-r)^2}\right) \\ &\quad -\left(\frac{y-r}{\sqrt{x^2+(y-r)^2}}\right)\left(-\frac{y-r}{x^2+(y-r)^2}\right) \\ &= \frac{x^2+(y-r)^2}{(\sqrt{x^2+(y-r)^2})(x^2+(y-r)^2)} \\ &= \frac{1}{\rho_r} \end{aligned}$$

We can now write the joint density function of ρ_r and θ as [67]

$$\begin{aligned} f\left(\rho_r,\theta\right) &= f(x,y)|J(x,y)|^{-1} \\ &= \frac{\rho_r}{\pi D^2 - 4\pi R^2} \end{aligned}$$

3.B Limits of Integration

Using the geometry of the network (Fig. 3.3) and applying the law of sines,

$$\frac{r}{\sin\beta} = \frac{2R}{\sin(\pi/2+\theta)} \;\Rightarrow\; \sin\beta = \frac{r\cos\theta}{2R}$$

$$\frac{l}{\sin\alpha} = \frac{r}{\sin\beta}$$

$$l = \frac{r}{\sin\beta}\left[\cos\theta\cos\beta - \sin\theta\sin\beta\right] = 2R\left(1-\frac{r^2}{4R^2}\cos^2\theta\right)^{\frac{1}{2}} - r\sin\theta.$$

Along the same lines we obtain,

$$h = D\left(1-\frac{r^2}{D^2}\cos^2\theta\right)^{\frac{1}{2}} - r\sin\theta.$$

3.C C.D.F. of d_i

The cumulative distribution function of $d_i = \sqrt{X^2 + Y^2}$ is as follows: for any $R \leq a \leq D$,

$$
\begin{aligned}
F_{d_i}(a) &= P\left\{\sqrt{X^2+Y^2} \leq a\right\} \\
&= \iint_{R^2 \leq X^2+Y^2 \leq a^2} f(x,y)\mathrm{d}x\mathrm{d}y \\
&= \frac{1}{\pi D^2 - \pi R^2} \iint_{R^2 \leq X^2+Y^2 \leq a^2} \mathrm{d}x\mathrm{d}y \\
&= \frac{a^2 - R^2}{D^2 - R^2}
\end{aligned}
$$

Chapter 4

Distributed Resource-Fair User Scheduling

In this chapter, we focus on the multicell co-channel scheduling sub-problem in view of mitigating interference in a wireless data network with full spectrum reuse. The centralized joint multicell scheduling optimization problem based on the complete co-channel gain information, has so far been justly considered impractical due to complexity and real-time cell-to-cell signaling overhead. However, we expose here the following remarkable result for a large network with a standard inverse power control policy: The capacity maximizing joint multicell scheduling problem admits a simple and fully distributed solution! This result is proved analytically for an idealized network based on the interference-ideal network model presented in the previous chapter. From the constructive proof, we propose a practical algorithm that is shown to achieve near maximum capacity for realistic cases of simulated networks of even small sizes.

4.1 Introduction

High data rate requirement for future wireless broadband services directly translates into a heavy demand for expensive and precious spectral resources. It is well known that full reuse of spectrum, in any of the dimensions allowed by the multiple access scheme (time or frequency slots, codes etc.) is key to achieving much greater capacity in wireless data networks. In practice however, aggressive reuse of the spectral resource leads to an increased, sometimes unbearable level of interference throughout the network. Traditionally, interference control is performed through the use of resource management techniques which, combined with power control algorithms, allow the network to operate under a satisfactory carrier to interference level (C/I) compatible with the receiver's sensitivity at the access points (base stations) and the user terminals. This is achieved by maintaining a sufficient spatial separation of most co-channel links, based on standard path loss and fading models. In addition to inter-cell interference mitigation, recently developed dynamic resource management techniques aim at better utilization of the spectrum inside each cell by encouraging channel access for users temporarily experiencing better (than others) propagation conditions, giving rise to the so-called multi-user diversity gain [17]. Clearly multi-user diversity is gained at the expense of throughput fairness, which may be restored by modifying the scheduling criteria in one of several possible manners [18]. As stated at the beginning of this dissertation, the joint multicell user scheduling problem offers an enormous number of degrees of freedom (governed by the number of cells times the number of user times the number of possible scheduling slots) that can be potentially used to maximize the *network capacity* in an interference-limited setting.

Notably, a number of recent channel allocation schemes [68] have been proposed to mitigate co-channel interference in the particular case of fixed wireless data networks [69] with aggressive spectral reuse. *Staggered Resource Allocation* (SRA) and variants [26] exploit directional antennae, user classification and ordering of users within sub-frames to obtain gains when traffic load is low. *Time-Slot Resource Partitioning* (TSRP) [25] turns off BS sector beams according to a determined sequence, which permits users to measure the interference received and then tell their respective BS their preferred sub-frame for reception. *Power-Shaped Advanced Resource Assignment* (PSARA) [23] allows the BS to transmit with different powers in different portions of the frame and users are allotted slots according to the amount of interference tolerated. In a similar vein, base-station coordination is achieved in [28], by exchanging information between the dominant interfering set of sectors and then making transmissions orthogonal in time for these BS. Such schemes can be extended to mobile networks, at the cost of increased overhead in signaling. The authors observe capacity gains associated with interference avoidance scheduling in interference-limited networks. These clever resource planning schemes are interesting as they offer some (limited) flexibility in mitigating interference. Nevertheless, they are far from fully exploiting the degrees of freedom provided by the joint multicell scheduling problem as they do not attempt to find the optimal scheduling rule for simultaneous transmission in all co-channel cells.

Unfortunately, the study of such optimal schemes faces two great challenges. One is complexity and the other, even more problematic, is the need for the joint processing of traffic and channel gain parameters for all network users. The latter requires a central control unit, which makes global network coordination hard to realize in practice, especially in mobile settings where the scheduler ought to track fast-fading channels. These issues remain problematic despite some interesting results such as [70], where a centralized heuristic algorithm works by inserting co-channel users one by one, as long as the channel throughput increases. Or that of [27] which provides a useful theoretical quantification of inter-cell coordination in terms of user queue stability regions for various network topologies.

This chapter takes a closer look at the challenging yet interesting multicell scheduling problem in view of network capacity maximization. We consider resource-fair schedulers under backlogged traffic for all users. Specifically, the contributions of this chapter are as follows:

- We begin by formulating the capacity maximization user scheduling problem for an arbitrary (realistic) network, given knowledge of the complete multicell channel gain information for a standard power control rule (gain inversion-based power control).

- Focusing on simplification in the case of interference-ideal networks, maximum network capacity can be reached by using a low-complexity *fully distributed* scheduling policy, based on local channel gains. This result admits a theoretical constructive proof which we further exploit to propose a multicell scheduling algorithm for realistic (non-ideal) networks.

- For fast-fading, the algorithm is a generalization of the single cell maximum capacity scheduler [17] to the multicell case. As a result, per-cell throughput maximization and multicell interference avoidance are

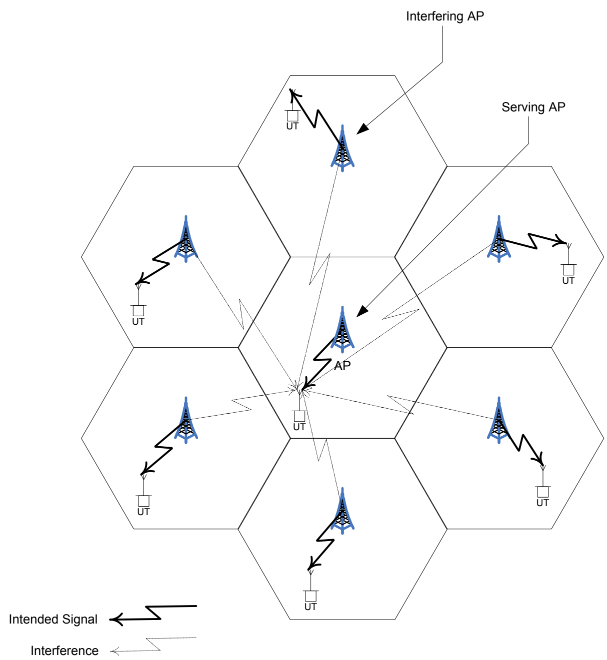

Figure 4.1: An interference limited cellular system employing full resource reuse

shown to go hand in hand and multi-user diversity scheduling can also be throughput optimal in a multicellular scenario.

- From the analysis, we derive a practical co-channel scheduling algorithm, called Power Matched Scheduling (PMS), that can trade-off resource fairness for system capacity.

These results have applications in cellular networks with interference-limited transmission. We test the algorithms over finite-size non-ideal cellular-type networks and show the throughput gains over a non-coordinated co-channel scheduler in the presence of interference.

The specific network model considered in this chapter is described in Section 4.2. The capacity maximization co-channel user scheduling sub-problem is formulated in Section 4.3. In Section 4.4, the interference-ideal network concept is employed to obtain a fully distributed optimal co-channel scheduling policy. We discuss issues related to multi-user diversity and fairness in Section 4.5. Finally, numerical results for capacity evaluation are presented in Section 4.6.

4.2 Network Model

As stated in Chapter 2, we consider a multicell system with N access points (AP) communicating with U user terminals (UT) in each cell. We are particularly interested in the downlink in which the AP sends data to the UT, but the results can be generalized to the uplink situation. The system employs the *same spectral resource* in each cell giving rise to an interference-limited system (fig. 4.1), although interference limitation is not a requirement for our approach. We also assume power control is used in the network in an effort to preserve power and limit interference and fading effects. Thus the signal model is that given in (2.1).

4.2.1 Resource Fair Partitioning

Within each cell, we consider a multiple access scheme in which an orthogonally divided resource (e.g. codes, time, frequency etc.) is used to separate the transmissions to the cell users. Each cell user is allocated a portion of the resource called a resource slot (fig. 4.2). A "frame" consists of a set of K slots. We enforce K-th order resource fairness, where $1 \leq K \leq U$. This means that a scheduling frame consists of K slots assigned to K distinct users per cell. If $K > U$, then users can be scheduled again in the same frame. Thus, this is by no means a constraint but only a simplification of exposition. Note that K-th order resource fairness does not necessarily yield throughput fairness, even with $K = U$, as users may not enjoy an equal throughput due to local channel conditions. Moreover, because of concurrent transmissions in all cells in any one slot, an assigned user "sees" interference from all co-channel cells.

4.2.2 Power Control

As is seen later, power control plays a key role in enabling the gains of network coordination. Typical power control strategies aim at adjusting the transmitter power to reduce co-channel interference experienced at the receivers. Power control policies may target a given signal-to-interference ratio (SIR) or a certain received signal power level. In [19], a distributed iterative algorithm is proposed for attaining the best possible common SIR and this is extended to an "if at all achievable" target SIR in [20]. Received signal-level based power control is studied in [58, 71] and also shown to contribute to mitigating co-channel interference although the performance of optimal interference balancing is slightly better than received signal-level

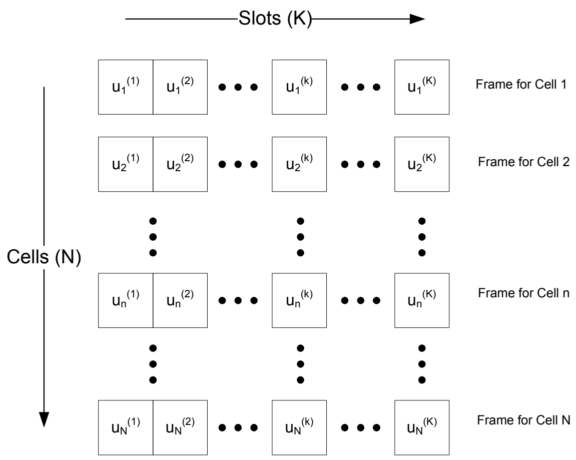

Figure 4.2: Frame structure and resource fair scheduling matrix for N co-channel cells with K orthogonal slots. User $u_n^{(k)}$ is the user scheduled in cell n during slot k. Dimension K can be sub-frequencies, orthogonal codes or time-slots.

power control [58]. Combining power control with cell diversity was subsequently shown to increase the number of supported users in the uplink [72]. For an overview on power control issues refer to [73].

The power control effect can be formulated simply in the following way: Assuming each AP has a peak transmission power constraint P_{MAX}^n, a multiplicative power control factor $0 < \rho \leq 1$ is used to adjust the transmitted power of the AP, such that we have for user u_n

$$P_{u_n} = \rho_{u_n} P_{MAX}^n$$

In what follows we assume that each AP has the same maximum power constraint P_{MAX}. Using $R_{u_n \leftarrow u_i} = G_{u_n,i} P_{u_i}$ to express the received power at user u_n (which is served by AP n) from the AP of cell i when it transmits to its user u_i, the SINR can be expressed as

$$\gamma_{u_n} = \frac{R_{u_n \leftarrow u_n}}{\eta + \sum_{i \neq n}^{N} R_{u_n \leftarrow u_i}} \tag{4.1}$$

where $R_{u_n \leftarrow u_n}$ is the received power from the *serving* AP of user u_n and η is the thermal noise power assumed the same for all users. $\sum_{i \neq n}^{N} R_{u_n \leftarrow u_i}$ is the total interference received by user u_n from other APs when they transmit to their respective scheduled users.

The value of ρ_{u_n} depends on the adopted power control policy. We assume a standard power inversion policy as this is a very common form of power control. We draw the reader's attention however to the fact that the optimal scheduling policy should ultimately be jointly optimized with the power control policy. This issue will be looked at in later chapters of this dissertation.

We define R^* as the target received power and assume that each user is able to measure and communicate back the power received from the serving AP so that the transmit power may be adjusted. The power control factor can then be obtained via:

$$\begin{aligned} G_{u_n,n}\rho_{u_n}P_{MAX} &= R^* \\ \rho_{u_n} &= \frac{R^*}{G_{u_n,n}P_{MAX}} \end{aligned}$$

But since there is a power constraint P_{MAX}, ρ is upper bounded by one:

$$\rho_{u_n} = \min\left\{\frac{R^*}{G_{u_n,n}P_{MAX}}, 1\right\} \tag{4.2}$$

Power control scenarios: Depending on the value of the R^* and the channel gain, a user will be receiving in full ($\rho = 1$) or reduced ($\rho < 1$) power mode. We consider three network scenarios. (1) *fully power controlled* (FPC) network: all users achieve R^* after power control. (2) *mixed power controlled* (MPC) network: Only a fraction of users achieve R^*. (3) *no power controlled* (NPC) network: all users use $\rho = 1$. As we will see shortly, different optimal multicell scheduling policies will arise in each network scenario.

4.3 The Co-Channel User Matching Problem

We assume that channel gains do not vary over the scheduling frame duration which is sized in accordance with the coherence period of the channel. Under the K-th order resource fairness constraint, the co-channel user matching problem consists in selecting K users in each cell and assigning these users to K slots so as to optimize the system utility function. To facilitate the formulation of the problem, we state the following definitions:

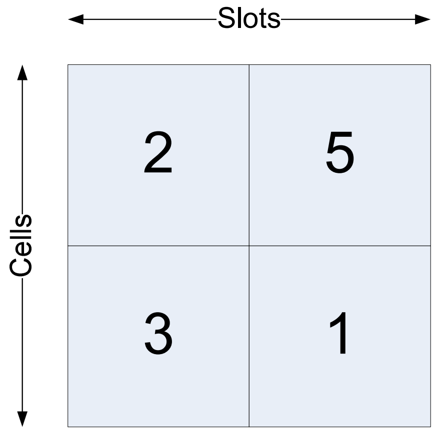

Figure 4.3: Example of Scheduling Matrix for $N = K = 2$.

Definition 4.1 *A* **scheduling policy** φ *is a bijective mapping of the subset* $\mathcal{U}_n$*, consisting of* K *users chosen from the set of all users in cell* n*, onto* $\mathcal{K}$*, the set of slots,* $\varphi_n : \mathcal{U}_n \mapsto \mathcal{K}$*.*

Definition 4.2 *A* **scheduling vector** $\mathscr{I}^{(k)}$ *contains the set of users scheduled in slot* k *across all cells (based on* φ*):*

$$\mathscr{I}^{(k)} = \left[u_1^{(k)} u_2^{(k)} \cdots u_n^{(k)} \cdots u_N^{(k)}\right]^{\mathrm{T}} \in [1, K]^N$$

where $[\mathscr{I}^{(k)}]_n = u_n^{(k)}$ *is the user scheduled during slot* k *in cell* n*.*

Note that because φ is a bijection, scheduling vectors are element-wise disjoint, $\mathscr{I}^{(a)} \bigcap \mathscr{I}^{(b)} = \varnothing \;\forall\; a \neq b$. The scheduling vector is the ensemble of users which interfere with each other and thus it determines the sum capacity for slot k.

Definition 4.3 *A* **scheduling matrix S** *is a* K*-column matrix composed of scheduling vectors given by the scheduling policy* φ*.*

$$\mathbf{S} = [\mathscr{I}^{(1)} \mathscr{I}^{(2)} \cdots \mathscr{I}^{(K)}]$$

This matrix describes the complete ordering of all users during one frame. For example, considering the scheduling matrix given in fig. 4.3, users 2 and 5 of cell 1 are scheduled with users 3 and 1 of cell 2, respectively.

4.3.1 System Performance

The SINR for users scheduled in slot k will depend on the scheduling vector $\mathscr{I}^{(k)}$. We can express the SINR during slot k in cell n as

$$\begin{aligned}\gamma(\mathscr{I}^{(k)}, n) &= \frac{R_{[\mathscr{I}^{(k)}]_n \leftarrow [\mathscr{I}^{(k)}]_n}}{\eta + \sum_{i \neq n}^{N} R_{[\mathscr{I}^{(k)}]_n \leftarrow [\mathscr{I}^{(k)}]_i}} \\ &= \frac{G_{u_n^{(k)}, n} \rho_{u_n^{(k)}} P_{MAX}}{\eta + \sum_{i \neq n}^{N} G_{u_n^{(k)}, i} \rho_{u_i^{(k)}} P_{MAX}},\end{aligned} \tag{4.3}$$

where $u_i^{(k)} = [\mathscr{I}^{(k)}]_i \; \forall \, i$ is the user scheduled during slot k in cell i. Assuming an ideal link adaptation protocol, from (2.3) the per cell capacity in slot k can be expressed in bits/sec/Hz/cell as

$$C(\mathscr{I}^{(k)}) = \frac{1}{N} \sum_{n=1}^{N} \log\Big(1 + \gamma(\mathscr{I}^{(k)}, n)\Big). \tag{4.4}$$

By averaging the per cell capacity over the total number of slots, we obtain the network capacity,

$$\begin{aligned}\mathcal{C}(\mathbf{S}) &\triangleq \frac{1}{K} \sum_{k=1}^{K} C(\mathscr{I}^{(k)}) \\ &\triangleq \frac{1}{NK} \sum_{k=1}^{K} \sum_{n=1}^{N} \log\left(1 + \frac{G_{u_n^{(k)}, n} \rho_{u_n^{(k)}} P_{MAX}}{\eta + \sum_{i \neq n}^{N} G_{u_n^{(k)}, i} \rho_{u_i^{(k)}} P_{MAX}}\right),\end{aligned} \tag{4.5}$$

which is a function of the scheduling matrix $\mathbf{S}$ and is the utility function for the multicell scheduling problem in this chapter.

4.3.2 Round Robin Scheduling

A standard approach for resource fair scheduling is round robin (RR) in which users are given slots turn by turn in each frame and thus, every possible permutation of a scheduling matrix is equiprobable. Letting $\mathbb{S}$ be the set of all scheduling matrices, the network capacity for RR will be the expectation over all scheduling matrix permutations given by

$$\mathcal{C}_{RR} \triangleq \mathbb{E}_{(\mathbf{S} \in \mathbb{S})}\Big\{\mathcal{C}(\mathbf{S})\Big\}. \tag{4.6}$$

4.3.3 Optimal Co-channel Scheduling

On the other hand, the scheduling policy for optimum network capacity (4.5) can be stated as

$$\mathbf{S}^* = \underbrace{\text{argmax}}_{\mathbf{S}\in\mathbb{S}}\{\mathcal{C}(\mathbf{S})\} \tag{4.7}$$

Notice that finding the optimal scheduling policy φ^* is equivalent to finding the optimal scheduling matrix $\mathbf{S}^*$. As $\mathbf{S}^*$ gives the optimal network capacity, we have in general:

$$\mathcal{C}(\mathbf{S}^*) \geq C_{RR},$$

where inequality will be strict in most cases, thus showing the gain of coordinated networks over uncoordinated ones.

4.3.4 Multicell Scheduling Gains vs. Power Control Scenarios

It is easy to see that some scenarios will result in no gain at all as shown below:

Lemma 4.1 For a no power control (NPC) network, the network capacity gain associated with multicell scheduling is zero.

Proof: With no power control, $\rho_{u_n} = 1 \ \forall \ u_n$, and thus all BS transmit at the same (maximum) power. Substituting this in (4.3) we obtain

$$\gamma(\mathscr{I}^{(k)}, n) = \frac{G_{u_n^{(k)},n} P_{MAX}}{\eta + \sum_{i \neq n}^{N} G_{u_n^{(k)},i} P_{MAX}}, \tag{4.8}$$

which is independent of the choice of co-channel users in other cells. It follows that the capacity will be the same no matter which users are scheduled with each other. ■

This result indicates that the gain can be intuitively expected to depend much on the degree of *variability* of channel *and* power control coefficients across the network users, as well as on the number of cells and users. We now turn to the issue of *finding* the optimal $\mathbf{S}$.

4.4 Optimum Network Capacity Scheduling

4.4.1 Exhaustive Search Approach

As $\mathbb{S}$ is a discrete finite set, clearly (4.7) is a non-linear *combinatorial optimization problem* for which, finding optimal solutions is NP-hard (Non-deterministic Polynomial-time hard).

Lemma 4.2 *For $K = U$, the cardinality of the search space for the optimization problem in $\mathbb{S}$ can be shown to be given by*

$$|\mathbb{S}| = (U!)^{N-1}. \tag{4.9}$$

Proof: The system has N frames each consisting of K slots. The problem is finding all possible permutations of size K from a set of U elements, N times. This is given by

$$\left(\frac{U!}{(U-K)!}\right)^N. \tag{4.10}$$

Notice that (4.10) gives all possible permutations of scheduling matrices including those of the same scheduling vectors ordered in different ways inside a scheduling matrix. Clearly, column-wise permutations of the same scheduling vectors give the same network capacity. By taking into account that a set of K scheduling vectors can be ordered in $K!$ ways, we obtain

$$|\mathbb{S}| = \frac{1}{K!}\left(\frac{U!}{(U-K)!}\right)^N,$$

and substituting $K = U$ gives (4.9). ■

Exhaustive search thus has factorial complexity in the number of users and exponential complexity in the number of cells. Even for a small network with $N = 7$ cells and $U = 5$ users, the complexity of this method remains prohibitive: $|\mathbb{S}| = (5!)^{7-1} \approx 2.9 \times 10^{12}$. Alternatively, *heuristic methods* offer sub-optimal solutions at reasonable computational cost and have been applied to the classical channel assignment problem [74, 75]. However, there is no guarantee on consistency and how close a heuristic solution is to the optimum [76].

Finally, another challenge of implementing the exhaustive search or greedy approaches is the need of a central control unit that collects all path gain information, processes it to find $\mathbf{S}$, then broadcasts the result to all APs within a time of much less than the coherence time of the channel. The delay and signaling overhead necessary for this approach makes it very hard to implement in practice.

We now proceed to find a *distributed* multicell scheduling algorithm instead. To this end, we employ the interference-ideal network model introduced in the previous chapter to simplify the network capacity and later used to approximate the actual capacity. The idealized network model serves as a tool to first establish our theoretical result, then construct a practical algorithm for a non-idealized (practical) setting.

4.4.2 Interference-Ideal Networks

Recall that an *interference-ideal network* is one in which *the total interference received by any cell user is independent of its location in the cell.* Though not rigorously true in practice, this model proves remarkably useful for certain large networks. Applying this to the system at hand, we have

$$\sum_{i \neq n}^{N} G_{u_n,i}\rho_{u_i}P_{MAX} = (N-1)\underbrace{\left(\frac{1}{N-1}\sum_{i \neq n}^{N} G_{u_n,i}\rho_{u_i}P_{MAX}\right)}_{\approx \mathrm{E}\left\{G_{u_n,i}\rho_{u_i}P_{MAX}\right\} \text{ (for large } N\text{)}}$$

and as inter-cell channel gains and power control factors are uncorrelated

$$\begin{aligned}\sum_{i \neq n}^{N} G_{u_n,i}\rho_{u_i}P_{MAX} &\approx (N-1)\mathrm{E}\left\{G_{u_n,i}\right\}\mathrm{E}\left\{\rho_{u_i}P_{MAX}\right\} \\ &\approx \mathrm{E}\left\{G_{u_n,i}\right\}(N-1)\frac{1}{N-1}\sum_{i \neq n}^{N}\rho_{u_i}P_{MAX} \\ &\approx \mathrm{E}\left\{G_{u_n,i}\right\}\sum_{i \neq n}^{N}\rho_{u_i}P_{MAX}. \qquad (4.11)\end{aligned}$$

We denote the expectation of the inter-cell channel gain as follows:

$$\mathrm{E}\left\{G_{u_n,i}\right\} = G(r),$$

where r is the distance of a user u_n from the cell center. Given this result we can model the best case or worst case interference by selecting $G = G(0)$ or $G(R)$. However, we will see later that the numerical value of G plays no role in the final multicell scheduling algorithm. Thus, based on the interference-ideal model we employ the following approximation

$$\sum_{i \neq n}^{N} G_{u_n,i}\rho_{u_i}P_{MAX} = G\sum_{i \neq n}^{N}\rho_{u_i}P_{MAX}, \qquad (4.12)$$

where G is a constant which does not depend on the location of u_n, but depends on pathloss and link budget parameters.

4.4.3 Optimum Scheduling in Interference-Ideal Networks

Armed with the idealized network model above, we proceed to present the main result of this chapter. We characterize the solution to the optimal network scheduling problem in an interference-ideal network and a *fully power controlled scenario*. Using (4.12) and (4.2) we can rewrite (4.3) as

$$\gamma(\mathscr{I}^{(k)}, n) = \frac{R^*}{\eta + GR^* \sum_{i \neq n}^{N} \frac{1}{G_{u_i^{(k)}, i}}} \tag{4.13}$$

The network capacity will be given by

$$\mathcal{C} = \frac{1}{NK} \sum_{k=1}^{K} \sum_{n=1}^{N} \log \left(1 + \frac{R^*}{\eta + GR^* \sum_{i \neq n}^{N} \frac{1}{G_{u_i^{(k)}, i}}} \right). \tag{4.14}$$

Next, we define a vector $\mathscr{U}_n\downarrow$, containing the K users of $\mathcal{U}_n$ ordered in descending order of intra-cell channel gains,

$$\mathscr{U}_n \downarrow = [u_{1,n} \dots u_{j,n} \dots u_{K,n}]^{\mathrm{T}}$$

where,

$$G_{u_{1,n},n} \geq \dots \geq G_{u_{j,n},n} \geq \dots \geq G_{u_{K,n},n}$$

We now present the following result:

Theorem 4.1 *Let* $\mathbf{S} \downarrow = [\mathscr{U}_1 \downarrow \dots \mathscr{U}_n \downarrow \dots \mathscr{U}_N \downarrow]^{\mathrm{T}}$*, then*

$$\mathbf{S} \downarrow = \begin{pmatrix} u_{1,1} & u_{2,1} & \dots & u_{k,1} & \dots & u_{K,1} \\ u_{1,2} & u_{2,2} & \dots & u_{k,2} & \dots & u_{K,2} \\ \vdots & \vdots & \ddots & \vdots & \ddots & \vdots \\ u_{1,n} & u_{2,n} & \dots & u_{k,n} & \dots & u_{K,n} \\ \vdots & \vdots & \ddots & \vdots & \ddots & \vdots \\ u_{1,N} & u_{2,N} & \dots & u_{k,N} & \dots & u_{K,N} \end{pmatrix} \tag{4.15}$$

Letting $\pi(\mathbf{S} \downarrow)$ *be the scheduling matrix obtained by applying any column-wise permutation on* $\mathbf{S} \downarrow$*. Then, for an interference-ideal network,* $\pi(\mathbf{S} \downarrow)$ *is an optimal scheduling matrix,* $\mathbf{S}^*$ *for the problem* (4.7)*.*

Proof: We prove the optimality of $\mathbf{S} \downarrow$ by first showing that it is valid for N cells and two slots. This is then extended to K slots.

Lemma 4.3 *For an arbitrary number of cells N and two slots, let*

$$\mathbf{S}\downarrow^{N\times 2} = \begin{pmatrix} u_{1,1} & u_{2,1} \\ u_{1,2} & u_{2,2} \\ \vdots & \vdots \\ u_{1,n} & u_{2,n} \\ \vdots & \vdots \\ u_{1,N} & u_{2,N} \end{pmatrix}$$

The optimal scheduling matrix for (4.7), $\mathbf{S}^* = \mathbf{S}\downarrow^{N\times 2}$.

Proof: We show that interchanging users in $M < N$ cells will result in either no change or a decrease in network capacity ($M = N$ will result in same capacity). Without loss of generality let these be the first M cells. We employ lighter notation by letting $G_{k,n}$ represent the channel gain between user scheduled in slot $k = 1, 2$ and it's serving AP n. Capacity before the swapping is given by

$$\begin{aligned} \mathcal{C}^* &= \sum_{n=1}^{N} \log\left(1 + \frac{R^*}{\eta + GR^*\left[\sum_{\substack{i=1\\ i\neq n}}^{M} \frac{1}{G_{1,i}} + \sum_{\substack{j=M+1\\ j\neq n}}^{N} \frac{1}{G_{1,j}}\right]}\right) \\ &+ \sum_{n=1}^{N} \log\left(1 + \frac{R^*}{\eta + GR^*\left[\sum_{\substack{i=1\\ i\neq n}}^{M} \frac{1}{G_{2,i}} + \sum_{\substack{j=M+1\\ j\neq n}}^{N} \frac{1}{G_{2,j}}\right]}\right) \end{aligned}$$

and after the swap,

$$\begin{aligned} \mathcal{C}' &= \sum_{n=1}^{N} \log\left(1 + \frac{R^*}{\eta + GR^*\left[\sum_{\substack{i=1\\ i\neq n}}^{M} \frac{1}{G_{2,i}} + \sum_{\substack{j=M+1\\ j\neq n}}^{N} \frac{1}{G_{1,j}}\right]}\right) \\ &+ \sum_{n=1}^{N} \log\left(1 + \frac{R^*}{\eta + GR^*\left[\sum_{\substack{i=1\\ i\neq n}}^{M} \frac{1}{G_{1,i}} + \sum_{\substack{j=M+1\\ j\neq n}}^{N} \frac{1}{G_{2,j}}\right]}\right). \end{aligned}$$

As $G_{1,n} \geq G_{2,n} \forall\ n$, we declare

$$\left(\beta_{1,n} = \sum_{\substack{i=1\\ i\neq n}}^{M} \frac{1}{G_{1,i}}\right) \leq \left(\beta_{2,n} = \sum_{\substack{i=1\\ i\neq n}}^{M} \frac{1}{G_{2,i}}\right)$$

$$\Big(\alpha_{1,n} = \sum_{\substack{j=M+1\\ j\neq n}}^{N} \frac{1}{G_{1,j}}\Big) \leq \Big(\alpha_{2,n} = \sum_{\substack{j=M+1\\ j\neq n}}^{N} \frac{1}{G_{2,j}}\Big)$$

Letting

$$\begin{aligned} g_n(x) \;=\; & \log\Big(1 + \frac{R^*}{\eta + GR^*(x+\beta_{1,n})}\Big) \\ & - \log\Big(1 + \frac{R^*}{\eta + GR^*(x+\beta_{2,n})}\Big) \end{aligned}$$

then we need to show

$$\mathcal{C}^* - \mathcal{C}' = \sum_{n=1}^{N} \Big(g_n(\alpha_{1,n}) - g_n(\alpha_{2,n})\Big) \geq 0 \;\forall\; \alpha_{1,n} \leq \alpha_{2,n}$$

Differentiating $g_n(x)$,

$$\begin{aligned} \frac{\mathrm{d}g_n(x)}{\mathrm{d}x} \;&=\; \frac{-R^*GR^*}{\ln(2)(1+\frac{R^*}{\eta+GR^*(x+\beta_{1,n})})(\eta+GR^*(x+\beta_{1,n}))^2} \\ &+\; \frac{R^*GR^*}{\ln(2)(1+\frac{R^*}{\eta+GR^*(x+\beta_{2,n})})(\eta+GR^*(x+\beta_{2,n}))^2} \end{aligned}$$

Letting

$$\Big(d_2 = \eta + GR^*(x+\beta_{2,n})\Big) \geq \Big(d_1 = \eta + GR^*(x+\beta_{1,n})\Big)$$

we have

$$\begin{aligned} \frac{\mathrm{d}g_n(x)}{\mathrm{d}x} \;&=\; \frac{-R^*GR^*}{\ln(2)(1+\frac{R^*}{d_1})d_1^2} + \frac{R^*GR^*}{\ln(2)(1+\frac{R^*}{d_2})d_2^2} \\ &=\; -\frac{R^*GR^*}{\ln(2)}\left(\frac{1}{d_1^2+R^*d_1} - \frac{1}{d_2^2+R^*d_2}\right) \end{aligned} \tag{4.16}$$

As $d_2 \geq d_1$, $\frac{\mathrm{d}g_n(x)}{\mathrm{d}x} \leq 0$ and $g_n(x)$ is a decreasing function. Thus $\mathcal{C}^* - \mathcal{C}' \geq 0$. This proves that $\mathbf{S}^* = \mathbf{S}\downarrow^{N\times 2}$. ∎

Next, we define an operator $\mathcal{Q}_{l,k}(\mathbf{S})$ which orders the users in columns (slots) l and k of the scheduling matrix in decreasing order of channel gain.

$$\begin{aligned} \mathcal{Q}_{l,k}(\mathbf{S}) \;=\; \Big[& \mathscr{I}^{(1)}\, \mathscr{I}^{(2)} \cdots \mathscr{I}^{(l-1)}\, \zeta(\mathscr{I}^{(l)}, \mathscr{I}^{(k)})_{:,1}\, \mathscr{I}^{(l+1)} \cdots \\ & \mathscr{I}^{(k-1)}\, \zeta(\mathscr{I}^{(l)}, \mathscr{I}^{(k)})_{:,2}\, \mathscr{I}^{(k+1)} \cdots \mathscr{I}^{(K)} \Big] \end{aligned}$$

where $\zeta(u,v) \in \mathbb{N}^{N\times 2}$ obtained through

$$\begin{aligned} \zeta(u,v)_{i,1} &= \max\left(G_{u_i,i}, G_{v_i,i}\right) \\ \zeta(u,v)_{i,2} &= \min\left(G_{u_i,i}, G_{v_i,i}\right) \end{aligned}$$

Lemma 4.4 *For an arbitrary scheduling matrix* $\mathbf{S}$, $\mathcal{C}(\mathcal{Q}_{l,k}(\mathbf{S})) \geq \mathcal{C}(\mathbf{S})$

Proof: As only columns l and k are manipulated, the capacity due to other columns remains unchanged. From Lemma 4.3, the capacity of two slots arranged in decreasing order of channel gains will be more than when they are arranged in any other fashion. Thus, $\mathcal{C}(\mathcal{Q}_{l,k}(\mathbf{S})) \geq \mathcal{C}(\mathbf{S})$. ∎

Lemma 4.5 *For an arbitrary scheduling matrix* $\mathbf{S}$

$$\mathcal{Q}_{K-1,K} \cdots \mathcal{Q}_{2,K} \cdots \mathcal{Q}_{2,3}\mathcal{Q}_{1,K} \cdots \mathcal{Q}_{1,3}(\mathcal{Q}_{1,2}(\mathbf{S})) = \mathbf{S}\downarrow$$

Proof: From Lemma 4.4, the capacity of the scheduling matrix after each $\mathcal{Q}$ operation will be greater than the previous. The successive $\frac{K(K-1)}{2}$ $\mathcal{Q}$ operations will result in the perfectly ordered matrix $\mathbf{S}\downarrow$. ∎

Since there is an increase in capacity at every step, $\mathcal{C}(\mathbf{S}\downarrow) \geq \mathcal{C}(\mathbf{S})$. This concludes the proof. ∎

Based on Theorem 4.1 an optimal scheduling policy is for each cell to rank its users by (say decreasing) order of channel gain and assign the best K users to the K available slots, regardless of the channel gains in other cells. As co-channel users are matched based on the rank of their channel gain, we call this scheduling policy *Power Matched Scheduling* (PMS). As local channel gain is the only scheduling criteria, PMS is completely distributed. Note that a side-effect of the policy is to group users with similar channel quality levels, possibly creating unfair service across resource slots.

4.5 Multi-user Diversity And Fairness

An interesting result from this study is the conclusion that scheduling based on multi-user diversity is also optimal in a multicellular scenario.

4.5.1 Multi-user Diversity

Lemma 4.6 *Throughput optimal multi-user scheduling in a single cell case is also throughput optimal in the multicell case if received signal-level power control is used.*

Proof: This can be easily seen by considering the frame size $K = 1$. Theorem 4.1 will result in the following scheduling matrix for $K = 1$

$$\mathbf{S}\downarrow^{N\times 1} = \begin{pmatrix} u_{1,1} \\ u_{1,2} \\ \vdots \\ u_{1,N} \end{pmatrix}$$

The users with the best channel gains in each cell are scheduled, which is also throughput optimal in the single cell case [17] as it maximizes the so called multi-user diversity in each and every cell. ∎

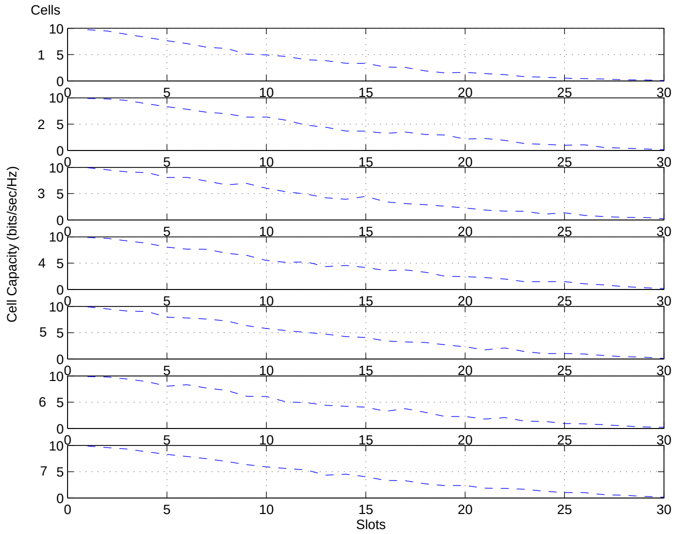

Figure 4.4: Slot capacities for N = 7 cells, each with K = 30 slots. The capacities are highest in the first slots and lowest in the last slots due to the coupled effect of lower channel gain and higher level of interference. As expected, optimal network capacity scheduling gives rise to greater lack of fairness.

4.5.2 Fairness

We have shown that the optimal multicell scheduling rule corresponds to grouping good users together and bad users together. Thus, network capacity is optimized at the expense of throughput fairness since weaker users will see their channel conditions worsened by the addition of the worst possible interference. This is demonstrated in fig. 4.4. Note that resource fairness can be guaranteed by choosing $K = U$, but not throughput fairness. The capacity maximization vs. fairness trade-off is not surprising since it gives an intuitive generalization of results derived previously for the single cell scenario [17, 47]. Notice that the value of K also has an effect on performance, where $K = 1$ gives only multi-user diversity gain without regard for fairness, while $K = U$ provides full resource fairness at the cost of capacity.

As in single cell scheduling, throughput fairness can be restored in several ways. One strategy is to use a clever admission control policy. An outage percentage can be imagined where a minimum SINR, γ_{min} is guaranteed to $(100 - \Delta)\%$ of the users. The $\Delta\%$ of the users which are not able to achieve γ_{min} can be compensated in a number of ways. One way is to increase access time for underprivileged users where slot duration is prolonged to increase throughput. In another way, these users can be put on an inter-cell orthogonal resource so that they see less interference.

Yet another way is to provide protection in dedicated slots by keeping some cells silent similar to TSRP [25], thereby improving SINR. The amount of protection can range from providing "exclusive access" to a cell user or removing cells from a slot turn by turn until the required SINR is achieved. The degree of protection will obviously depend on the degree of degradation as well as the number of users needing compensation. We point out however, that implementing these kinds of schemes will require global knowledge of the system and will result in a loss of capacity as compared to the full power matching scheduling algorithm.

4.6 Numerical Results

The performance of Power Matched Scheduling (PMS) is compared with RR in terms of network capacity based on Monte Carlo simulations under a full resource fairness constraint ($K = U$). A hexagonal cellular system functioning at 1800 MHz is considered, consisting of 1 km. radius cells with users randomly spread according to a uniform distribution. Channel gains for *both inter-cell and intra-cell* AP-UT links are based on a COST-231 path loss model [77] including log-normal shadowing plus fast-fading. Log-normal shadowing is a zero mean Gaussian distributed random variable in dB with a standard deviation of 10 dB. Fast-fading is modeled by i.i.d. random variables $h_{u_n,i} \sim \mathcal{CN}(0,1)$. R^* corresponds to an SNR target of 30 dB and $P_{MAX} = 1$W. These network settings result in a mixed power control (MPC) system which serves to test the robustness of PMS in a realistic scenario.

4.6.1 PMS vs. Optimal Scheduler

We first compare PMS with an optimal scheduler which in theory performs an exhaustive search over all possible scheduling matrices to find the optimal solution. In practice, this would amount to a centralized entity collecting information about all AP-UT links in the network in order to compute the system capacity for every scheduling matrix. For PMS, users are scheduled according to Theorem 4.1. As mentioned earlier the exhaustive search approach entails significant computational complexity and thus we consider a network with $N = 12$ and $U = 2$. Fig. 4.5 demonstrates the performance of PMS compared to that of exhaustive search where we trace the frame network capacity for both schemes. Mean network capacity is then obtained by averaging over the total number of frames. We see that the difference in performance between PMS and exhaustive search is quite small, showing that even for a modest network size, the interference-ideal model allows us to conveniently obtain a distributed scheduling solution.

4.6.2 PMS vs. Round Robin

In accordance with (4.6), round robin (RR) is modeled by selecting a random permutation of the scheduling matrix for each frame. For this comparison, we assume that there are 30 users/cell. We first show traces of network capacity obtained using RR and PMS with $N = 19$ (fig. 4.6) and we see that PMS provides substantial gain over RR. The proposed scheme is robust even for a small network size of $N = 3$ (fig. 4.7). We observe that as the number of cells increases, interference averaging reduces variation in network capacity and yields an increase in gain. The relative performance of the two scheduling policies is represented by the Network Capacity Gain τ, of PMS over RR, which is given by

$$\tau = \frac{\mathcal{C}(\mathbf{S}^*)}{\mathcal{C}_{RR}}.$$

Fig. 4.8 shows the variation of network capacity gain with the size of the network. We notice that the gain is greater in the presence of both shadowing and fast-fading leading to the conclusion that greater channel variation improves performance and mobile environments will also benefit from this scheduling policy. The PMS scheme outperforms RR in all cases and moreover, the gain increases with system size.

4.7 Conclusion

In this chapter we studied the problem of multi-user multicell scheduling for wireless networks. An optimal scheduler is proposed for asymptotically large networks. We show that large gains are obtained from inter-cell coordination thanks to the inter-cell channel gain variability which stems from power control and fading. In the optimal scheduler each cell ranks its users according to decreasing channel gains. As *local* channel gains are used the optimal scheduler can be efficiently approximated by a fully distributed multicell scheduler. The multi-cell scheduler is also consistent with maximizing the capacity of each cell independently through multi-user diversity. Simulations on a realistic network show substantial gains over uncoordinated scheduling and these gains increase with the size of the network.

From this chapter we see that power control also plays a major role in determining the achievable gain of multicell coordination. Thus, having proposed an optimal and distributed multicell user scheduling scheme, in the forthcoming chapters we will look at multicell power allocation. There we will characterize the optimal solution to the power allocation problem for interfering links and then go on to propose algorithms for joint power allocation and scheduling.

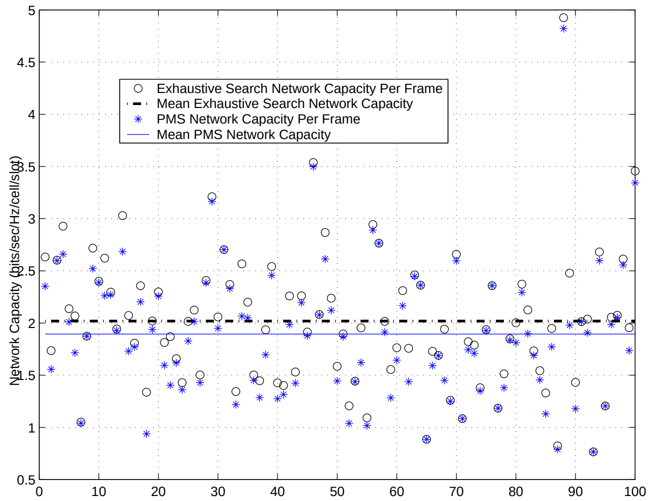

Figure 4.5: Trace of network capacity for $N = 12$ and $U = 2$ comparing Power Matched Scheduling (PMS) with the optimal scheduler based on exhaustive search. Independent channel realizations are generated on a frame by frame basis. The performance gap between PMS and the optimal scheduler is quite small.

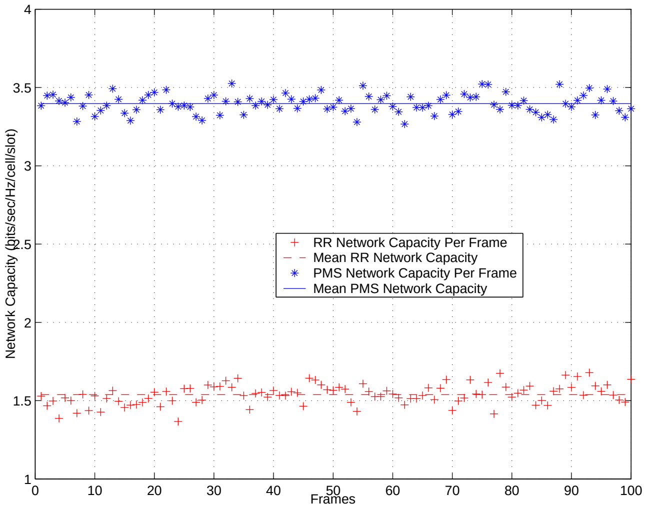

Figure 4.6: Trace of network capacity values for 19 cells and 30 users per cell. Independent channel realizations are generated on a frame by frame basis. Power Matched Scheduling (PMS) provides substantial improvement as compared to Round Robin (RR) for large network sizes

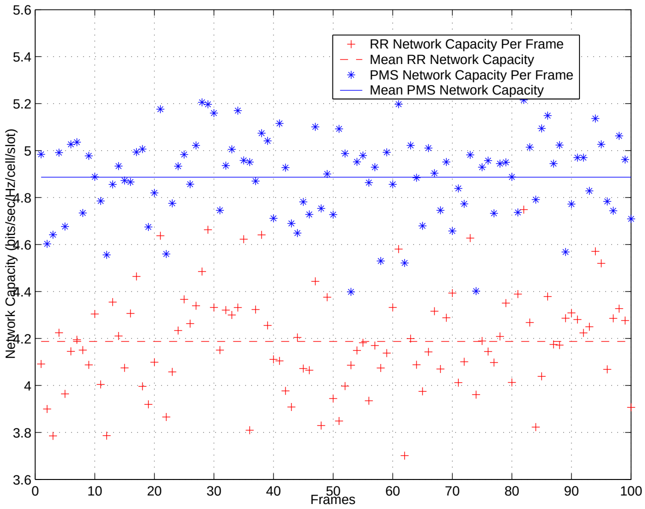

Figure 4.7: Trace of network capacity values for 3 cells and 30 users per cell. Independent channel realizations are generated on a frame by frame basis. PMS provides better multicell capacity gain than RR even for small network sizes.

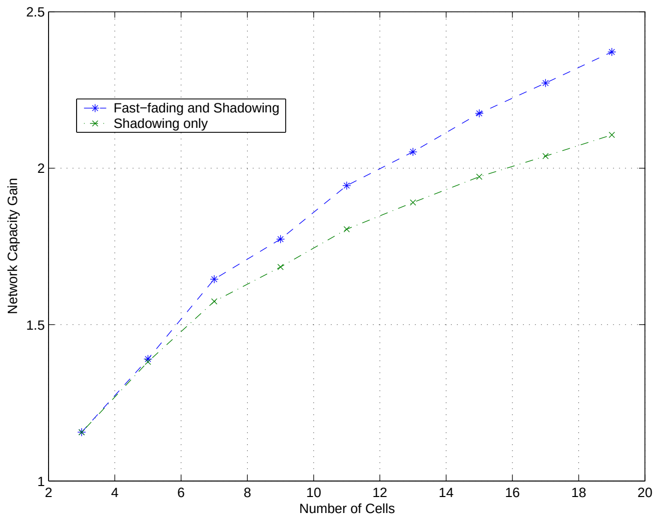

Figure 4.8: Network capacity gain versus number of cells for different propagation scenarios. Network capacity gain is the ratio given by PMS network capacity upon RR network capacity. Gain increases with system size as optimization space increases. Greater channel variation increases performance gap between the two scheduling policies thereby increasing gain.

Chapter 5

Weighted Sum-Rate Maximizing Power Allocation

Having studied user scheduling in the multicell context, in this chapter we now consider the optimal power allocation sub-problem for mutually interfering wireless links. Specifically, we focus on the maximization of the weighted sum-rate capacity, which is a more generalized version of the sum network capacity. The motivation behind considering this kind of utility is that it allows the incorporation of quality of service (QoS) criteria in the objective function. By virtue of the weights, the priority of a link can be adapted according to numerous criteria, e.g. delay-constraints, fairness, grade of service etc. Although this problem is non-convex, for two interfering links, we are able to analytically characterize the optimal solution to this problem. For the case of equal link weights, a surprisingly simple binary solution to the power allocation is obtained. These results are exploited in later chapters of this thesis where we consider practical algorithms for power allocation and scheduling.

5.1 Introduction

System level performance of future wireless data networks like WiMAX, 3G/4G etc. are adversely affected by an intolerable level of interference in case of full reuse (in any dimension e.g. time or frequency slots, codes etc.) of the spectral resource. As we have seen in previous chapters, some form of coordination between the different cells occupying the same spectral resource can offer significant improvement. Apart from scheduling, *power control* serves as a means to mitigate the effect of interference and has been an extensively researched topic for more than 30 years. In traditional voice-centric wireless networks, power control was found to be an effective method to enhance the reliability of the system. A number of approaches have been proposed to address this problem [78, 19, 58, 71, 20, 21, 73]. The key idea here is to either aim for a certain target received power at the receiver or, balance the transmit powers to achieve a minimum acceptable level of signal-to-interference-plus-noise ratio (SINR) for each user. This is to guarantee a target outage probability for the communication link, which is the measure of QoS in connection-oriented voice networks. An extension to minimizing the power while achieving predefined rates is done in [79], where a cost is introduced for transmission, resulting in solving a convex optimization problem. Power allocation in sensor networks has also been studied where the design criteria are geared towards gathering data and communicating them back to a central unit with as few errors as possible [80]. In [81], two interfering links are considered under the assumption of symmetric interference. Based on a sum power constraint over the links, the power allocation is derived as a function of the interference level. However, these assumptions are not applicable to our cellular system, where there is an individual peak power constraint at every link, and the interference is dependent on respective propagation conditions and thus cannot be the same for both links.

Moreover, we investigate power allocation in the context of future data wireless networks enabled with link adaptation protocols. Based upon underlying channel conditions, such systems are able adapt (or select) the transmit rate through adaptive modulation and coding. Moreover, due to the elastic nature of data traffic (web browsing, email, etc.), guaranteeing a strict SINR requirement is not always required. Rather, maximizing the amount of data transferred becomes a more relevant performance goal. However, having some form of QoS constraints on performance is none the less desirable for the operator, which may offer different grades of service to end users. In light of these arguments, we consider *weighted sum-rate capacity* of the system as our performance criterion and formulate the power allocation problem to maximize this metric. Specifically, this choice of objective function proves useful for adaptive resource allocation policies, where, by virtue of the weights, a link can be more or less prioritized with respect to the resources depending on QoS or fairness constraints. With the goal of maximizing this objective, in this chapter we present the following results:

- We formulate the weighted sum-rate capacity maximizing power allocation problem, and characterize the optimal solution for the case of two links.

- For the special case of equal weights, the objective function is the same as the sum network capacity and for two links, we find *binary power control* is optimal. In this case, a link transmits with either the maximum power or remains silent.

5.2 Optimal Power Allocation Problem

In this section, we formulate the optimal power allocation problem for maximizing a certain metric based on the sum of individual link capacities. We consider the same network model as that described in Chapter 2, where N transmit-receive active pairs are simultaneously communicating at a given time instant, while others remain silent (Fig. 2.1). Recall that the transmit power vector $\boldsymbol{P}$ contains transmit power values used by each transmitter to communicate with its respective receiver:

$$\boldsymbol{P} = [P_1, P_2, \ldots, P_n, \ldots, P_N],$$

where $[\boldsymbol{P}]_n = P_n$, and the feasible set of transmit power vectors is given by:

$$\Omega = \{\boldsymbol{P} \mid 0 \leq P_n \leq P_{\max} \; \forall \; n = 1, \ldots, N\}.$$

The signal to interference-plus-noise ratio (SINR) at the receiver of link n is then given by

$$\gamma_n(\boldsymbol{P}) = \frac{G_{n,n}P_n}{\eta_n + \sum\limits_{\substack{i=1 \\ i \neq n}}^{N} G_{n,i}P_i}, \tag{5.1}$$

where $G_{n,i}$ is the channel gain from the transmitter of link i to the receiver of link n. Assuming an ideal link adaptation protocol and perfect CSI at the transmitter, the rate of link n can then be expressed in bits/sec/Hz using the Shannon capacity [45] as

$$\mathcal{R}_n(\boldsymbol{P}) = \log_2\Big(1 + \gamma_n(\boldsymbol{P})\Big), \tag{5.2}$$

which is clearly dependent upon the complete transmit power vector.

5.2.1 Weighted Sum-Rate Capacity

The objective function we consider here is the weighted sum-rate capacity, defined as

$$\mathcal{C}(\boldsymbol{P}) \triangleq \sum_{n=1}^{N} w_n \mathcal{R}_n(\boldsymbol{P}). \tag{5.3}$$

Here, $w_n \geq 0$ is the weight associated with the receiver of link n. For the particular case of a cellular network, if there are U_n users in each cell n, the weights are associated with each user $u_n \in [1, \ldots, U_n]$ which may be scheduled at any given instant. This choice of objective function is of particular interest in adaptive resource allocation policies. Specifically, a resource allocation unit can prioritize users by adjusting their respective weights, so as to achieve some sort of fairness or to fulfill delay constraints. For example, traffic queue states can be observed for each user and the weights set accordingly so as to minimize the delay. Another scheme can be imagined where the weights are adjusted according to the throughput the users have already experienced so as to obtain some sort of rate fairness. Thus, this choice of objective function finds relevance in scenarios where QoS constraints may need to be met. We also point out here that sum-rate maximization is a special case of (5.3) when $w_n = 1 \ \forall \ n$. We will touch upon this special case later on in the chapter.

5.2.2 Optimal Power Allocation Problem

Taking (5.3) as the objective function we want to maximize, the optimal power allocation problem can be stated as

$$\boldsymbol{P}^* = \arg\max_{\boldsymbol{P}\in\Omega} \mathcal{C}(\boldsymbol{P}). \tag{5.4}$$

This problem is known to be non-convex [48], and an optimal solution would require an exhaustive search over the feasible set of transmit powers which entails high complexity as well as centralized processing.

However, by considering $N = 2$, i.e., just two links, we hope to gain some more insight into the problem at hand. Thus, in the next section, we investigate the optimal solution to the weighted sum-rate maximization power allocation problem for two interfering links.

5.3 Optimal Power Allocation for $N = 2$

For two links, problem (5.4) can be written as

$$\boldsymbol{P}^* = \arg\max_{\boldsymbol{P}\in\Omega} \left(w_1 \mathcal{R}_1(\boldsymbol{P}) + w_2 \mathcal{R}_2(\boldsymbol{P})\right), \tag{5.5}$$

We will now characterize the optimal solution to the power allocation problem for weighted sum-rate maximization. We first present the following lemma:

Lemma 5.1 *The optimal solution to the weighted sum-rate maximizing power allocation problem (5.4), has at least one link operating at $P_{\max}$.*

Proof: Along the same lines as in Lemma 1 of [82], consider for $\epsilon > 1$ and $\boldsymbol{P} \in \Omega$,

$$\mathcal{C}(\epsilon\boldsymbol{P}) = \sum_{n=1}^{N} w_n \log_2\left(1 + \frac{G_{n,n}P_n}{\dfrac{\eta_n}{\epsilon} + \sum\limits_{\substack{i=1\\ i\neq n}}^{N} G_{n,i}P_i}\right) > \mathcal{C}(\boldsymbol{P}).$$

Increasing the value of ϵ increases the weighted sum-rate, until at least one of the powers hits $P_{\max}$. ■

Letting

$$J(P_1, P_2) = w_1 \log_2(1 + \frac{G_{1,1}P_1}{\eta_1 + G_{1,2}P_2}) + w_2 \log_2(1 + \frac{G_{2,2}P_2}{\eta_2 + G_{2,1}P_1}),$$

through Lemma 5.1 we may let one of the links operate at maximum power by setting $P_2 = P_{\max}$. Our task is then reduced to finding the optimal P_1. The derivative of $J(P_1, P_{\max})$ w.r.t P_1 can be expressed as

$$\frac{\partial J(P_1, P_{\max})}{\partial P_1} = \frac{aP_1^2 + bP_1 + c}{f(P_1)},$$

where

$$\begin{aligned}
a &= w_1 G_{1,1} G_{2,1}^2, \\
b &= 2w_1 G_{1,1} \eta_2 G_{2,1} + G_{1,1} G_{2,1} G_{2,2} P_{\max}(w_1 - w_2), \\
c &= w_1 G_{1,1} \eta_2^2 + w_1 G_{1,1} \eta_2 P_{\max} G_{2,2} - w_2 P_{\max} G_{2,2} G_{2,1} \eta_1 \\
&\quad - w_2 P_{\max}^2 G_{2,2} G_{2,1} G_{1,2}, \\
f(P_1) &= (\eta_2 + P_1 G_{2,1} + P_{\max} G_{2,2})(\eta_2 + P_1 G_{2,1})(\eta_1 + P_{\max} G_{1,2} + P_1 G_{1,1}).
\end{aligned}$$

We see that $f(P_1)$ is always positive, and in order to find P_1 such that $\frac{\partial J(P_1, P_{\max})}{\partial P_1} = 0$, we need to solve $aP_1^2 + bP_1 + c = 0$.

Note that when $w_1 = w_2$, i.e. the links are symmetric, $a, b > 0$ and this results in the scenario already treated in [82, 83]. In this case the optimal power allocation is for a link to be either on or off. We term this *binary power control.*

Lemma 5.2 *The optimal sum-rate capacity maximizing power allocation for 2 interfering links, i.e.*

$$\boldsymbol{P}^* = \arg\max_{\boldsymbol{P}\in\Omega} \sum_{n=1}^{2} \mathcal{R}_n(\boldsymbol{P}),$$

lies in the binary feasible set

$$\Omega^B = \{\boldsymbol{P} \mid P_n = 0 \text{ or } P_n = P_{\max}]\}. \tag{5.6}$$

Proof: For $a, b > 0$ and $P_1 \in [0, P_{\max}]$, the quadratic equation has either no root, or one root where it changes sign from - to +. The maximum will thus be attained at the boundaries, either 0 or $P_{\max}$. Due to symmetry (as $w_1 = w_2$) the same holds for P_2. See [82, 84, 83]. ■

When $w_1 > w_2$, the links are no longer symmetric. In this case $a, b > 0$, and P_1 is either 0 or $P_{\max}$ if P_2 is set to $P_{\max}$. However, when $w_1 < w_2$, b may no longer be positive and thus the potential non-binary solution may also be possible as well:

$$P_1' = \frac{-b \pm \sqrt{b^2 - 4ac}}{2a}$$

For P_2, a similar analysis can be carried out to see that when $w_1 > w_2$, we need to check P_2', obtained similar to P_1' by simply inverting the indices of a, b, and c. Only positive real solutions which satisfy the power constraint need to be considered. This leads us to state the following theorem:

Theorem 5.1 *The optimal power allocation for weighted sum-rate capacity maximization of 2 interfering links is given as*

$$(P_1^*, P_2^*) = \begin{cases} \arg\max_{(P_1,P_2)\in\Omega^B} J(P_1,P_2) & w_1 = w_2 \\ \arg\max_{(P_1,P_2)\in\{\Omega^B\cup(P_{\max},P_2')\}} J(P_1,P_2) & w_1 > w_2 \\ \arg\max_{(P_1,P_2)\in\{\Omega^B\cup(P_1',P_{\max})\}} J(P_1,P_2) & w_1 < w_2 \end{cases} \tag{5.7}$$

As an example, consider the weights $w_1 = 0.1369$, $w_2 = 0.4544$, and the following channel gain matrix

$$\mathbf{G} = \begin{pmatrix} 0.9611 & 0.2004 \\ 0.0940 & 0.5219 \end{pmatrix}.$$

We take the maximum power to be 1 and assume from here on that the noise powers are the same for all links, i.e. $\eta_1 = \eta_2 = \eta = 0.1$. By employing the conditions in (5.7), allocating the power $(P_1^*, P_2^*) = (0.1203, 1)$ yields a weighted sum-rate of $\mathcal{C}(P_1^*, P_2^*) = 1.2040$, which is slightly better than $\mathcal{C}(P_1, P_2) = 1.1981$, obtained by the best binary allocation, here $(P_1, P_2) = (0, 1)$. We also show the effect of varying the weights on the optimal power allocation in Fig. 5.1. Here we keep $w_2 = 0.4544$ and take $w_1 = \alpha w_2$, where α is varied from 0 to 1. We observe that for certain values of weights, intermediate power values (other than 0 or $P_{\max}$) are indeed optimal for weighted sum-rate maximization, which is in contrast to the equal weights (or no weights) case where binary power allocation is optimal. However, we also compare the weighted sum-rate obtained by searching over the optimal power allocation set (5.7), to searching over only the binary power allocation given by (5.6). Interestingly, Fig. 5.2 shows that although binary power allocation is not optimal, the difference between the two in terms of weighted sum-rate is quite small.

5.3.1 Binary Power Allocation for $N > 2$

For the case of when there are more than two links, it has been shown that binary power allocation is not optimal [83]. However, by considering approximations of the capacity term, or the high and low SINR regimes, binary power control is found to be capacity optimal. Interestingly, by using a geometric programming (GP) approach for power control and comparing that with the simple binary power allocation, a negligible difference in capacity is found [83]. We will take advantage of this observation in the chapters that follow, where we propose distributed algorithms for power allocation and user scheduling based on binary power control.

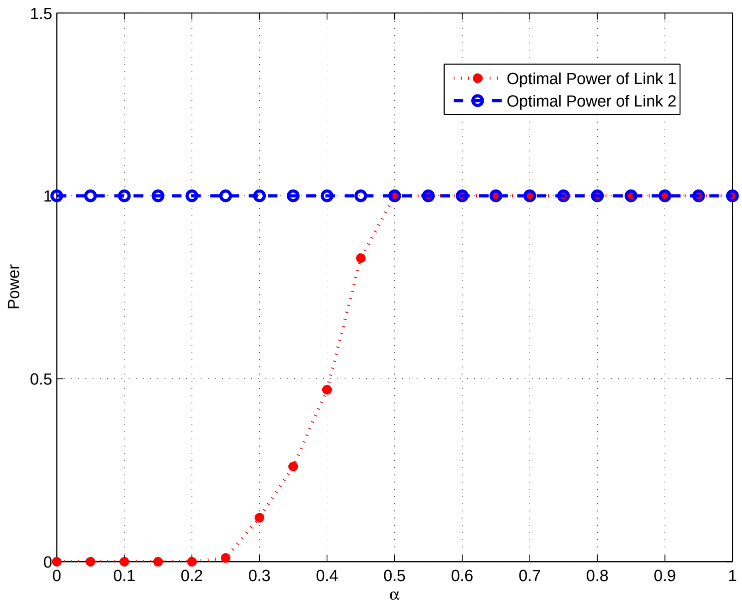

Figure 5.1: Variation of transmit powers with changing weights for 2 interfering links. Channel gains are taken as $G_{1,1} = 0.9611$, $G_{1,2} = 0.2004$, $G_{2,2} = 0.5219$, $G_{2,1} = 0.0940$ and noise power is considered to be $\eta_1 = \eta_2 = 0.1$. Weight of link 2 is set as $w_2 = 0.4544$ and $w_1 = \alpha w_2$, where α is varied from 0 to 1.

5.4 Conclusions

In this chapter, we formulated the weighted sum-rate maximizing power allocation problem for mutually interfering links which is a generalization of sum-rate maximization. For the case of two links, we analytically characterized the optimal solution set to this problem. Moreover, for the case of equal link weights, we obtained a surprisingly simple result: the optimal power allocation is binary. Obtaining the optimal solution however requires centralized processing of the link state information and link weights. This is hard to realize in practice, as feeding back and processing all network information presents significant signaling and computational overhead. In the following chapters, we focus on distributed solutions to the joint power allocation and user scheduling problem, thus making the promised gains realizable in practice.

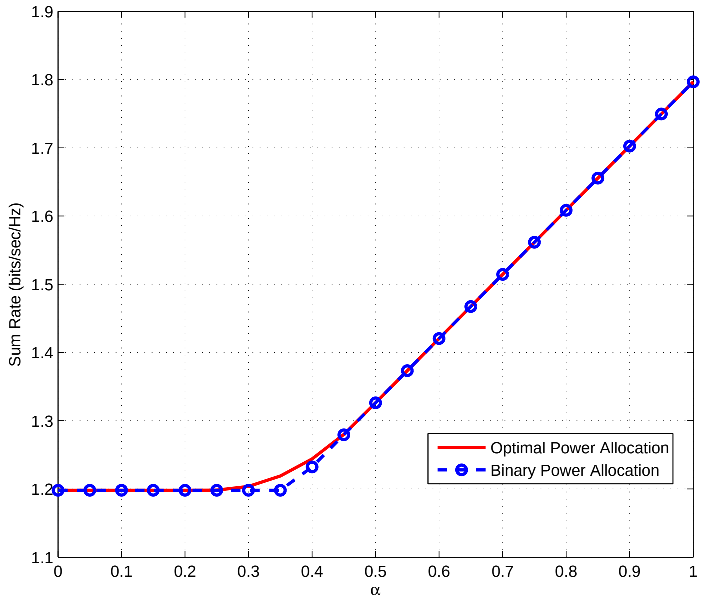

Figure 5.2: Variation of weighted sum-rate with changing weights for 2 interfering links. By searching over the optimal power allocation set a very small gain is obtained as compared to just searching over binary power allocation.

Chapter 6

Joint Power Allocation and Scheduling

In this chapter, we consider the joint optimization of transmit power and user scheduling in wireless data networks. Although it promises significant system-wide capacity gains, this problem is known to be non-convex and thus difficult to tackle in practice. We analyze this problem for the downlink of a large multicell full reuse network with the goal of maximizing the overall network capacity. Based on the centralized optimal power allocation studied in the previous chapter, we propose a distributed power allocation and scheduling algorithm which provides significant capacity gain for any finite number of users. This distributed cell coordination scheme, in effect, achieves a form of dynamic spectral reuse, whereby the amount of reuse varies as a function of the underlying channel conditions and only limited, or no inter-cell signaling is required.

6.1 Introduction

As we have seen in previous chapters, optimal resource allocation requires complete information about the network in order to decide which users in which cells should transmit simultaneously with a given power, while incurring the least loss of capacity due to inter-cell interference. Some interesting results exist exploiting inter-cell coordination with goals such as maximizing system throughput [85, 70, 34, 35], achieving a target carrier-to-interference ratio [23] or maintaining user queue stabilities [27]. All of these results however, rely on some form of centralized control to obtain gains at various layers of the communication stack.

In a realistic network however, centralized multicell coordination is hard to realize in practice, especially in fast-fading environments. Thus, in this chapter we address the problem of *distributed inter-cell coordination* to maximize the sum network capacity. Distributed coordination signifies the fact that the cells take independent decisions based on knowledge of their local conditions. As such they have information on the channel state information (CSI) of their own users, but no information about channel conditions of other cell users. Based on this knowledge constraint, each cell needs to decide which user to schedule and to transmit with how much power.

By employing the interference-ideal model and binary power allocation, we propose a distributed algorithm which allows a subset of the total number of cells to transmit simultaneously during a given scheduling period. The key idea behind this algorithm is to *switch off transmission in cells which do not contribute enough capacity to outweigh the interference degradation caused by them to the rest of the network*. Though other cells stay silent, they may be active during the next scheduling period or on an alternate resource slot. This approach can be considered as a distributed mechanism for *dynamic spectral reuse*. In contrast with traditional cellular networks, the reuse pattern obtained with this method is random, possibly highly irregular (Fig. 6.1) and varies from one scheduling period to the next as a function of the channel state information of the cell users. We show that the proposed power allocation and scheduling algorithm thus offers two types of gain:

- a dynamic spectral reuse gain thanks to the reduction of interference.
- a multi-user diversity gain through scheduling within each cell.

6.2 Joint Power Allocation and User Scheduling

Having looked at both power allocation and user scheduling individually, we now consider the joint allocation of transmit power and scheduling. For simplicity, we will consider each link has equal weight and thus the sum network capacity will be our utility function. We will exploit binary power control and the interference-ideal model introduced in the beginning of this thesis to obtain a completely distributed algorithm for this purpose.

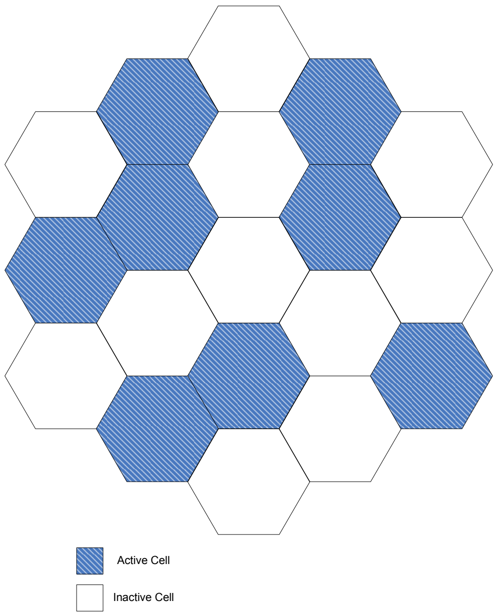

Figure 6.1: Possible irregular reuse pattern at a given scheduling period due to dynamic spectral reuse.

Here we recapitulate that the joint power allocation and scheduling problem consists of finding the power allocation vector $\boldsymbol{P}$ and scheduling vector $\boldsymbol{U}$ that will maximize the sum network capacity:

$$(\boldsymbol{U}^*, \boldsymbol{P}^*) = \arg\max_{\substack{\boldsymbol{U}\in\Upsilon \\ \boldsymbol{P}\in\Omega}} \frac{1}{N}\sum_{n=1}^{N} \log_2 \Big(1 + \gamma([\boldsymbol{U}]_n, \boldsymbol{P})\Big). \tag{6.1}$$

where

$$\gamma([\boldsymbol{U}]_n, \boldsymbol{P}) = \frac{G_{u_n,n}P_{u_n}}{\eta + \sum_{i\neq n}^{N} G_{u_n,i}P_{u_i}}.$$

6.2.1 Distributed Power Allocation and Scheduling

A straightforward approach to problem (2.4) would be an exhaustive search over the sets Υ and Ω to find $\mathcal{C}^*$. But clearly, this approach entails a significant computational cost as well as feedback overhead. Moreover, due to the dependency of the capacity equation on global network knowledge, centralized processing would be required. We thus proceed to obtain a computationally simple and distributed, though sub-optimal, algorithm instead.

Distributed Iterative Approach in the Interference Limited Regime

Let $\mathscr{N}$ be the set of indices of all presently active cells. A cell should be deactivated if this action results in an increase in network capacity. Denoting the cell which is to be potentially turned off by m, the network capacities with and without cell m turned off are respectively given by the R.H.S. and the L.H.S. of

$$\sum_{n\in\mathscr{N}} \log_2\left(1+\frac{G_{n,n}P_n}{\eta+\sum\limits_{\substack{i\neq n\\ i\in\mathscr{N}}} G_{n,i}P_i}\right) < \sum_{\substack{n\in\mathscr{N}\\ n\neq m}} \log_2\left(1+\frac{G_{n,n}P_n}{\eta+\sum\limits_{\substack{i\neq n,m\\ i\in\mathscr{N}}} G_{n,i}P_i}\right), \tag{6.2}$$

and after simple manipulations

$$\left(1+\frac{G_{m,m}P_m}{\eta+\sum\limits_{\substack{i\neq m\\ i\in\mathscr{N}}} G_{m,i}P_i}\right)\prod_{\substack{n\in\mathscr{N}\\ n\neq m}}\left(1+\frac{G_{n,n}P_n}{\eta+\sum\limits_{\substack{i\neq n\\ i\in\mathscr{N}}} G_{n,i}P_i}\right) < \prod_{\substack{n\in\mathscr{N}\\ n\neq m}}\left(1+\frac{G_{n,n}P_n}{\eta+\sum\limits_{\substack{i\neq n,m\\ i\in\mathscr{N}}} G_{n,i}P_i}\right). \tag{6.3}$$

Assuming high SINR regime in all "on" cells, and an interference-limited system, we can simplify the condition (6.3) as

$$\frac{G_{m,m}P_m}{\sum\limits_{\substack{i\neq m\\ i\in\mathscr{N}}} G_{m,i}P_i} < \frac{\prod\limits_{\substack{n\in\mathscr{N}\\ n\neq m}}\sum\limits_{\substack{i\neq n\\ i\in\mathscr{N}}} G_{n,i}P_i}{\prod\limits_{\substack{n\in\mathscr{N}\\ n\neq m}}\sum\limits_{\substack{i\neq n,m\\ i\in\mathscr{N}}} G_{n,i}P_i} \tag{6.4}$$

Evaluating (6.4) still requires global channel state knowledge as well as searching over the sets Υ and Ω. We therefore exploit the following results which will allow us to further simplify the problem in the case of large network size (N).

Interference Modeling: In order to obtain a distributed algorithm dependent only on locally available information, we use the *interference-ideal* model proposed earlier in this thesis. This allows us to simplify modeling of the interference in large full-reuse networks by stating that the total interference at a receiver is only weakly dependent on its position in the cell when there are a large number of interferers, i.e. a dense network. This can be formalized as

$$\sum_{i\neq n}^{N} G_{u_n,i}P_i \approx G\sum_{i\neq n}^{N} P_i$$

where G is a constant which does not depend on the location of u_n, but depends on pathloss and link budget parameters. One of the key ideas in our approach is that G (average interference gain) need *not* be estimated.

Binary Power Allocation The results of the previous chapter showed that the optimal power allocation for 2 interfering link for any scheduling vector, lies in the binary feasible set

$$\Omega^B = \{\boldsymbol{P} \mid P_{u_n} = 0 \text{ or } P_{u_n} = P_{\max}]\}.$$

Moreover, numerical results suggest that with a greater number of cells this binary allocation, although not strictly globally capacity-optimal in the Shannon sense, results in negligible capacity loss compared to a Geometric Programming optimization approach [85, 83]. As the binary feasible significantly reduces the power allocation search space, this motivates restricting the search for power levels to Ω^B also for an arbitrary number of cells.

Armed with these results and simplifications we now proceed to obtain a distributed algorithm. Using the interference-ideal model on the R.H.S. of (6.4), for cell m to be deactivated (all other cells being static) we require

$$\frac{G_{m,m}P_m}{\sum\limits_{\substack{i\neq m\\ i\in\mathcal{N}}} G_{m,i}P_i} < \frac{\prod\limits_{\substack{n\in\mathcal{N}\\ n\neq m}} G \sum\limits_{\substack{i\neq n\\ i\in\mathcal{N}}} P_i}{\prod\limits_{\substack{n\in\mathcal{N}\\ n\neq m}} G \sum\limits_{\substack{i\neq n\neq m\\ i\in\mathcal{N}}} P_i}.$$

As all "on" cells transmit with $P_{\max}$ and denoting $|\mathcal{N}| = \tilde{N}$, cell m will be active if

$$\frac{G_{m,m}}{\sum\limits_{\substack{i\neq m\\ i\in\mathcal{N}}} G_{m,i}} > \left(\frac{\tilde{N}-1}{\tilde{N}-2}\right)^{(\tilde{N}-1)}. \tag{6.5a}$$

Evaluating this condition requires knowledge of the number of active cells, which can be easily determined by measuring the number of received pilot signals. Additionally, we see that as the size of the network increases,

$$\lim_{N\to\infty} \left(\frac{\tilde{N}-1}{\tilde{N}-2}\right)^{(\tilde{N}-1)} = e.$$

Thus, for a large network size, a cell m will be active if the signal-to-interference ratio of the scheduled user is more than e,

$$\mathrm{SIR}([\boldsymbol{U}]_m) = \frac{G_{m,m}}{\sum\limits_{\substack{i\neq m\\ i\in\mathcal{N}}} G_{m,i}} > e. \tag{6.5b}$$

Notice that evaluating (6.5b) requires knowledge of only the cell user SIR, which can be measured during a training phase and communicated back to the AP. We thus obtain a surprisingly simple, yet powerful condition allowing an AP to determine in a distributed manner, whether it should be active or inactive. Moreover, for each cell to fulfill the condition (6.5b) and thus contribute to the system capacity, the user with the best SINR for a given power allocation should be scheduled. Depending on the size of the network either (6.5a) or (6.5b) could be used. In what follows, we use (6.5b) as the activity condition in order to demonstrate its robustness for realistic network sizes.

Distributed Algorithm: An iterative approach is adopted to obtain a fully distributed algorithm for power allocation and user scheduling. Starting with a full power allocation vector, each cell simultaneously selects the user with the best SINR and based on (6.5b) remains active or inactive during the next iteration. Similarly, at every iteration, inequality (6.5b) is evaluated for the user with the best SINR based on the power allocation resulting from the previous iteration, and the power allocation is updated. The algorithm is run until the cell capacity stabilizes or for a given number of iterations. The pseudo-code for this approach is given in Algorithm 1.

Algorithm 1 A Distributed Iterative Power Allocation and Scheduling Algorithm

$[\boldsymbol{P}^{(1)}]_n = P_{\max} \; \forall \; n$
for $t = 1 : IT_{\max}$ **do**
  $[\boldsymbol{U}^{(t)}]_n = \arg\max_{u_n} \gamma(u_n, \boldsymbol{P}^{(t)})$
  if $\gamma([\boldsymbol{U}^{(t)}]_n, \boldsymbol{P}^{(t)}) > e$ **then**
    $[\boldsymbol{P}^{(t+1)}]_n = P_{\max}$
  else
    $[\boldsymbol{P}^{(t+1)}]_n = 0$
  end if
end for

Extension to Multicell OFDMA Networks

With the same goal of sum network capacity maximization, the proposed algorithm can be extended to multicell multi-carrier systems. Consider a full reuse multicell OFDMA network in which the available frequency band is divided into a number of intra-cell orthogonal sub-carriers. The advantage of OFDMA lies in frequency-selective channels where a user experiencing fading on one sub-carrier, can be scheduled on another where it sees a better channel. For OFDMA, the proposed algorithm is simply run independently over all sub-carriers in parallel. In this case, the algorithm will jointly schedule the user and power for *each sub-carrier* in the same way as described in the single-carrier case. If a cell cannot schedule a user which contributes enough capacity to the system to outweigh the interference produced, it will remain silent on that specific sub-carrier. As we focus on

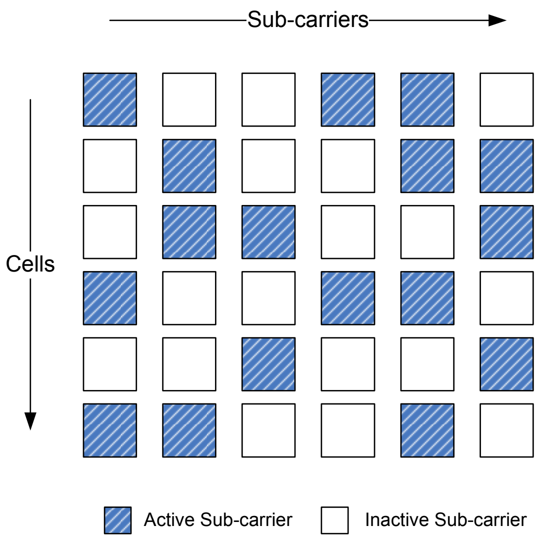

Figure 6.2: Snapshot of a full reuse multicell OFDMA network. Possible sub-carrier reuse pattern at a given scheduling period due to dynamic sub-carrier allocation.

system capacity maximization, no user to sub-carrier allocation fairness constraint is imposed, and at a given scheduling instant a user may be allocated a number of sub-carriers or none at all. The result of this algorithm on OFDMA systems is illustrated in Fig. 6.2, where we show a possible sub-carrier reuse pattern. Note however, that a sum power constraint can be considered over the sub-carriers and as such power allocation may also be performed *across sub-carriers* to take into account frequency selective fading. This adds a new dimension to the power allocation problem and is left as future work.

Fairness Issues

As we focus on capacity maximization schemes, it is expected that fairness issues will arise with regard to some cells that might experience long periods of silence due to prolonged detrimental fading conditions or a poor user distribution. However, we draw the reader's attention to the fact that solutions akin to the single-cell scheduling scenario, giving various levels of fairness-capacity trade-off, can be used also in the multicell context, e.g. use of proportional-fair type measures [47]. Hence, we may alternatively use a capacity measure for each cell that is normalized by the throughput of the cell. Moreover, when multiple orthogonal units are employed, a cell that is inactive for one code, frequency, or time slot may be active on another. Investigations of the fairness-capacity trade-off are however, left for future work.

Table 6.1: Simulation Parameters

Parameter	Value
Hexagonal Cell Radius	200 m
Square Cell Side	500 m
Operating Frequency	1800 MHz
System Bandwidth	5 MHz
σ_X	10 dB
Transmit antenna gain	16 dB
Receive antenna gain	6 dB
$P_{\max}$	1 Watt

6.3 Numerical Results

In this section, we present performance results of the distributed algorithm based on Monte-Carlo simulations. Two system layouts are considered: a hexagonal cellular system with 19 cells and a square grid with 100 cells. Gains for *all inter-cell and intra-cell* AP-UT channels are based on a path loss model including log-normal shadowing plus fast fading. Distance-based pathloss is obtained through the COST-231 model [77] and includes antenna gains as well. Log-normal shadowing is a zero mean Gaussian distributed random variable in dB with a standard deviation of σ_XdB. Fast fading is i.i.d. with distribution $\mathcal{CN}(0,1)$. All simulation parameters are detailed in Table 6.1. We compare the distributed approach with full reuse, as well as with traditional fixed reuse patterns under a max-SINR scheduling policy i.e. the user with the best SINR is scheduled.

6.3.1 Comparison with Exhaustive Search

We first compare the distributed algorithm with an exhaustive search approach. The exhaustive search algorithm considers all possible combinations of binary power allocation vectors $\boldsymbol{P} \in \Omega^B$, and schedules the user with the maximum SINR based on the chosen $\boldsymbol{P}$. This will thus serve as an optimal solution for problem (2.4) if $\boldsymbol{P}$ is restricted to Ω^B instead of Ω, and will demonstrate just how much gain may be exploited through joint power allocation and scheduling. We consider for this case only a 7 cell hexagonal network, as Monte-Carlo simulations of the exhaustive search approach prove cumbersome even for a small network (e.g. if $N = 7$ and $U = 8$, then the number of combinations are $(2^N - 1)(U^N) = 1.27 \times 10^9$). For one user there is no multiuser diversity gain and the distributed algorithm is able to exploit approximately 50% of the available dynamic spectral reuse gain (Fig. 6.3). As the number of users increases, all the algorithms converge as full reuse becomes optimal. This is due to the fact that as the number of users increases, the chance of a cell finding a user which has high direct channel gain and is sufficiently shielded from interference increases [86]. Thus, more and more cells will be active with full power. Notice also in Fig. 6.4 that with exhaustive search fewer cells are active

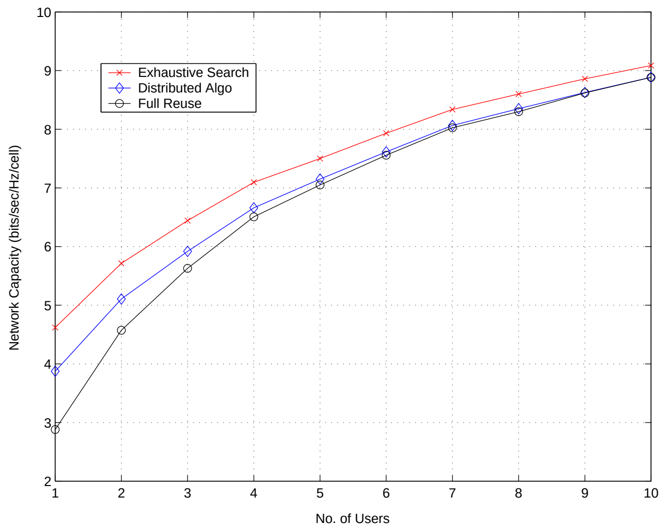

Figure 6.3: Network capacity vs. number of users for hexagonal cellular system with 7 cells. Distributed approach lies between the optimal exhaustive search approach and full reuse. Convergence to full reuse occurs as the number of users increases.

than with the distributed algorithm.

6.3.2 Comparison with Static Schemes

We next compare the distributed algorithm against fixed reuse pattern schemes. In order to ensure a fair comparison, the fixed reuse schemes also select users based on the maximum SINR rule, like full reuse and the distributed algorithm. For the hexagonal cell system the algorithms are compared with fixed reuse of cluster size 3 and 4 (Fig. 6.5). The variation of network capacity with the number of users is shown in Fig. 6.6. As the number of users increase, capacity for all schemes improves due to the multi-user diversity gain. Full reuse and the distributed algorithm both outperform fixed reuse, clearly due to both having greater reuse than fixed schemes. Moreover, as the number of users increases both full reuse and the distributed algorithm converge, due to the maximum SINR scheduling rule and the fact that it is always best to keep all cells on. Figure 6.7 demonstrates this by showing that even for as few as 10 users, more than 95% of the cells are active. This reinforces the conjecture that for a network with many users, binary power allocation and maximum SINR scheduling are optimal. The results for just one user are of particular interest. In this case there is no multiuser diversity gain, and therefore this demonstrates the performance of only power allocation for a round robin type of scheduling policy. The gain of the distributed approach over full reuse

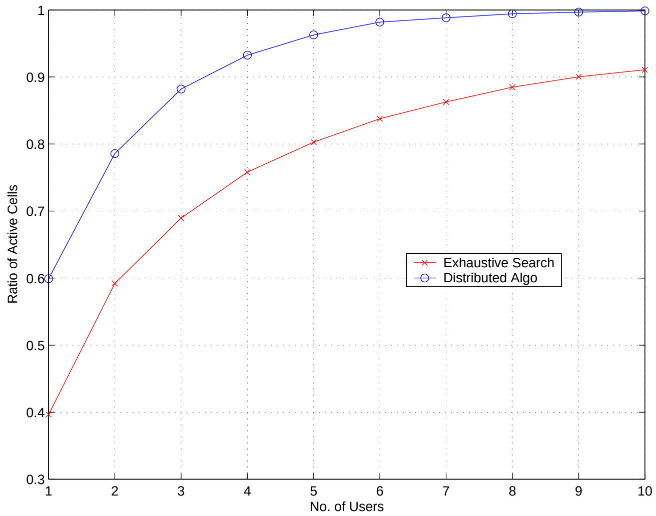

Figure 6.4: Number of active cells vs. number of users for hexagonal cellular system with 7 cells.

is at its greatest and this demonstrates the merit of dynamic spectral reuse.

For the square grid the algorithms are compared with fixed reuse having cell activity ratios of 0.25 and 0.5 (Fig. 6.8). The performance of the distributed algorithm and full reuse (Fig. 6.9) is as already explained in the hexagonal network scenario. Notice in this simulation scenario for one user the activity ratio for the distributed algorithm is approximately 0.45 (Fig. 6.7), which lies between the simulated fixed activity ratios of 0.25 and 0.5. However, the network capacity is significantly more for the distributed approach. This gain is due to the dynamic spectral reuse which adapts the reuse pattern to the channel conditions as opposed to the static schemes.

6.4 Conclusion

We presented in this chapter, a novel distributed algorithm for power allocation and scheduling for capacity maximization in multicell networks. The key idea is to combine intra-cell multi-user diversity gain with dynamic spectral reuse gain through inter-cell coordination to maximize the overall system capacity. Relying on local cell information, cells which do not offer enough capacity to outweigh interference caused to the network are deactivated. Comparisons with traditional fixed reuse schemes in a realistic network demonstrated significant capacity gains.

However, the algorithm is derived under a large network assumption, as well as high SINR regime. We would expect the performance to degrade in the limited number of cells case. Thus it is of interest to explore a more generalized approach,

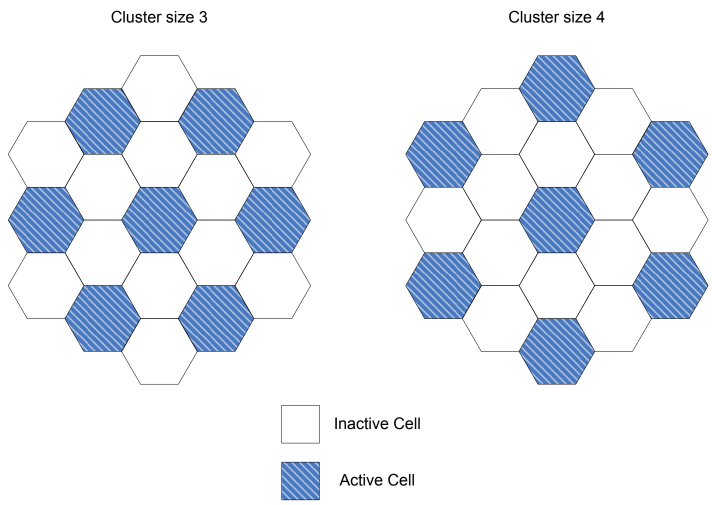

Figure 6.5: Hexagonal reuse patterns for cluster size 3 and 4.

without imposing constraints on the network parameters. In the next chapter, we present an alternate approach for power allocation and scheduling based on statistical information about the network.

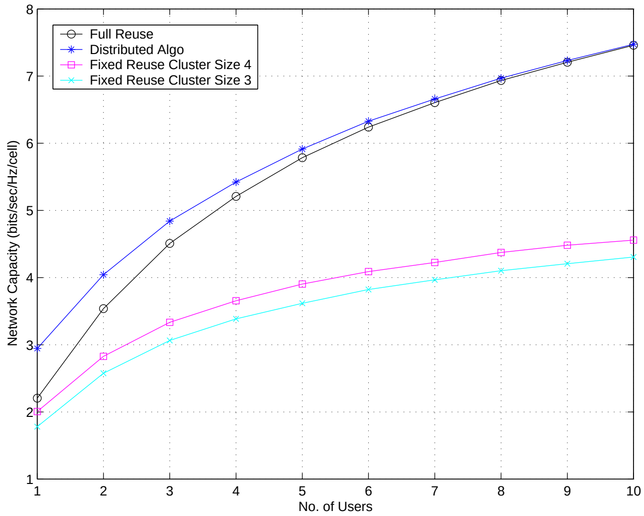

Figure 6.6: Network capacity vs. number of users for hexagonal cellular system with 19 cells. Distributed approach provides gain for small number of users and converges to the asymptotically optimal solution. Dynamic resource allocation outperforms fixed spectral reuse schemes.

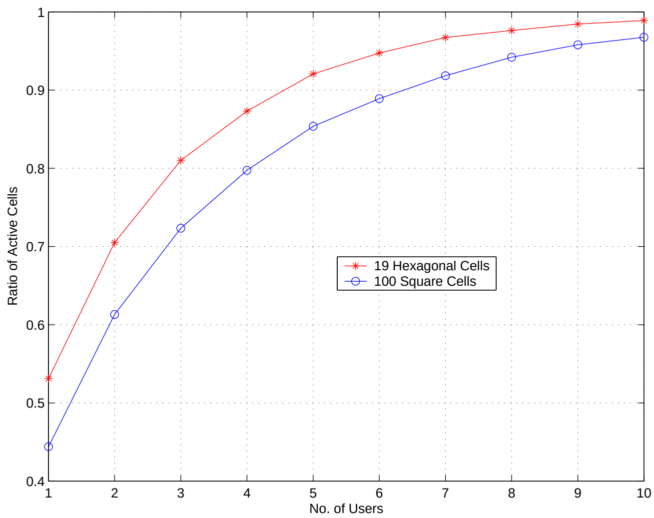

Figure 6.7: Number of active cells vs. number of users. As the number of users increases the full reuse solution becomes network capacity optimal.

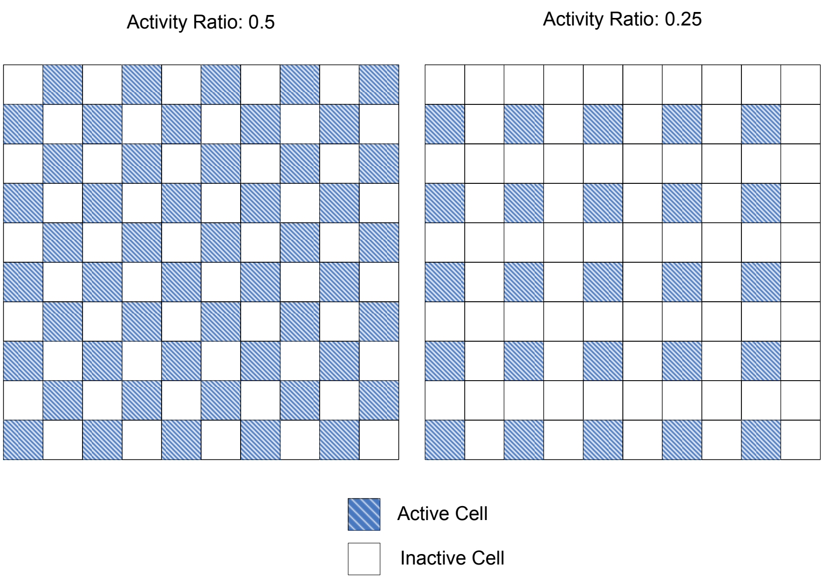

Figure 6.8: Square grid reuse patterns for activity ratios 0.5 and 0.25.

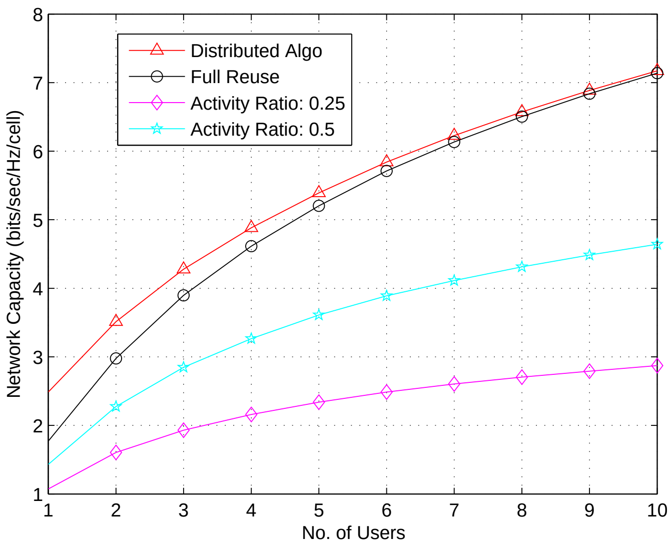

Figure 6.9: Network capacity vs. number of users for a square grid with 100 cells. Due to dynamic spectral reuse, the distributed algorithm achieves higher network capacity for $U = 1$ although it has activity ratio between 0.5 and 0.25.

Chapter 7

Power Allocation Based on Statistical Knowledge

As we have seen, joint power allocation and scheduling promises significant system capacity gains in interference-limited data networks. However, the approach presented in the previous chapter relies on an interference averaging effect necessitating a large network, as well as a high SINR regime. In this chapter, we formulate a general framework for the distributed power allocation problem in view of sum network capacity maximization. The approach is based on partitioning system knowledge into local and non-local information, and is independent of the underlying network architecture, size, or the power regime of operation. By considering instantaneous knowledge of local information and statistical knowledge of non-local information, distributed optimization may be performed. For the case of two links, we derive a distributed power allocation algorithm based on this framework. Although a gain is observed as compared to no power allocation, the power allocation algorithm shows a performance gap as compared to a centralized algorithm. We thus investigate how minimal information message passing (in this case one bit) between interfering links can help reduce this gap substantially. Finally, we also show how user scheduling can be easily incorporated into the distributed power allocation algorithm.

7.1 Introduction

As we have seen, the system capacity for mutually interfering links can be substantially improved through power allocation and scheduling. If we are to realize this gain in practice, distributed solutions to this problem are desirable. We have proposed distributed iterative power allocation and scheduling algorithms in the previous chapter which take advantage of a simplifying interference model. Such approaches rely however, on statistical averaging properties of large random networks and thus are not applicable for all networks [87]. We are more interested in a more general approach which does not rely on assumptions on the underlying network.

A number of approaches exist for power allocation, one of which is game theory already discussed in the introduction of this thesis. As an alternative to game theoretic approaches, the power allocation problem can be solved through *geometric programming* techniques which by considering the high and low SINR regimes, render the problem convex[88, 89, 49]. Power allocation over parallel channels is also studied in [90, 91], but here the authors consider the uplink of a single cell.

In this chapter, we take a different and, more importantly, simpler approach to the power allocation problem.

- We first propose a framework for sum-rate maximizing power allocation in an arbitrary network with several interfering cells or links based on statistical knowledge of non-local network parameters. The key advantage of this framework is that it allows a fully distributed optimization of the power allocation.
- By considering the two-cell case, we derive simple conditions for link activation based on signal-to-noise ratio (SNR) and SINR. These conditions allow us to derive a novel, fully distributed power allocation algorithm.
- As each link has no information about the actions taken by other links, we investigate how one bit information message passing between interfering links may provide substantial improvement in the capacity performance.
- Finally, we also show how user scheduling can be incorporated into the power allocation algorithm, so as to exploit an added multi-user diversity gain.

Numerical results show that the fully distributed and near distributed power allocation algorithms largely outperforms a system with fixed (or no) power control and are close to the performance given by centralized power control.

7.2 Distributed Power Allocation Framework

Distributed optimization is important as it enables the implementation of an otherwise unpractical centralized solution, especially for large systems. Finding good distributed optimization algorithms however proves to be a formidable task, as the objective function being optimized usually depends on all system parameters; even those not locally available. Obtaining the optimal solution would thus require the gathering and processing of all system information, which is difficult in practice. In order to obtain a distributed solution, one can however imagine compromising on the amount of information available, so that a pragmatic, though sub-optimal, solution is obtained.

We propose a distributed optimization framework based on partitioning network information into two classes: *local information* of which we have instantaneous knowledge, and *non-local information* of which there is statistical knowledge. Later on, we will see that user scheduling can be jointly performed with power allocation, thus, in effect addressing problem (2.4). For the power allocation problem being considered, each link would make a decision based on what the transmitter or receiver can measure locally, plus information fed back from the receiver to the transmitter, i.e. local information to the cell. This would indeed be sub-optimal, as some kind of assumption would have to be made about other links' behavior. None the less, this is a very practical form of distributed control in terms of both complexity and information exchange. In what follows, we formulate the distributed power allocation problem under the assumption of statistical knowledge of unknown non-local information. Note that this knowledge can be acquired a priori, during a network calibration phase.

7.2.1 Network Capacity Maximization Framework Under Statistical Knowledge

As stated, we assume that each transmitter has instantaneous local knowledge. Let us denote the set of complete network information by $\mathcal{G}$. The local information of which transmitter n has instantaneous knowledge is given by $\mathcal{G}_n^{\text{local}}$. Thus, unknown or non-local information for transmitter n can be denoted as $\tilde{\mathcal{G}}_n = \mathcal{G} \backslash \mathcal{G}_n^{\text{local}}$, of which we assume only statistical knowledge. Based on this knowledge, link n then tries to maximize the *expected network capacity* defined as

$$\overline{\mathcal{C}}_n(\boldsymbol{P}) \triangleq \mathbb{E}_{\tilde{\mathcal{G}}_n|\mathcal{G}_n^{\text{local}}} \left\{ \sum_{m=1}^{N} w_m \log_2 \left(1 + \frac{G_{m,m} P_m}{\eta + \sum_{\substack{i=1 \\ i \neq m}}^{N} G_{m,i} P_i} \right) \right\}. \tag{7.1}$$

$\mathbb{E}_{\tilde{\mathcal{G}}_n|\mathcal{G}_n^{\text{local}}}\{\cdot\}$ is the expectation operator averaging the capacity over all realizations of $\tilde{\mathcal{G}}_n$, conditioned on full knowledge of $\mathcal{G}_n^{\text{local}}$. The distributed power allocation problem under this framework can thus be written as

$$[\boldsymbol{P}^*]_n = \left[\arg\max_{\boldsymbol{P} \in \Omega} \overline{\mathcal{C}_n}(\boldsymbol{P}) \right]_n . \tag{7.2}$$

7.2.2 Local v.s. Non-Local Channel Knowledge Partitioning: One Example

Clearly the choice of local and non-local information will significantly impact the distributed solution of the power allocation problem. The sets of local and non-local information can be partitioned in a number of ways, depending on the knowledge each link has. For the problem at hand, we consider the set of all network information as $\mathcal{G} = \{G_{i,j}, w_i\} \ \forall \ i, j$, and we let the *local* information be $\mathcal{G}_n^{\text{local}} = \{G_{n,j}, w_n \ \forall \ j\}$. This means that a transmitter has knowledge of the direct channel, the interference from other cells to its intended receiver, and the weight of the user it is serving. This is a natural choice for local information, as these values allow us to measure the SINR at the receiver, which can be fed back to the transmitter. Practically, channel information can be periodically fed back by the receiver to the transmitter through a pilot/dedicated channel. Thus, the unknown information at the transmitter is given by $\tilde{\mathcal{G}}_n = \{G_{i,j}, w_i \ \forall \ j, i \neq n\}$. Under this knowledge, the expected network capacity that transmitter n tries to maximize is given by

$$\begin{aligned}\overline{\mathcal{C}_n}(\boldsymbol{P}) \ \triangleq \ & w_n \log_2 \left(1 + \frac{G_{n,n} P_n}{\eta + \sum_{\substack{i=1 \\ i \neq n}}^{N} G_{n,i} P_i} \right) \\ & + \mathbb{E}_{\tilde{\mathcal{G}}_n} \left\{ \sum_{m \neq n}^{N} w_m \log_2 \left(1 + \frac{G_{m,m} P_m}{\eta + \sum_{\substack{i=1 \\ i \neq m}}^{N} G_{m,i} P_i} \right) \right\}. \end{aligned} \tag{7.3}$$

From the power allocation vector resulting from this maximization, link n uses $[\boldsymbol{P}^*]_n$ as the transmission power to its respective user.

However, calculation of the expected capacity from all other links is not so trivial. In the next section, we thus focus on the two-link case which offers insight into the potential gain offered by this distributed approach. We propose a simple distributed algorithm to solve this problem, as well as a modified version of this algorithm incorporating 1-bit information exchange between neighboring links to enhance performance. We then discuss how user scheduling can be easily incorporated into the power allocation algorithm.

7.3 Distributed Power Allocation for Two Links

The case of problem (7.2) for two links is particular. However, the algorithm developed here can be used in a wider network with more links, where links are previously paired up in clusters of two links. Forming of the clusters should favor strongly interfering links, for which a distributed resource allocation technique will exhibit the largest benefits. For example, in a cellular network, adjacent cells are

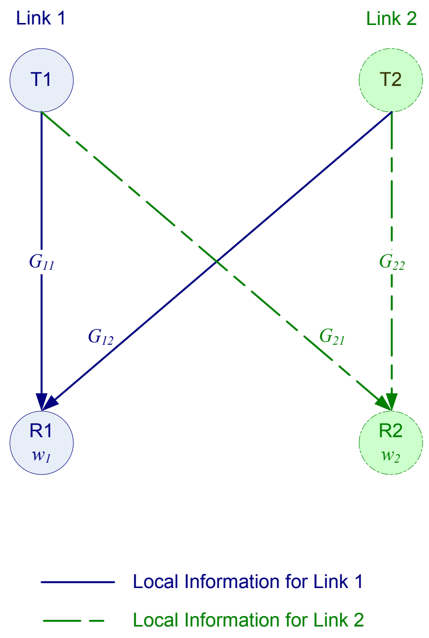

Figure 7.1: A 2 cell/link scenario with mutual interference. Local information of link n is given by $\mathcal{G}_n^{\text{local}} = \{G_{n,i}, w_n \ \forall\ i\}$, i.e. the direct channel and interfering channel at the receiver.

often the dominant interferers as the pathloss degradation between them is the least. A potential clustering method would be to determine the pairs of cells that interfere the most with each other based on average pathloss statistics.

Notice also that the proposed framework exploits statistical information about other links, *including* the weights of other links. Guaranteeing QoS usually requires the weights to be adapted at each scheduling instant, making the weights instantaneous parameters. If the weights correspond to a grade of service that a user has purchased, then we can assume the weights to be independent of the channel gains. Moreover, as the grade of service of all users is known to the network, we also assume knowledge of the *average weight* $\mathbb{E}\{w_n\} = \overline{w}$, of the user population in the network. Focusing on link 1, we have knowledge of $G_{1,1}$, $G_{1,2}$ and w_1 (Fig. 7.1). We can write the expected network capacity as a function of the transmit powers as

$$\begin{aligned} \overline{\mathcal{C}}_1(P_1, P_2) &= w_1 \log_2\left(1 + \frac{G_{1,1}P_1}{\eta + G_{1,2}P_2}\right) \\ &+ \overline{w}\, \mathbb{E}\left\{\log_2\left(1 + \frac{G_{2,2}P_2}{\eta + G_{2,1}P_1}\right)\right\}, \end{aligned} \tag{7.4}$$

where the expectation is taken over the distribution of other link channel gains, namely $G_{2,2}$ and $G_{2,1}$. The expected capacity for link 2 can be expressed similarly, by inverting the indices. Thus, each link will search over all possible power values to find the optimal expected capacity.

However, from (5.7) we know the centralized optimal power allocation set for weighted sum-rate maximization. Motivated from this result, we adopt the reduced optimization search space given by (5.7) for the distributed problem as well. However, we point out that the centralized optimal power allocation (5.4) is not necessarily optimal for the distributed problem formulation (7.2) as the objective functions in the two cases are not the same. The distributed power allocation problem for weighted sum-rate maximization can thus be written as

$$\boldsymbol{P}_i^* = \left[\arg \max_{(P_1,P_2)\in\Omega'} \overline{\mathcal{C}_i}(P_1,P_2)\right]_i \quad \forall\ i = 1,2 \tag{7.5}$$

where $\Omega' = \Omega^B \cup (P_{\max}, P_2') \cup (P_1', P_{\max})$. Each link would thus need to independently search over five possible power allocation points to find the one that maximizes (7.5). However, evaluating the non-binary values for the powers still requires knowledge of instantaneous information of the other link, e.g. link 1 would require knowledge of $G_{2,2}, G_{2,1}$ and w_2. Thus, motivated by the result exhibited in Fig. 5.2, we adopt the binary feasible set Ω^B given by (5.6), accepting a little loss in weighted sum-rate. In this case, we can formally write the distributed optimization problem for equal link weights as

$$\boldsymbol{P}_i^* = \left[\arg \max_{(P_1,P_2)\in\Omega^B} \overline{\mathcal{C}_i}(P_1,P_2)\right]_i \quad \forall\ i = 1,2 \tag{7.6}$$

The advantage gained from this simplification is that a completely distributed algorithm can be derived, as the powers can now only be either 0 or $P_{\max}$.

7.3.1 Fully Distributed Power Allocation

As already stated, by adopting binary power control a link will either transmit at $P_{\max}$ (from now on assumed to be 1 for simplicity) or remain inactive. Thus, solving problem (7.6) is equivalent to each link determining if it should be active or not, depending on knowledge of local information.

A cell i needs to consider the following cases to determine which power allocation maximizes the expected capacity defined in (7.4):

1. Expected capacity of both cells being active: $\overline{\mathcal{C}}(1,1)$.
2. Expected capacity of only cell i being active: $\overline{\mathcal{C}}(0,1)$ or $\overline{\mathcal{C}}(1,0)$.

Focusing on link 1, the activity conditions can thus be summarized as follows:

$$P_1 = \begin{cases} 1 & \text{if } \overline{\mathcal{C}}_1(1,1) \geq \overline{\mathcal{C}}_1(0,1) \\ 1 & \text{if } \overline{\mathcal{C}}_1(1,0) \geq \overline{\mathcal{C}}_1(0,1) \\ 0 & \text{otherwise} \end{cases}$$

Algorithm 2 Fully Distributed Power Allocation

Steps performed at link 1:
if $(\gamma_1([1,1]) \geq 2^{\left(\beta_1[\overline{\mathcal{R}}(0,1)-\overline{\mathcal{R}}(1,1)]\right)} - 1)$ or $(\gamma_1([1,0]) \geq 2^{\left(\beta_1\overline{\mathcal{R}}(0,1)\right)} - 1)$ **then**
    $P_1 = 1$
else
    $P_1 = 0$
end if
Steps performed at link 2:
if $(\gamma_2([1,1]) \geq 2^{\left(\beta_2[\overline{\mathcal{R}}(0,1)-\overline{\mathcal{R}}(1,1)]\right)} - 1)$ or $(\gamma_2([0,1]) \geq 2^{\left(\beta_2\overline{\mathcal{R}}(0,1)\right)} - 1)$ **then**
    $P_2 = 1$
else
    $P_2 = 0$
end if

Note that there is no need to compare the expected capacity of both cells being active and only cell 1 being active, as cell 1 will be active in either case. By simple manipulation of the above conditions, link 1 will be active if either

$$\mathrm{SINR}_1 = \gamma_1([1,1]) \geq 2^{\left(\beta_1[\overline{\mathcal{R}}(0,1)-\overline{\mathcal{R}}(1,1)]\right)} - 1 \tag{7.7}$$

or

$$\mathrm{SNR}_1 = \gamma_1([1,0]) \geq 2^{\left(\beta_1\overline{\mathcal{R}}(0,1)\right)} - 1, \tag{7.8}$$

where $\overline{\mathcal{R}}(0,1)$ and $\overline{\mathcal{R}}(1,1)$ are the expected capacities of link 2 under the respective power allocations and $\beta_1 = \frac{\overline{w}}{w_1}$. Due to symmetry, the expected capacities will be the same for both links and the conditions for link 2 can be expressed in a similar fashion. The steps performed at each link are given in Algorithm 2.

In what follows, based on a simplified distance pathloss channel model, we derive the expected capacities. The utility of such a model is that it applies to scenarios where large-scale attenuation dominates and also enables us to investigate the expected capacities in the high and low interference regimes.

Random Exponential Pathloss Channel Model

Assume that users are located according to a uniform spatial distribution over the cell area. Let the cell radius be R, and the distance between cells D (Fig. 7.2). An exponential pathloss model is assumed for the channel gains, with pathloss exponent ξ; and thus $G_{n,i} = d_{n,i}^{-\xi}$, where $d_{n,i}$ is the distance between transmitter i and receiver n.

We first calculate the distribution of the distance r of the direct path, assuming the cell under consideration to be centered at the origin of the cartesian plane (Fig.

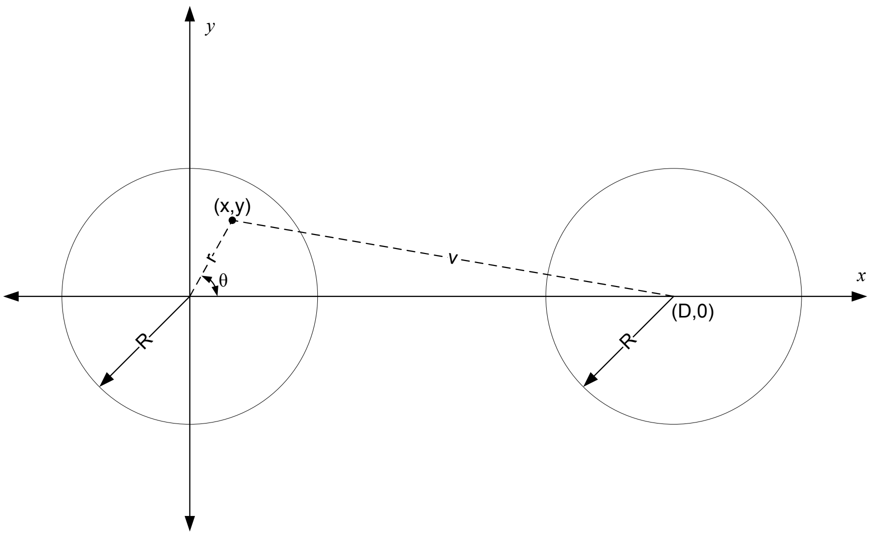

Figure 7.2: Two cells of radius R at a distance D from each other. A user in the cell under consideration lies at a random point (x,y) drawn from a uniform distribution over the cartesian plane.

7.2). The joint distribution of x and y is given by

$$f(x,y) = \frac{1}{\pi R^2} \text{ for } 0 \leq x^2 + y^2 \leq R^2.$$

Since

$$r = \sqrt{x^2 + y^2}, \quad \theta = \tan^{-1} \frac{y}{x},$$

we can easily find the Jacobian

$$J(x,y) = \begin{vmatrix} \frac{\delta r}{\delta x} & \frac{\delta r}{\delta y} \\ \frac{\delta \theta}{\delta x} & \frac{\delta \theta}{\delta y} \end{vmatrix} = \frac{1}{r}.$$

Then we have

$$f(r,\theta) = f(x,y)|J(x,y)^{-1}| = \frac{r}{\pi R^2}$$

for

$$0 \leq r \leq R, \quad 0 \leq \theta \leq 2\pi.$$

With no interference the expected capacity is given (in bits/sec/Hz) by

$$\begin{aligned}
\overline{\mathcal{R}}(0,1) &= \mathbb{E}\left\{\log_2\left(1+\frac{r^{-\xi}}{\eta}\right)\right\} \\
&= \int_0^{2\pi}\int_0^R \log_2\left(1+\frac{r^{-\xi}}{\eta}\right) f(r,\theta)\mathrm{d}r\mathrm{d}\theta \\
&= \int_0^{2\pi}\int_0^R \log_2\left(1+\frac{r^{-\xi}}{\eta}\right) \frac{r}{\pi R^2}\mathrm{d}r\mathrm{d}\theta \\
&= \frac{2}{\ln(2)R^2}\left[\frac{\xi r^2}{4} - \frac{1}{4}\xi{}_2F_1(-\frac{2}{\xi},1;1-\frac{2}{\xi};-\frac{r^{-\xi}}{\eta})r^2 + \frac{1}{2}\ln(\frac{r^{-\xi}+\eta}{\eta})r^2\right]_0^R \\
&= \frac{1}{\ln(2)}\left[\frac{\xi}{2} - \frac{1}{2}\xi{}_2F_1(-\frac{2}{\xi},1;1-\frac{2}{\xi};-\frac{R^{-\xi}}{\eta}) + \ln\left(\frac{R^{-\xi}+\eta}{\eta}\right)\right], \qquad (7.9)
\end{aligned}$$

where ${}_2F_1$ denotes the hypergeometric function.

For the case of interference being present, the interfering channel distance is given by $v = \sqrt{r^2 + D^2 - 2rD\cos\theta}$ (Fig. 7.2). Thus, we have

$$\begin{aligned}
\overline{\mathcal{R}}(1,1) &= \mathbb{E}\left\{\log_2\left(1+\frac{r^{-\xi}}{\eta+v^{-\xi}}\right)\right\} \\
&= \int_0^{2\pi}\int_0^R \log_2\left(1+\frac{r^{-\xi}}{\eta+(r^2+D^2-2rD\cos\theta)^{-\xi/2}}\right) f(r,\theta)\mathrm{d}r\mathrm{d}\theta.
\end{aligned}$$

Although a closed form for this integral is too complicated to derive, it can be easily evaluated numerically to find the expected capacity when both cells are active. In Fig. 7.3, we plot the expected capacities $\overline{\mathcal{R}}(0,1)$ and $\overline{\mathcal{R}}(1,1)$ as a function of the distance D between cells (normalized w.r.t. $2R$) for $R = 500$m and $\xi = 4$. Clearly, as the distance D increases the effect of interference diminishes and the two capacities approach each other as expected.

Practically, $\overline{\mathcal{R}}(0,1)$ and $\overline{\mathcal{R}}(1,1)$ for any channel model can be calculated offline, by generation of a sufficient number of channel realizations, and plugged into conditions (7.7) and (7.8) to determine if the cell should be active. Thus, based on simple conditions and in a fully distributed way, each link decides based on local channel information whether it should transmit or not based on criteria (7.7) and (7.8). We call this algorithm *Fully Distributed Power Allocation* (FDPA).

7.3.2 Capacity Enhancement with 1-bit Message Passing

The FDPA algorithm presented in the previous section is completely distributed, i.e. it requires no real-time information exchange from other links. However, due to each link being ignorant of the other link, a sub-optimal decision is taken and in certain cases a very detrimental result would be each link shutting itself off, resulting in zero network capacity.

It is thus interesting to explore if somehow a minimum amount of information exchange could be used to enhance performance. We let this amount of information

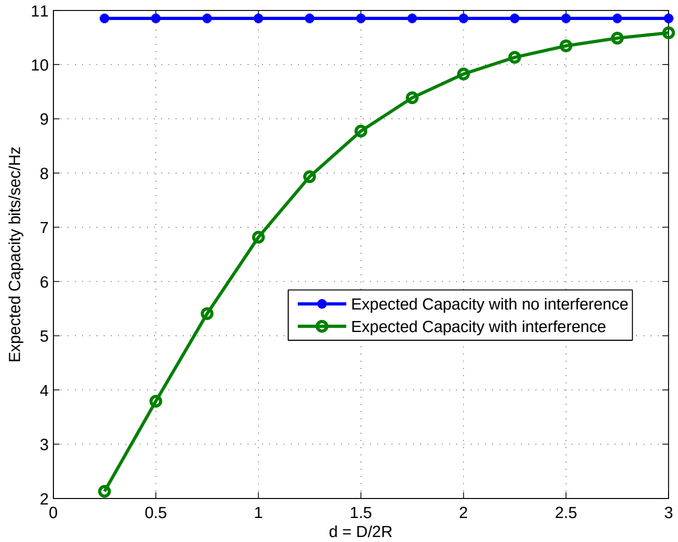

Figure 7.3: Variation of expected capacities with distance between cells based on exponential pathloss model, with pathloss exponent 4. The expected capacity with interference will approach that without interference as the distance between cells is increased.

be one bit. More precisely, a link is allowed to send a 1-bit message to the other link. The most natural choice of information to send would be the result of its distributed (using FDPA criteria) optimization solution. We call this algorithm *1-Bit Distributed Power Allocation* (1-BDPA) and describe it as follows:

1. Link 1 performs the optimization (7.6) based on criteria (7.7) and (7.8), and then sends a 1-bit message to the other link to indicate whether it is active or not.

2. Link 2 then performs the optimization (7.6) to calculate P_2, under the knowledge of P_1.

If the message bit is a 0, then link 2 will obviously be active. If a 1 is sent, then link 2 needs only to consider if both cells being active gives better performance than the expected capacity of the other link. Clearly this algorithm will perform better than FDPA as with the 1-bit signal from link 1, a more *informed* decision can be made by link 2, thus avoiding shutting down both links simultaneously. Details are given in Algorithm 3.

Algorithm 3 1-Bit Distributed Power Allocation

```
Steps performed at Link 1:
if (γ1([1,1]) ≥ 2^(β1[R̄(0,1)−R̄(1,1)]) − 1) or (γ1([1,]) ≥ 2^(β1 R̄(0,1)) − 1) then
    P1 = 1
    msg_bit = 1
else
    P1 = 0
    msg_bit = 0
end if
Steps Performed at Link 2:
if msg_bit = 0 then
    P2 = 1
else if γ2([1,1]) ≥ 2^(β2[R̄(0,1)−R̄(1,1)]) − 1 then
    P2 = 1
else
    P2 = 0
end if
```

7.3.3 Power Allocation and Scheduling

In cellular networks, there are normally a number of users in each cell requesting data from the AP. In this context, user scheduling can be exploited to obtain multi-user diversity gain [17]. The idea is to schedule a user which has comparatively better channel conditions than other users, so that higher throughput can be achieved.

In order to obtain a multi-user diversity gain, user scheduling can also be incorporated into the power allocation framework. This is easily done by observing that for a cell to be active and thus contribute capacity to the system, either of the conditions (7.7) and (7.8) should be satisfied. Thus, scheduling a user with the maximum SNR or SINR increases the probability of satisfying these conditions. If we suppose that there are U_n users in cell n, then the activation conditions can be written as

$$\max_{u_n \in [1,U_n]} \mathrm{SINR}_n(u_n) \geq 2^{\left(\beta_{u_n}[\overline{\mathcal{R}}_{(U_n)}(0,1) - \overline{\mathcal{R}}_{(U_n)}(1,1)]\right)} - 1 \tag{7.10}$$

or

$$\max_{u_n \in [1,U_n]} \mathrm{SNR}_n(u_n) \geq 2^{\left(\beta_{u_n}\overline{\mathcal{R}}_{(U_n)}(0,1)\right)} - 1 \tag{7.11}$$

where $\overline{\mathcal{R}}_{(U_n)}(0,1)$ and $\overline{\mathcal{R}}_{(U_n)}(1,1)$ are the expected capacities based on employing the max-SNR and max-SINR scheduling policies. These will be different from the previously calculated expected capacities because scheduling in general changes the distributions of the channel gains. In this case, the U_n order statistics of the expected capacities have to be calculated. Similarly, $\beta_{u_n} = \frac{\overline{w}_{U_n}}{w_{u_n}}$, where $\overline{w}_{U_n}$ is the

U_n order statistic of the average weights, and w_{u_n} is the weight associated with user u_n. Although these can be analytically calculated, they can also be easily obtained through sufficient Monte-Carlo simulations. Thus, the scheduling rule is to find the max-SNR and max-SINR users and see which one satisfies its respective condition. If both satisfy their respective conditions then the user which offers higher *expected* capacity is scheduled, i.e., either the max-SINR or the max-SNR user.

7.4 Numerical Results

As stated previously, the formulation of the distributed power allocation is independent of the system architecture (cellular or ad-hoc). Thus for ease of simulation, we adopt a cellular network layout for evaluating the performance of the proposed power allocation algorithms. This will also allow us to investigate user scheduling jointly with power allocation. In this case, we consider the downlink, i.e., the transmitter is the AP, and the receiver is the user terminal (UT). We set both link weights equal to 1, as this will simplify presentation of the numerical results, thereby allowing us to focus more on the performance of the proposed techniques. Monte-Carlo simulations over random UT positions are carried out for 2 cells with an operating frequency of 1.8 GHz, each with a radius $R = 500$ meters. A UT position is drawn randomly from a uniform distribution over the cell area. Gains for *all inter-cell and intra-cell* AP-UT links are based on the COST-231 [77] path loss model, including log-normal shadowing with standard deviation of 10 dB, as well as fast fading which is assumed i.i.d. with distribution $\mathcal{CN}(0, 1)$. The peak power constraint is given by $P_{\max} = 1$ Watts. In order to compute the expected capacity of the other cell, offline calculations based on an adequate number of channel realizations are done for when both cells are active or just the other cell is active.

The performance of FDPA and 1-BDPA is compared with "No Power Allocation" (i.e. both cells always on at $P_{\max}$) and centralized "Optimal Allocation" (i.e. exhaustive search over all points). To gain insight into the effects of power allocation we vary the distance between the two cells. Denoting the distance between APs by D, we vary the ratio $\frac{D}{2R}$, $2R$ being the distance between neighboring APs in a reuse one cellular system. When $\frac{D}{2R} < 1$ then the cells overlap and this results in severe interference, akin to that in ad-hoc networks. When $\frac{D}{2R} > 1$ the cells are further apart and thus the effects of interference diminish. In Fig. 7.4 we plot the *average network capacity per cell* versus $\frac{D}{2R}$. It can be seen that power allocation provides the most benefit when $\frac{D}{2R}$ is small, i.e. when there is strong interference. Turning off one of the cells will then provide more overall capacity than when both cells are transmitting. The FDPA algorithm achieves 50% of the gain offered by optimal power allocation, whereas with 1-BDPA a substantial amount of the gain is exploited. As $\frac{D}{2R}$ increases, the gain from power allocation decreases and all the schemes converge to the same capacity. This is quite straightforward due to the fact that increasing the distance between the cells diminishes the effect of interference, and both cells become more or less "shielded" from interference. This can equivalently be seen from Fig. 7.3 where the expected capacity with interference increases as $\frac{D}{2R}$ increases. Thus, from a network capacity maximization point of view, both links should transmit at full power when $\frac{D}{2R}$ becomes large.

In Fig. 7.5 we depict the percentage of erroneous decisions made in the power allocation by each algorithm as compared to the optimal solution, where an erroneous decision is defined as a deviation from the centralized binary power allocation. FDPA makes a significant amount of errors in the high interference case. This is due to the fact that under severe interference both cells can become inactive as both cells may come to the conclusion that they will not contribute enough capacity to outweigh the interference caused. This is demonstrated by the fact that FDPA turns both cells off 28% of the time in the high interference scenario, whereas, clearly at least one cell should be active. This type of error becomes more rare in the low interference case, as each cell decides it will offer enough capacity without causing too much interference and thus both cells being active becomes the optimal thing to do. We see that with 1-BDPA, in the high interference scenario the percentage of errors is relatively smaller. This is due to the fact that it can exploit the 1-bit information exchange to make a better decision, which in the severe interference case is to keep one, but not both, of the cells active. At the other extreme, when cells are far apart, the error percentage is small due to the fact that both cells are kept active in the presence of low interference.

Finally, we compare the performance of power allocation and user scheduling in Fig. 7.6 for $U = 1, 5$ and 10. We see a gain in absolute capacity values when employing user scheduling. Notice that as the number of users increases, the gain from power allocation diminishes. This is due to the fact that the probability of finding users which have good direct gains, while still being sufficiently protected from interference, increases by the process of scheduling alone. Thus, keeping both cells active is better in terms of network capacity and all the curves lie closer together. However, FDPA starts to suffer when user scheduling is employed. This can be due to the fact that it still results in both links being inactive, although through user scheduling full power allocation becomes more and more likely. The rate of increase in expected capacity of user scheduling is overshadowed by the damaging effect of making wrong decisions.

7.5 Conclusions

In this work, we proposed a framework for distributed weighted sum-rate maximizing power control, exploiting statistical knowledge of non-local information. We again analyzed the particular case of two links, deriving simple conditions on SNR and SINR for link activation. Based on these conditions, computationally simple distributed algorithms were proposed which were shown to exploit a major part of the gain offered by the centralized optimal power allocation. Moreover, we also demonstrated how user scheduling can be incorporated into the power allocation algorithm. Through numerical results, the proposed power allocation algorithms exhibited significant sum-rate gains over no power allocation.

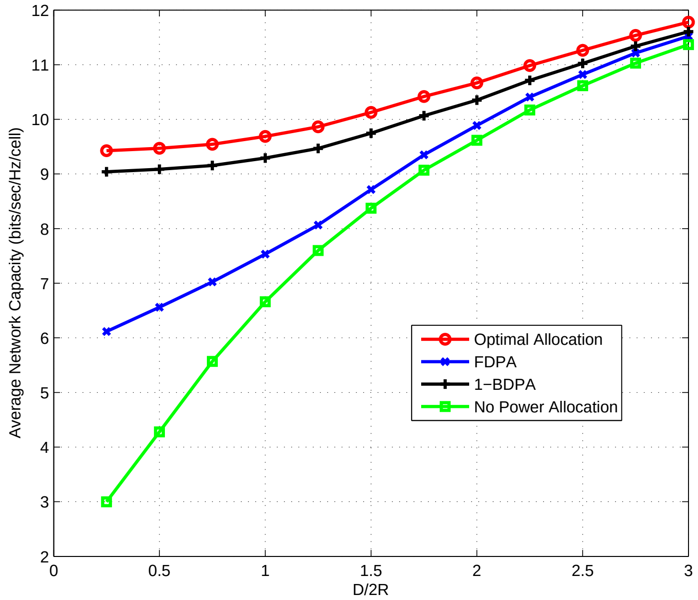

Figure 7.4: Comparison of average network capacity per cell for the fully distributed algorithm (FDPA) and 1-bit message passing approach (1-BDPA) with Optimal and No Power Allocation. The two algorithms exhibit marked gain over no power allocation with the 1-bit message passing approach providing a significant amount of capacity gain. All the approaches converge when the separation between links increases as interference decreases and both cells transmitting at full power becomes optimal.

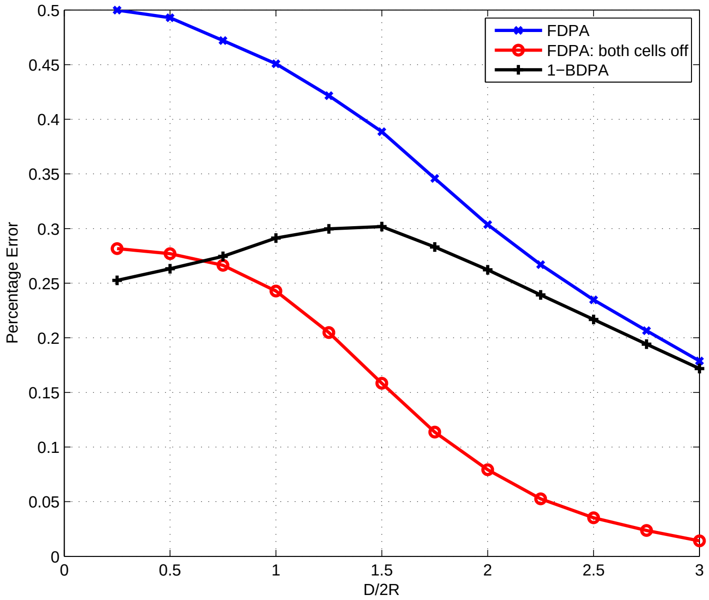

Figure 7.5: Percentage Error of FDPA and 1-BDPA compared with the optimal binary power allocation. FDPA turns off both cells 28% of the time in the high interference scenario thus resulting in zero sum-rate. Allowing 1-bit signaling reduces the number of errors made and thus 1-BDPA outperforms FDPA.

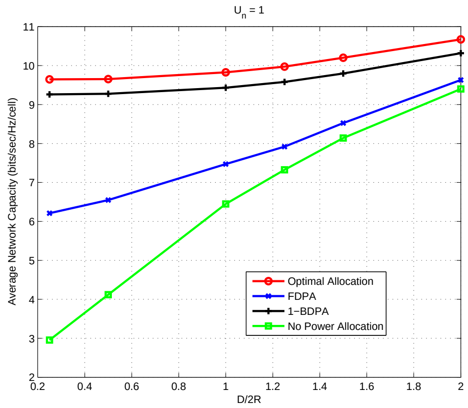

(a) With one user per cell

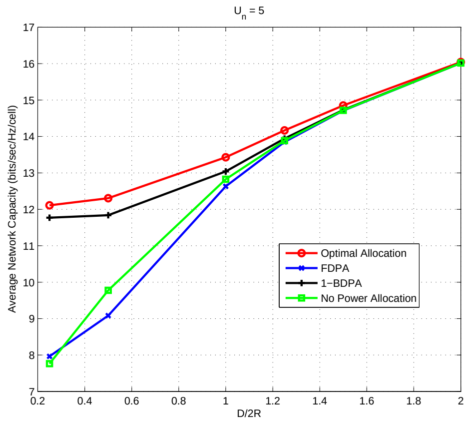

(b) With five users per cell

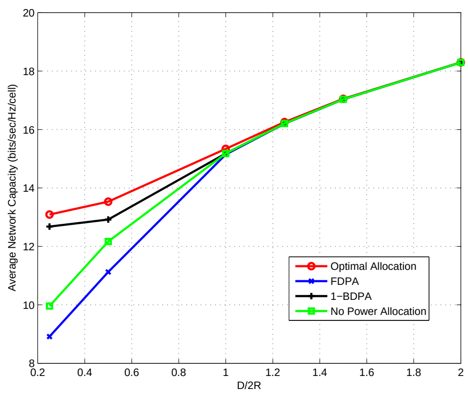

(c) With ten users per cell

Figure 7.6: Effect of power allocation and user scheduling on average network capacity. Incorporating user scheduling makes full reuse more probable in terms of optimality for sum-rate maximization.

Chapter 8

Probabilistic Access Schemes

An alternate approach to multicell power allocation and scheduling called multicell access schemes (MCA) has been proposed in [64]. In this approach, cells compete for a chance to transmit to their users and is reminiscent of random access protocols in multiuser networks. Thus at any given instant out of N cells, only K cells are allowed to be active simultaneously. MCA schemes are similar to the modified ALOHA protocol proposed in [92], where the authors optimize the uplink transmit probability to exploit multiuser diversity, thus maximizing system throughput. However, here parallel interfering transmissions are considered (multicell) instead of simultaneous transmission to a common receiver (single-cell). Moreover, not only is multi-user diversity exploited, but interference management is also taken into account to maximize sum network capacity [64].

In the proposed MCA scheme, a cell obtains permission to transmit when it has enough *credit*. To keep the algorithm distributed, the credit is based on local knowledge; specifically, the channel gain of the scheduled user. Thus, an *access function* maps the credit (channel gain) onto a probability of a cell gaining access and transmitting to its user. The problem is then to maximize the *expected network capacity*. The expected network capacity is analyzed based on a simple access function motivated by our previous results. That is, when the channel gain is above a certain threshold, the cell is active with full power. Otherwise, the cell remains silent. This results in a step function for the probability of access for a cell. Based on this simple access function, numerical results for a 19 cell network show that at the optimal threshold, a capacity gain of approximately 20% is achieved over transmitting with full power. Subsequently, the access function which optimizes the system capacity is also investigated [93]. Discretizing the access function gives rise to a combinatorial optimization problem for maximzing the expected capacity. An algorithm based on *Simmulated Annealing* is used to optimze the access function. Interestingly, it is found that a binary probability of access function (threshold) optimizes the expected network capacity, thus corroborating the initial choice of access function [93].

Chapter 9

Conclusions and Future Work Directions

In this thesis, we studied *Multicell Resource Allocation* techniques for full reuse cellular networks. We considered a very general system model applicable to a number of access techniques (TDMA, O/FDMA, orthogonal-CDMA), in which transmissions mutually interfere due to full resource reuse. Based on this model, we formulated the *joint power allocation and scheduling problem* for sum network capacity maximization. Our goal was to not only quantify the gains achievable through power allocation and scheduling, but also to propose practical solutions, i.e. distributed algorithms for this problem.

We initially studied the behavior of interference in large random cellular networks by proposing a simple geometric model in which access points were randomly placed over the coverage area. We derived analytical expressions for the expected interference as a function of different network parameters, which demonstrated it to increase monotonically but slowly from cell center to cell edge. We then obtained lower bounds on the SIR, which can be used to evaluate cell capacity. We showed cell capacity to be independent of network density and to increase with the pathloss exponent and as a result, concluded that the sum capacity increases with network density. The proposed model was also shown to be easily extendable to ad-hoc networks for certain classes of MAC protocols where this proves valuable in predicting expected interference. Intuition from this study allowed us to propose the *interference-ideal network* model in which the intercell interference is approximated by its expectation. This model proves useful for obtaining distributed solutions for multicell resource allocation problems.

We next focused on the problem of multiuser, multicell scheduling for cellular networks with a resource-fairness constraint. An optimal scheduler was proposed for large networks based on a standard channel inversion power control policy. In the optimal scheduler, each cell ranks its users according to decreasing channel gains. As *local* knowledge of channel gains is used, the optimal scheduler can be efficiently approximated by a fully distributed multicell scheduler. The multicell scheduler is also consistent with maximizing the capacity of each cell independently through multi-user diversity. Large gains were shown to be obtainable from inter-cell coordination thanks to the inter-cell channel gain variability which stems from power control and fading.

Having looked at scheduling, we next turned our attention to multicell power allocation. Specifically, we formulated the weighted sum-rate maximizing power allocation problem for mutually interfering links which is a generalization of sum network capacity maximization. Though this problem is non-convex, for the case of two links, we analytically characterized the optimal solution set to this problem. An interesting result was obtained for the case of equal link weights, where the optimal power allocation was shown to lie at the boundary points of the feasible power allocation set. This translates into a cell being either on or off, and we termed this as *binary power control*. This result substantially reduced the complexity of resulting algorithms by transforming the search space into a continuous set to just three possible power allocations. Obtaining the optimal power allocation solution however, requires centralized processing.

We thus proceeded with tackling the joint power allocation and scheduling problem. For this, we first presented a novel distributed algorithm based on the interference-ideal model and binary power control. Relying on local cell information, cells which do not offer enough capacity to outweigh interference caused to the network are deactivated. A simple iterative algorithm was derived which scheduled the cell user with the maximum SINR compared to a simple threshold condition to determine activity. However, this algorithm is dependent on a large network assumption.

Therefore, we proposed a framework for distributed weighted sum-rate maximizing power control exploiting statistical knowledge of non-local information, which does not rely on a large network size or a specific power regime of operation. In this approach, each link independently maximizes the expected network capacity conditioned on local information. We analyzed the particular case of two links, deriving simple conditions on SNR and SINR for link activation. Based on these conditions, a computationally simple and fully distributed algorithm for power allocation was proposed. We also investigated how 1-bit message passing could be used to substantially improve the performance of the fully distributed algorithm. Moreover, we also demonstrated how user scheduling can be incorporated into the power allocation algorithm. The proposed power allocation algorithms exhibited significant network capacity gains over no power allocation and were shown to exploit a significant portion of the gain offered by the centralized optimal power allocation.

Future Work Directions

Although we have tried to solve some of the problems linked to multicell resource allocation, a number of issues arise as a consequence. The most notable of these, is the notion of fairness. The PMS algorithm results in good users gaining benefit and bad users being harmed even further. Similarly, the distributed iterative algorithm results in some cells being completely shut off. If a cell has an unfavorable propagation environment, this will result in it suffering in terms of throughput and delay. Investigating methods of guaranteeing different kinds of fairness *at the cell, as well as the user level* is thus of great importance.

For the distributed framework based upon statistical non-local information a number of issues also remain to be investigated. First of all, investigating different kinds of local and non-local knowledge is interesting, as it would impact the outcome of the power allocation and hence the network capacity. Secondly, the FDPA and 1-BDPA algorithms have been presented considering a simple two-cell network. Extending these algorithms to a larger network size or developing new algorithms based on this framework would be the next step.

We have considered a single channel model in this work and though some of the results presented here might be applicable over multiple channels independently, the dimension offered by performing power allocation and scheduling over multichannel, multicell networks would come as a significant extension of this work. For the power allocation problem, this would result in a peak power constraint per cell and a sum power constraint over the channels. The problem would then be to find the appropriate power per channel and the corresponding user which would maximize the network capacity (which in this case would be summed over the channels as well).

Bibliography

[1] *Physical and Medium Access Control Layers for Combined Fixed and Mobile Operation in Licensed Bands*, IEEE Std. Std 802.16e-2005, 2005.

[2] 3rd generation - Long Term Evolution. 3rd Generation Partnership Project. [Online]. Available: http://www.3ggp.org

[3] G. J. Foschini and M. J. Gans, "On limits of wireless communications in a fading environment when using multiple antennas," *Wirel. Pers. Commun.*, vol. 6, no. 3, pp. 311–335, 1998.

[4] A. Paulraj, R. Nabar, and D. Gore, *Introduction to Space-Time Wireless Communications*. United Kingdom: Cambridge University Press, 2003.

[5] H. Bölcskei, D. Gesbert, C. B. Papadias, and A.-J. van der Veen, *Space-Time Wireless Systems: From Array Processing to MIMO Communications*. New York: Cambridge University Press, 2006.

[6] S. Lin and J. Daniel J. Costello, *Error Control Coding*. New Jersey: Prentice Hall, 2004.

[7] J.-C. Belfiore, G. Rekaya, and E. Viterbo, "The golden code: A 2 x 2 full-rate space-time code with non-vanishing determinants," *IEEE Trans. Inform. Theory*, vol. 51, pp. 1432–1436, April 2005.

[8] S. Catreux, P. F. Driessen, and L. J. Greenstein, "Simulation results for an interference-limited multiple-input multiple-output cellular system," *IEEE Commun. Lett.*, vol. 4, no. 11, pp. 334–336, 2000.

[9] R. S. Blum, J. H. Winters, and N. R. Sollenberger, "On the capacity of cellular systems with mimo," *IEEE Commun. Lett.*, vol. 6, no. 6, pp. 242–244, 2002.

[10] J. Zander and S.-L. Kim, *Radio Resource Management for Wireless Networks*. Massachusetts: Artech House, 2001.

[11] M. Xiao, N. B. Shroff, and E. K. P. Chong, "Resource management in power-controlled cellular wireless systems," *Wireless Communications and Mobile Computing*, vol. 1, pp. 185–199, 2001, invited paper.

[12] V. H. Macdonald, "The cellular concept," *Bell Technical Journal*, vol. 58, pp. 15–42, 1979.

[13] A. Goldsmith, *Wireless Communications*. New York: Cambridge Univ. Press, 2005.

[14] U. Madhow and M. L. Honig, "Interference suppression for directed-sequence spread spectrum cdma," *IEEE Trans. Commun.*, vol. 42, no. 9, pp. 3178–3188, Dec. 1994.

[15] S. Verdu, *Multiuser Detection*. New York: Cambridge University Press, 1998.

[16] G. Song and Y. Li, "Utility-based resource allocation and scheduling in OFDM-based wireless broadband networks," *IEEE Communications Magazine*, vol. 43, pp. 127–134, Dec. 2005.

[17] R. Knopp and P. Humblet, "Information capacity and power control in single-cell multiuser communications," in *Proc. IEEE International Conference on Communications*, Seattle, June 1995, pp. 331–335.

[18] M. Andrews, K. Kumaran, K. Ramanan, A. Stoylar, P. Whiting, and R. Vijayakumar, "Providing quality of service over a shared wireless link," *IEEE Commun. Mag.*, pp. 150–154, Feb. 2001.

[19] J. Zander, "Distributed cochannel interference control in cellular radio systems," *IEEE Trans. Veh. Technol.*, vol. 41, pp. 305–311, Aug. 1992.

[20] G. J. Foschini and Z. Miljanic, "A simple distributed autonomous power control algorithm and its convergence," *IEEE Trans. Veh. Technol.*, vol. 42, no. 4, pp. 641–646, Nov. 1993.

[21] R. D. Yates, "A framework for uplink power control in cellular radio systems," *IEEE J. Select. Areas Commun.*, vol. 13, pp. 1341–1347, 1995.

[22] A. J. Goldsmith and S.-G. Chua, "Adaptive coded modulation for fading channels," *IEEE Trans. Commun.*, vol. 46, pp. 595–602, May 1998.

[23] V. Tralli, R. Veronesi, and M. Zorzi, "Power-shaped advanced resource assignment for fixed broadband wireless access systems," *IEEE Trans. Wireless Commun.*, vol. 3, pp. 2207–2220, Nov. 2004.

[24] R. Veronesi, V. Tralli, J. Zander, and M. Zorzi, "Distributed dynamic resource allocation for multicell sdma packet access networks," *IEEE Trans. Wireless Commun.*, vol. 5, pp. 1–12, 2006.

[25] K. Chawla and X. Qiu, "Quasi-static resource allocation with interference avoidance for fixed wireless systems," *IEEE J. Select. Areas Commun.*, vol. 17, pp. 493–504, Mar. 1999.

[26] K. K. Leung and A. Srivastava, "Dynamic allocation of downlink and uplink resource for broadband services in fixed wireless networks," *IEEE J. Select. Areas Commun.*, vol. 17, pp. 990–1006, May 1999.

[27] T. Bonald, S. Borst, and A. Proutière, "Inter-cell scheduling in wireless data networks," in *Proc. European Wireless*, Cyprus, Apr. 2005.

[28] M. H. Ahmed, H. Yanikomeroglu, and S. Mahmoud, “Interference management using basestation coordination in broadband wireless access networks,” *Wireless Communications and Mobile Computing*, vol. 6, pp. 95–103, 2006.

[29] D. J. Love, R. W. Heath, W. Santipach, and M. Honig, “What is the value of limited feedback for MIMO channels?” *IEEE Communications Magazine*, vol. 42, pp. 54–59, Oct. 2004.

[30] A. Gjendemsjø, D. Gesbert, G. E. Øien, and S. G. Kiani, “Optimal power allocation and scheduling for two-cell capacity maximization,” in *Proc. Modeling and Optimization in Mobile, Ad Hoc, and Wireless Networks*, Boston, MA, April 2006, pp. 1–6.

[31] K. N. Lau, “Analytical framework for MIMO uplink space-time scheduling design with convex utility functions,” *IEEE Trans. on Wireless Communications*, pp. 1832–1843, Sept. 2004.

[32] C. Y. Wong, R. S. Cheng, K. B. Letaief, and R. D. Murch, “Multiuser OFDM with adaptive subcarrier, bit, and power allocation,” *IEEE J. Select. Areas Commun.*, vol. 17, pp. 1747–1758, Oct. 1999.

[33] J. Jang and K. B. Lee, “Transmit power adaptation for multiuser OFDM systems,” *IEEE J. Select. Areas Commun.*, vol. 21, pp. 171–178, Feb. 2003.

[34] G. Li and H. Liu, “Downlink dynamic resource allocation for multi-cell OFDMA system,” in *Proc. IEEE VTC*, Oct. 2003.

[35] H. Kim, Y. Han, and J. Koo, “Optimal subchannel allocation scheme in multicell OFDMA systems,” in *Proc. IEEE VTC*, May 2004.

[36] D. Fudenberg and J. Tirole, *Game Theory.* Cambridge,MA: MIT Press, 1991.

[37] E. Altman, T. Boulogne, R. El-Azouzi, T. Jimenez, and L. Wynter, “A survey on networking games in telecommunication,” *Comput. Oper. Res.*, vol. 33, pp. 286–311, Feb. 2006.

[38] M. Xiao, N. B. Shroff, and E. K. P. Chong, “A utility-based power-control scheme in wireless cellular systems,” *IEEE/ACM Trans. Networking*, vol. 11, pp. 210–221, Apr. 2003.

[39] D. Goodman and N. Mandayam, “Power control for wireless data,” *IEEE Personal Commun. Mag.*, vol. 7, pp. 48–54, Apr. 2000.

[40] C. Saraydar, N. B. Mandayam, and D. J. Goodman, “Pricing and power control in a multicell wireless data network,” *IEEE Trans. Commun.*, vol. 19, pp. 1883–1892, Oct. 2001.

[41] ——, “Efficient power control via pricing in wireless data networks,” *IEEE Trans. Commun.*, vol. 50, pp. 291–303, Feb. 2002.

[42] C. Zhou, M. L. Honig, and S. Jordan, “Utility-based power-control for a two-cell CDMA data network,” *IEEE Trans. Wireless Commun.*, vol. 4, pp. 2764–2776, Nov. 2005.

[43] J. Huang, R. Berry, and M. L. Honig, "Distributed interference compensation for wireless networks," *IEEE J. Select. Areas Commun.*, vol. 24, pp. 1074–1084, May 2006.

[44] E. G. Larsson and E. A. Jorwieck, "Competition and collaboration on the MISO interference channel," in *Allerton Conference*, Illinois, USA, Sep. 2007.

[45] T. M. Cover and J. A. Thomas, *Elements of Information Theory.* New York: John Wiley & Sons, 1991.

[46] F. P. Kelly, "Charging and rate control for elastic traffic," *European Transactions on Telecommunications*, vol. 8, pp. 33–37, 1997.

[47] P. Viswanath, D. Tse, and R. Laroia, "Opportunistic beamforming using dumb antennas," *IEEE Trans. Inform. Theory*, vol. 48, pp. 1277–1294, June 2002.

[48] M. Chiang, "Geometric programming for communications systems," *Foundations and Trends in Communications and Information Theory*, vol. 2, no. 1/2, pp. 1–156, Aug. 2005.

[49] M. Chiang, C. W. Tan, D. P. Palomar, D. O'Neill, and D. Julian, "Power control by geometric programming," *IEEE Trans. Wireless Commun.*, vol. 6, no. 7, pp. 2640–2651, July 2007.

[50] E. S. Sousa, "Interference modeling in a direct-sequence spread-spectrum packet radio network," *IEEE Trans. Commun.*, vol. 38, pp. 1475–1482, Sept. 1990.

[51] K. S. Gilhousen, I. M. Jacobs, R. Padovani, A. J. Viterbi, L. A. Weaver, and C. E. Wheatley, "On the capacity of a cellular cdma system," *IEEE Trans. Veh. Technol.*, vol. 40, pp. 303–312, May 1991.

[52] M. Zorzi, "On the analytical computation of interference statistics with applications to the performance evaluation of mobile radio systems," *IEEE Trans. Commun.*, vol. 45, pp. 103–109, Jan. 1997.

[53] S. Hanly and R. Mathar, "On the optimal base-station density for cdma cellular networks," *IEEE Trans. Commun.*, vol. 50, pp. 1274–1281, Aug. 2002.

[54] J.-M. Kelif and E. Altman, "Downlink fluid model of CDMA networks," in *Proc. IEEE VTC*, Stockholm, May 2005.

[55] S. Gobriel, R. Melhem, and D. Moss, "A unified interference/collision analysis for power-aware adhoc networks," in *Proc. IEEE Conference on Computer Communications*, Hong Kong, March 2004.

[56] R. Hekmat and P. V. Mieghiem, "Interference in wireless multi-hop ad-hoc networks and its effects on network capacity," *Wireless Networks Journal*, vol. 10, pp. 389–399, July 2004.

[57] ——, "Interference power sum with log-normal components in ad-hoc and sensor networks," in *Proc. WiOpt*, Trentino, Italy, April 2005.

[58] J. F. Whitehead, "Signal-level-based dynamic power control for cochannel interference management," in *Proc. IEEE Vehicular Technology Conference*, May 1993, pp. 499–502.

[59] T. S. Rappaport, *Wireless Communications: Principles and Practice*. Upper Saddle River, NJ: Prentice Hall, 2002.

[60] W. C. Y. Lee and D. Lee, "CDMA capacity on pathloss and power control," in *Proc. IEEE Vehicular Technology Conference*, 2000, pp. 624–629.

[61] *Wireless LAN Medium Access Control (MAC) and Physical Layer (PHY) Specifications*, IEEE Std. 802.11, 1999.

[62] N. Jain, S. R. Das, and A. Nasipuri, "A multichannel CSMA MAC protocol with receiver-based channel selection for multihop wireless networks," in *Proc. IC3N*, Scottsdale, AZ, USA, Oct. 2001.

[63] Z. J. Haas and J. Deng, "Dual busy tone multiple access (DBTMA) - a multiple access scheme for ad-hoc networks," *IEEE Trans. Commun.*, vol. 50, pp. 975–985, June 2002.

[64] J.-E. Kirkebø, D. Gesbert, and S. G. Kiani, "Maximizing the capacity of wireless networks using multi-cell access schemes," in *Proc. IEEE SPAWC*, Cannes, France, July 2006.

[65] S. G. Kiani and D. Gesbert, "Optimal and distributed scheduling for multicell capacity maximization," *IEEE Trans. Wireless Commun.*, vol. 7, Jan. 2008.

[66] S. G. Kiani, G. E. Øien, and D. Gesbert, "Maximizing multi-cell capacity using distributed power allocation and scheduling," in *Proc. IEEE Wireless Communications and Networking Conference (WCNC)*, Hong Kong, China, March 2007.

[67] A. Papoulis and S. U. Pillai, *Probability, Random Variables and Stochastic Processes*. New York: McGraw Hill, 2002.

[68] I. Katzela and M. Naghshineh, "Channel assignment schemes for cellular mobile telecommunication systems: A comprehensive survey," *IEEE Personal Commun. Mag.*, pp. 10–31, June 1996.

[69] H. Bölcskei, A. J. Paulraj, K. V. S. Hari, R. U. Nabar, and W. W. Lu, "Fixed broadband wireless access: State of the art, challenges, and future directions," *IEEE Commun. Mag.*, vol. 39, pp. 100–108, Jan. 2001, invited paper.

[70] I. Koutsopoulos and L. Tassiulas, "Channel state-adaptive techniques for throughput enhancement in wireless broadband networks," in *Proc. IEEE Conference on Computer Communications*, Alaska, Apr. 2001.

[71] J. F. Whitehead, "Performance and capacity of distributed dynamic channel assignment and power control in shadow fading," in *Proc. IEEE International Conference on Communications*, May 1993, pp. 910–914.

[72] S. V. Hanly, "An algorithm for combined cell-site selection and power control to maximize cellular spread spectrum capacity," *IEEE J. Select. Areas Commun.*, vol. 13, pp. 1332–1340, 1995, invited paper.

[73] N. Bambos, "Toward power-sensitive network architectures in wireless communications: Concepts, issues and design aspects," *IEEE Personal Commun. Mag.*, pp. 50–59, June 1998.

[74] M. Duque-Antón, D. Kunz, and B. Rüber, "Channel assignment for cellular radio using simulated annealing," *IEEE Trans. Veh. Technol.*, vol. 42, pp. 14–21, 1993.

[75] G. Wang and N. Ansari, "Optimal broadcast scheduling in packet radio networks using mean field annealing," *IEEE J. Select. Areas Commun.*, vol. 15, pp. 250–260, Feb. 1997.

[76] C. R. Reeves, *Modern Heuristic Techniques for Combinatorial Problems,* Advanced Topics in Computer Science. McGraw-Hill Book Company, 1995.

[77] *Urban Transmission Loss Models for Mobile Radio in the 900 and 1800 MHz Bands*, EURO-COST Std. 231, 1991.

[78] J. Zander, "Performance of optimum transmitter power control in cellular radio systems," *IEEE Trans. Veh. Technol.*, vol. 41, no. 1, pp. 57–62, Feb. 1992.

[79] Y.-H. Lin and R. L. Cruz, "Power control and scheduling for interfering links," in *Proc. IEEE ITW*, San Antonio, TX, October 2004.

[80] J. Matamoros and C. Antón-Haro, "Opportunistic power allocation schemes for wireless sensor networks," in *submitted to IEEE Int'l Symposium on Signal Processing and Information Technology (ISSPIT)*, Dec. 2007.

[81] T. Park, J. Jang, O.-S. Shin, and K. B. Lee, "Transmit power allocation for a downlink two-user interference channel," *IEEE Commun. Lett.*, vol. 9, no. 1, pp. 13–15, 2005.

[82] A. Gjendemsjø, D. Gesbert, G. E. ien, and S. G. Kiani, "Optimal power allocation and scheduling for two-cell capacity maximization," in *Proc. RAWNET (WiOpt)*, Boston, 2006.

[83] A. Gjendemsjø, D. Gesbert, G. E. Øien, and S. G. Kiani, "Binary power control for multi-cell capacity maximization," *to appear in the IEEE Trans. Wireless Comm.*, accepted Aug. 2007.

[84] M. Ebrahimi, M. A. Maddah-Ali, and A. K. Khandani, "Power allocation and asymptotic achievable sum-rates in single-hop wireless networks," in *Proc. CISS*, Princeton, NJ, March 2006.

[85] A. Bedekar, S. Borst, K. Ramanan, P. Whiting, and E. Yeh, "Downlink scheduling in CDMA data networks," in *Proc. IEEE Global Telecommunications Conference*, Rio de Janeiro, 1999, pp. 2653–2657.

[86] D. Gesbert and M. Kountouris, "Resource allocation in multicell wireless networks: Some capacity scaling laws," in *Workshop on Resource Allocation in Wireless Networks (RAWNET)*, Limassol, Cyprus, April 2007.

[87] J. Abouei, M. Ebrahimi, and A. K. Khandani, "A new decentralized power allocation strategy in single-hop wireless networks," in *Proc. CISS*, Princeton, NJ, March 2007.

[88] S. Kandukuri and S. Boyd, "Optimal power control in interference-limited fading wireless channels with outage-probability specifications," *IEEE Trans. Wireless Commun.*, vol. 1, pp. 46–55, January 2002.

[89] C. W. Tan, D. P. Palomar, and M. Chiang, "Solving non-convex power control problems in wireless networks: Low SIR regime and distributed algorithms," in *Proc. IEEE GLOBECOM*, St. Louis, MO, Nov.-Dec. 2005, pp. 3445–3450.

[90] X. Qin and R. Berry, "Distributed power allocation and scheduling for parallel channel wireless networks," in *Proc. Modeling and Optimization in Mobile, Ad Hoc, and Wireless Networks (WIOPT)*, Trentino, Italy, April 2005.

[91] M. Moustafa, I. Habib, and M. N. Naghineh, "Efficient radio resource control in wireless networks," *IEEE Trans. Wireless Commun.*, vol. 33, pp. 2385–2395, November 2004.

[92] X. Qin and R. Berry, "Exploiting multiuser diversity for medium access control in wireless networks," in *Proc. IEEE INFOCOM*, San Francisco, CA, April 2003, pp. 1084–1094.

[93] J.-E. Kirkebø, D. Gesbert, and S. G. Kiani, "Probabilistic access functions for multi-cell wireless schemes," in *Proc. IEEE International Telecommunication Symposium (ITS)*, Fortaleza, Brazil, September 2006.